Aino Valli

Accounting for imprecisions in image-guided radiotherapy: bladder cancer as an example

School of Electrical Engineering

Thesis submitted for examination for the degree of Master of Science in Technology.

Espoo 23.2.2015

Thesis supervisor:

Prof. Lauri Parkkonen

Thesis advisors:

M.Sc. Laura Tuomikoski

Docent Mikko Tenhunen

Aalto University
School of Electrical
Engineering

AALTO UNIVERSITY
SCHOOL OF ELECTRICAL ENGINEERING

ABSTRACT OF THE
MASTER'S THESIS

Author: Aino Valli

Title: Accounting for imprecisions in image-guided radiotherapy: bladder cancer as an example

Date: 23.2.2015 Language: English Number of pages: 8+79

Department of Department of Neuroscience and Biomedical Engineering

Professorship: Biomedical Engineering Code: Tfy-99

Supervisor: Prof. Lauri Parkkonen

Advisors: M.Sc. Laura Tuomikoski, Docent Mikko Tenhunen

There are many sources of imprecision in delivering external beam radiotherapy. Some of the errors can be eliminated with image guidance, but still, some inaccuracies have to be accounted for by using margins around the target volume. For mobile targets, such as the bladder, the internal motion of the target can be even the most important source of imprecision. Treating such targets with radiation therapy is challenging, since the margins needed to account for the possible target position variation inevitably include some normal tissue, which can lead to serious side-effects, limiting the treatment dose and preventing dose escalation. Adaptive radiation therapy (ART) addresses this challenge. In bladder ART, the target volume is modified daily to accommodate the daily bladder volume as conformally as possible, but without compromising dose coverage of the bladder. Different strategies for bladder ART have been suggested, but there is not yet a consensus of which strategy is the optimal one.

In this study, the adaptive radiotherapy methods applied in Helsinki University Central Hospital (Helsinki method) and Aarhus University Hospital (Aarhus method) for bladder cancer were compared. The treatment according to both methods was simulated for 10 patients in three different ways. There was no statistically significant difference between the methods in terms of the chosen planning target volume size. The selected alternative planning target volumes were more evenly distributed in the Aarhus method. Comparison of the modified methods with centroid registration suggested a possibility of a more even selection of treatment volumes if the current Helsinki method plan selection volumes (PSVs) were expanded with a 3-mm margin. However, for both methods, the smaller planning target volumes were selected more often in the actual treatment than in this simulation, suggesting that utilizing the bladder contours in the plan selection in the simulation affected the selections in an unexpected way.

Keywords: imprecision sources, adaptive radiotherapy, bladder cancer, treatment simulation

AALTO-YLIOPISTO
SÄHKÖTEKNIIKAN KORKEAKOULU

DIPLOMITYÖN
TIIVISTELMÄ

Tekijä: Aino Valli

Työn nimi: Epätarkkuuksien huomiointi kuvantaohjatussa sädehoidossa: esimerkkinä virtsarakon syöpä

Päivämäärä: 23.2.2015 Kieli: Englanti Sivumäärä: 8+79

Neurotieteen ja lääketieteellisen tekniikan laitos

Professuuri: Lääketieteellinen tekniikka Koodi: Tfy-99

Valvoja: Prof. Lauri Parkkonen

Ohjaajat: FM Laura Tuomikoski, Dosent Mikko Tenhunen

Ulkoisessa sädehoidossa on epätarkkuuden lähteitä. Jotkin näistä virhelähteistä voidaan poistaa käyttämällä kuvantaohjausta, mutta jotkin epätarkkuudet täytyy huomioida käyttämällä marginaaleja kohdealueen ympärillä. Liikkuville hoitokohteille, kuten virtsarakolle, kudosten liike potilaassa voi olla jopa suurin epävarmuuden lähde. Tällaisten kudosten sädehoito on haastavaa, sillä kohteen mahdollisen liikkeen kompensoiviin marginaaleihin sisältyy väistämättä myös normaalia kudosta. Tämä voi johtaa vakaviin sivuvaikutuksiin, jotka rajoittavat käytetyn säteilyannoksen suuruutta. Ongelmaa pyritään ratkaisemaan adaptiivisella sädehoidolla. Virtsarakon adaptiivisessa sädehoidossa kohdealuetta muokataan joka hoitokerta kattamaan rakon tilavuus mahdollisimman pienellä kohdealueen tilavuudella, kuitenkaan tinkimättä rakon annoskattavuudesta. Virtsarakon adaptiiviseen sädehoitoon on ehdotettu monia toteutustapoja, mutta parhaasta mahdollisesta menetelmästä ei ole vielä päästy selvyyteen.

Tässä tutkimuksesssa verrattiin Helsingin Yliopistollisessa Keskussairaalassa ja Aarhusin Yliopistollisessa Sairaalassa (Engl. Aarhus University Hospital) käytettyjä virtsarakon adaptiivisia sädehoitomenetelmiä. Menetelmien mukainen hoito simuloitiin kymmenelle potilaalle kolmella eri tavalla. Menetelmien välillä ei ollut tilastollisesti merkitsevää eroa valitun kohdealueen koossa. Vaihtoehtoisia kohdealueita valittiin tasaisemmin Aarhusin menetelmässä. Muokattujen menetelmien vertailusta kävi ilmi, että Helsingin menetelmän mukaisten suunnitelmanvalintavolyymien (Engl. plan selection volume, PSV) laajentaminen 3 mm marginaalilla voisi johtaa tasaisempaan vaihtoehtoisten kohdealueiden valintaan. Pienempiä kohdealueita valittiin kuitenkin molempien menetelmien tapauksessa todellisessa hoidossa simulaatiota enemmän, joten rakon ääriviivojen käyttö suunnitelmanvalinnassa saattoi vaikuttaa valintoihin odottamattomalla tavalla.

Avainsanat: virhelähteet, adaptiivinen sädehoito, virtsarakon syöpä, hoidon simulaatio

Preface

I would like to thank my instructor, Docent Mikko Tenhunen, for the opportunity to work with this fascinating research topic and for all his guidance. I highly appreciate all the advice he has given me regarding my studies and my future ambitions. My other instructor, M.Sc. Laura Tuomikoski also earns my most sincere gratitude for her priceless advice and support during the course of this work. Thank you for your constructive comments and most valuable discussions. I also want to thank Prof. Lauri Parkkonen for detailed comments and excellent thesis supervision. In addition, I want to acknowledge the generous grant of Fanny Palmén's Fund that supported my thesis work. Furthermore, it has been a pleasure to work at the Department of Oncology of Helsinki University Central Hospital and I want to thank all my co-workers for help, understanding and inspiring discussions.

I am also grateful to my family for their support and encouragement during my studies. Knowing that you believe in me and discussions with you have meant me more than you ever guess. Finally, thank you, Teemu for all your endless love and patient support. I could not imagine my life without my safe place in your arms.

Espoo, February 23, 2015

Aino Valli

Contents

Symbols and abbreviations

Symbols and Operators

Margin theory

$\boldsymbol{\Sigma}$	Standard deviation of systematic errors
$\boldsymbol{\sigma}$	Standard deviation of random errors
σ_{p}	Standard deviation describing the penumbra width
$\boldsymbol{\Sigma}_i$	Standard deviation of systematic error component i
$\boldsymbol{\sigma}_i$	Standard deviation of random error component i
α	Parameter depending on the level of confidence
β	Parameter depending on the beam configuration
a	Treatment planning system photon beam algorithm error
$\mathbf{b}$	Breathing positional error
$\mathbf{M}$	Group systematic error

Statistical analysis

ϵ_i	Linear regression error term
β	Parameter chosen to minimize the error terms
x	Linear regression explanatory variable
y	Linear regression dependent variable
R^2	R^2-value, describes how many % of y variation is explained by x
n	Number of observations
F	F-test quantity
t	t-test quantity
D_i	Difference between the ith pair of observations
s_D	Variance of the D_i
r_{xy}	Pearson correlation coefficient
p	p-value

Abbreviations

AUH	Aarhus University Hospital
ART	Adaptive radiotherapy
CBCT	Cone-beam computed tomography
Cine-MRI	Cine-magnetic resonance imaging
CT	Computerized tomography
CTV	Clinical target volume
GTV	Gross tumour volume
HUCH	Helsinki University Central Hospital
ICRU	International Commission of Radiation Units and Measurements
IMRT	Intensity-modulated radiotherapy
ITV	Internal target volume
Linac	Linear accelerator
MLC	Multileaf collimator
NTCP	Normal tissue complication probability
PSV	Plan selection volume
PTV	Planning target volume
PUC	Probability of uncomplicated cure
RF	Radio frequency
TCP	Tumour control probability
TPS	Treatment planning system
VMAT	Volumetric-modulated arc therapy

1 Introduction

In external beam radiotherapy, radiation is produced with a linear accelerator and delivered to the target volume based on positional information of the computerized tomography (CT) image of the patient. The aim is to treat the target volume with a dose that is high enough to kill the malign cells while keeping the dose to healthy tissue at minimum. Fulfilment of this goal is challenging, mainly because of geometric inaccuracies in the treatment process. The total dose is usually divided into smaller fractions, and therefore, the daily positional variation of the target poses an additional challenge in the case of moving tissue.

The accuracy can be improved with careful patient positioning and maintenance of the imaging and treatment devices [1]. The movement of the target can be attempted to be restricted or compensated for with tracking [2]. Image-guided radiation therapy solves many of the problems in precisely delivering radiation to the target. However, there is always some remaining inaccuracy, which is taken into account by adding margins to the treatment volume [2]. In this thesis, the different sources of imprecision in the radiation therapy process are examined. The ways to deal with these sources of error are addressed and the remaining problems are discussed.

The urinary bladder is a mobile organ and with its changing volume a problematic target for radiation therapy [3; 4]. The position and volume of the planning target volume varies from day to day not only due to the gradual changes of the tumour and the surrounding normal tissues, but also because of the changes in urinary bladder dimensions that cannot be avoided by instructing the patients to empty their bladder [4; 5]. Also the adjacent organs change the bladder shape [6]. Thus, daily imaging is required.

Image guidance enables adjusting the patient's position on the treatment machine immediately before the treatment based on the imaging information acquired [2]. The patient can be positioned to the treatment by registering the treatment planning computerized tomography image and the image acquired on the treatment machine. In this registration the patient's anatomy (e.g. bones or soft tissues) in the treatment planning CT is matched to that of the image acquired in the treatment.

In radiation therapy of the bladder, some problems remain to be solved even with image guidance. The tolerance of the surrounding normal tissues restrain the dose that can be given to the target volume, since large margins need to be added to the target volume in order to achieve adequate dose coverage to the bladder [7]. Adaptive radiation therapy (ART) aims at increasing the precision of the treatment while minimizing the treated volume. In adaptive radiotherapy, the target volume is adapted to the daily target volume shape and position [8]. Different strategies for adaptive radiation therapy of the bladder have been suggested, but it is still unclear, what would be the optimal way to minimize the treated volume without compromising the target coverage.

Two methods for image-guided adaptive radiotherapy of the bladder have been recently proposed [9; 10]. In the method used in Helsinki University Central Hospital (Helsinki method), four treatment planning CT images with different bladder

volumes are acquired and based on the bladder volumes delineated on the images, a set of treatment plans is made [9]. The plan of the day is chosen based on the visible extent of bladder wall in cone-beam computed tomography (CBCT) images.

In the method used in Aarhus University Hospital (Aarhus method) the treatment of the first week is given conventionally. The treatment plan for the first week is made based on one treatment planning CT image with margins large enough to account for the changes of the bladder volume. CBCT-images of the patient are acquired every day during the first week and three alternative planning target volumes are constructed with Boolean operations performed on the bladder contours of the four different CBCT images and the treatment planning CT image [10].

The aim of this study is to compare these two methods for adaptive radiation therapy of the bladder in terms of hitting the target and saving the surrounding normal tissues. This is done by simulating the treatment up to the point where the target volumes for the daily treatments are chosen. The simulation is repeated with three ways, with the aim of critically analysing which factors have an effect on the results and to evaluate the pros and cons of the methods.

There are situations that the lymph nodal areas surrounding the bladder need to be included to the target volume. The usual procedure in these cases is to register the images according to the bony anatomy. In this study, the treatment of the bladder and the lymph nodal areas is simulated, positioning the patient according to the bladder. The margin needed to account for this positional error induced to the lymph nodes is calculated.

Chapter 1 is an introduction. In Chapter 2, the theoretical background of the study is addressed. The central idea and concepts of radiation therapy are reviewed and the ways to classify errors in radiotherapy are introduced. The ways to minimize the imprecisions and to compensate for the remaining inaccuracies are also described. After this, the sources of inaccuracy present during the course of radiotherapy treatment are reviewed, making a division to the errors in the treatment simulation and those in the treatment delivery. In addition, radiotherapy of the urinary bladder cancer is reviewed and the adaptive radiotherapy methods of Helsinki [9] and Aarhus [10] are introduced. Chapter 3 describes the methods of the study, discussing the patients, the three different ways to simulate the treatment, and simulation of the treatment with the lymph nodes included. Also the statistical methods used in the study are reviewed. Chapter 4 presents the results of the study and Chapter 5 discusses the findings. In Chapter 6, the conclusions of the study are reported.

2 Background

2.1 Introduction to radiotherapy

In this chapter, the aim and principles of external beam radiotherapy are reviewed. First, the fundamental idea behind radiotherapy, the dose–response relationship, is clarified. Second, the radiotherapy treatment process is briefly reviewed. Furthermore, the definition and classification of errors are introduced and the ways to minimize errors as well as the principle of accounting for the errors with margin addition are described.

2.1.1 Dose–response relationship

The goal of external radiotherapy is to give the patient a radiation dose which maximizes the probability for tumour local control, yet minimizing the side effects for normal tissues. When the treatment fulfils these two goals in the best possible manner, its therapeutic ratio is optimized. When planning the treatment one must take into account not only the therapeutic dose to the tumour but also the tolerance of the normal tissues. The distance between the dose producing the tumour control and the dose causing unwanted side effects is usually narrow. Usually, megavoltage (MV) photons or electrons are used in the radiation therapy. Both the electrons and the photons interact in the tissue ionizing the atoms on their way. The recombination of these ionized atoms provides energy for the production of highly reactive chemical radicals. These mostly water-based radicals can then attack the DNA and other critical structures of the cell nucleus, which interferes with cell reproduction thus sterilizing the cell.

If a cancer cell can form a number of copies of itself by dividing itself, it is called a clonogenic unit [11]. The curation of the tumour can be accomplished only by destroying each individual clonogenic unit of the tumour. It is essential that the entire target volume receives the prescribed dose as even a small volume of the target not receiving the total dose might contain living tumour cells. If these cells did not achieve the prescribed dose, this might lead to local recurrence.

The effect of radiotherapy on the normal tissues and the tumour can be described with dose–response relationship curves. The term tumour control probability (TCP) means the dose–response relationship of the tumour and the term normal tissue complication probability (NTCP) is used for the normal tissues, respectively. The curve presents the probability of a given reaction as a function of the absorbed dose D. Probability of uncomplicated cure (PUC) describes the probability that the tumour is cured without having any side effects. It can be calculated with the formula:

$$\mathrm{PUC} = \mathrm{TCP}\,(1 - \mathrm{NTCP}) \tag{1}$$

The absorbed dose in matter is defined as the energy that has been absorbed from ionizing radiation to a certain point of matter per unit mass. Its unit is gray (Gy).

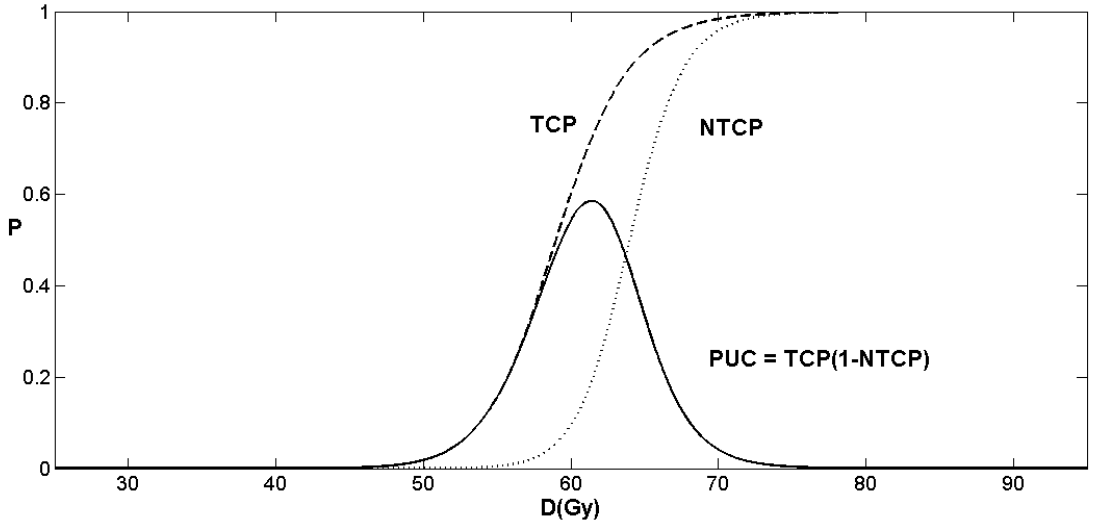

Figure 1: Dose–response relationship curves. The TCP is the tumour control probability describing the radiation response of the tumour. NTCP is the normal tissue complication probability describing the response of the normal tissues to radiation. The PUC curve describes the probability of uncomplicated cure. However, in clinical situations, the dose maximizing the value of PUC may lead to unacceptable side-effects.

The dose–response relationship curve of both normal tissue and the tumour has approximately a logistic form [11]. An example of the dose–response relationship curves for normal tissues and tumour is shown in Figure 1. The form of the curve shows that the probability for a response to the radiation is very modest with small doses. Also, one can see that with doses higher than some threshold dose, which depends on the tissue, the probability of the response grows rapidly.

These dose–response relationship curves are typically steep, and thus it is important to deliver the precisely correct dose to the precisely correct target. If the actually received dose is smaller than expected, this can reduce the probability of the cure. The normal tissue complication probability curve often lies close to the tumour control probability curve and thus, the target dose cannot be escalated more than to the threshold dose of the normal tissue complication probability curve. The precision of the dose as well as the geometrical precision while delivering the dose is important. The geometrical deviation between the planned and the actual received dose distribution can lead to both smaller tumour dose and larger normal tissue dose [12].

2.1.2 Radiotherapy treatment process

The different phases of the radiotherapy treatment are the treatment planning and treatment delivery. In the treatment planning, a planning computerized tomography image is first acquired. Then the target volume and the adjacent normal structures are delineated in the CT image and a treatment plan is made. The treatment delivery phase comprises the treatment, where several treatment fractions are given.

Most often a medical linear accelerator (linac) is used for producing the radiation and directing it at the patient. The linac accelerates electrons, which can be used to treat the patient or to produce photons. Photons are attenuated with only about a factor of 2 in passing through the body and thus can treat deep-lying tumours [13]. The absorbed dose of photons builds up over the first a few centimetres which is useful for limiting the dose to the sensitive layers of the skin. More superficial targets can be treated with electrons, which penetrate the body only to a distance of a few centimetres [13]. This reduces dose to the deeper-lying critical structures.

Most modern linacs have an isocentric set-up with the treatment head, i.e. gantry, rotating 360 degrees around one certain point; the isocentre [13] (Figure 2). This is the point of intersection of the gantry axis and the collimator axis, which is moving in the vertical plane [14]. The treatment couch also rotates with respect to the isocentre, around an axis perpendicular to the couch surface and parallel with the collimator axis. The couch is a flat, even board that can be moved in three orthogonal directions. It is made of a material that minimally attenuates radiation. The location of the isocentre is indicated by the lasers on the sides of the treatment room.

In the treatment simulation, a computerized tomography scan is acquired, the patient being in the treatment position. The treatment position is chosen so that it is as suitable as possible for image acquisition and treatment [13]. This means that the position is easily reproducible and comfortable for the patient. Being able to reproduce and hold the position can be aided by using different patient positioning systems and rigid immobilization devices [12; 13].

During treatment simulation, the position of the isocentre in the patient is chosen from the CT images and sent to the laser indicators on each side of the patient. The projections of the isocentre location on each side of the patient are tattooed to the spots shown by the lasers. The initial patient positioning during the treatment is based on these tattooed marks.

The next step in the radiotherapy treatment process is to delineate the target volume and the adjacent critical normal structures to the treatment simulation CT images. To get standardized, reproducible procedures in this task, international organizations have published recommendations for the purpose. In the following, the most common recommendations by International Commission of Radiation Units and Measurements (ICRU) are presented. A radiographer delineates the critical normal tissues surrounding the target in the planning CT image. After this the radiation oncologist delineates the gross tumour volume (GTV) and defines the clinical target volume (CTV) and the planning target volume (PTV).

The gross tumour volume is the primary tumour volume containing the maximum

Figure 2: A linear accelerator with an isocentric set-up, Elekta Versa HD in HUCH. The gantry of the linac rotates a whole circle around the isocentre. The treatment table can also be moved and rotates around the vertical axis going through the isocentre. Opposite to the gantry there is a flat panel MV radiation detector for MV imaging. On the right there is an X-ray tube and on the left there is a detector for kV imaging. The imaging equipment is turned off the way of the treatment radiation.

tumour cell density. The shape, size and location of the GTV can be observed by clinical examination, e.g. palpation or imaging. The clinical target volume contains the tumour plus the suspected microscopic growth around the tumour, which cannot be observed, palpated or visualized. The CTV needs to be derived from information of the characteristics of similar tumours in the past [15]. To account for the small deviations between the planned and delivered treatment, the clinical target volume is expanded with a safety margin. The planning target volume is the volume to which a high dose is directed merely in order to ensure that the CTV receives adequate dose despite the geometric errors in the treatment [16]. Delineating the PTV, one must have knowledge of the possible uncertainties and variations in the tumour location and machine parameters [17]. The treated volume is the volume which gets the full prescribed dose. The irradiated volume is defined as the volume receiving a dose that is considered significant for the normal tissue tolerance. The target volumes are illustrated in Figure 3.

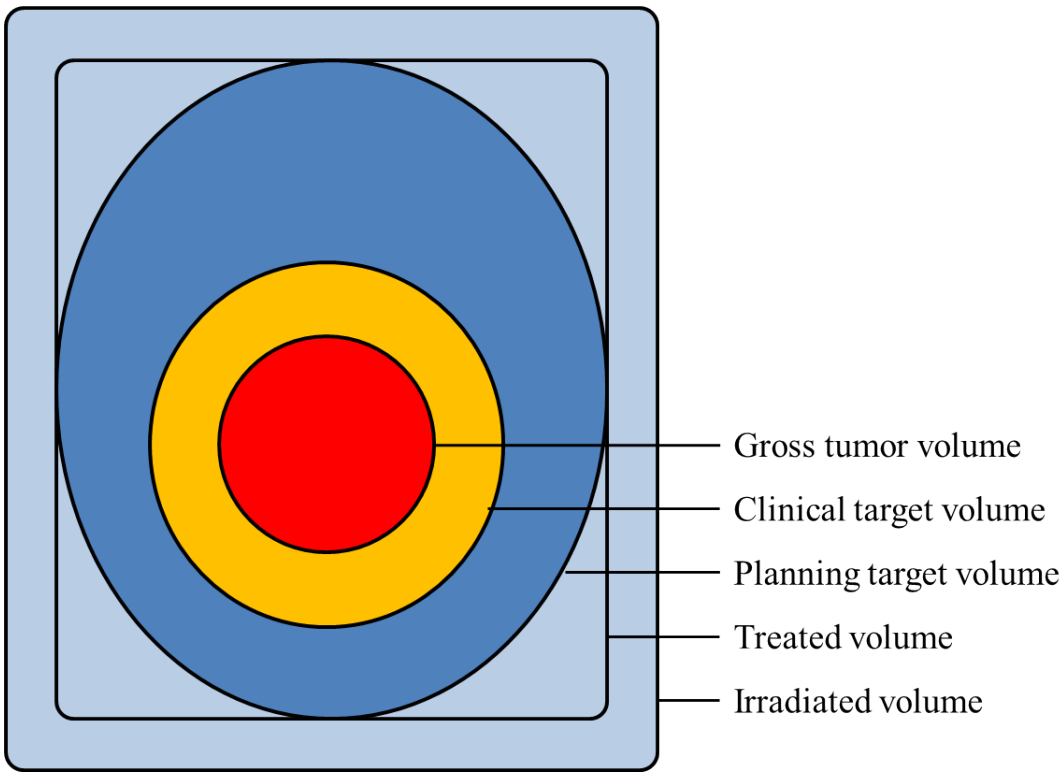

Figure 3: Definition of volumes in radiotherapy. Figure modified from Ref. 19.

The total treatment dose is usually divided to smaller fractions. This way it is possible to enable the healthy tissues to repair the damage produced by the radiation while the more radiosensitive tumour cells are irreversibly damaged. The radiation fields are aimed at the target of the treatment from many different directions so that only the target receives the prescribed total dose and the surrounding healthy tissues only get a part of the dose [19].

After the radiation oncologist has defined the planning target volume and assigned the dose and fractionation to the PTV, the physicist makes the treatment

plan. The field set-up that gives the most uniform dosage to the PTV minimising the dose to the normal tissues is chosen. According to ICRU recommendations the PTV dose should be 95–107% of the dose prescribed by the radiation oncologist [18]. In addition to the constraints set to the PTV dose, the normal tissue tolerances are taken into account when planning the treatment. There are specific tolerance criteria for every organ.

The treatment is planned with a computerized treatment planning system (TPS), which calculates the dose distribution in the patient by utilizing the tissue density information from the planning CT image. In the case of conformal radiotherapy, the physicist chooses the number and directions of the beams. The beams are formed with the collimators and the multi-leaf collimator (MLC). The latter has leaves that are set to certain positions according to the shape of the target. It is possible to control the relative amount of radiation produced by each of the beams by adjusting field weights.

When making an intensity-modulated radiation therapy (IMRT) plan, the treatment planning process is inversed. The physicist sets the normal tissue tolerance criteria and the field directions to the treatment planning system. The TPS optimizes the field weights and intensity patterns from each field that produce the most conformal and uniform dose filling the criteria. The intensity pattern in the fields is modulated by the means of closing and opening the MLC leaves during irradiation. The technique is especially powerful in sparing of normal tissues from the treatment dose in the case of concave targets. Another method with a similar optimization process as in IMRT is volumetric-modulated arc treatment (VMAT), which utilizes beams that turn along an arc during the radiation production. VMAT is especially practical for approximately round targets.

Each treatment fraction begins with patient set-up to the treatment machine. The patient is positioned to the treatment machine in the same way in the treatment delivery as in the treatment simulation CT. It is important to make a good documentation of the patient positioning and immobilization devices in the simulation in order to be able to reproduce the position also during the treatment. At present, in the majority of treatments, the target volume is further localized by imaging on the treatment machine immediately before each fraction. The imaging can be done with planar kV or MV imaging or different 3D-imaging methods, such as cone-beam CT imaging. Depending on the target and on the imaging method, either the target or a surrogate, e.g. the surrounding bony anatomy, is imaged. The possible misalignments of the beams that would be left undetected without imaging can then be corrected with translations and rotations of the treatment table. The prescribed single fraction of the total radiation dose is then given with the treatment machine.

2.1.3 Definition and classification of errors

In this thesis, the word 'error' does not mean a major mistake in the treatment that should have been detected by quality assurance procedures, i.e. a gross error, but instead the small deviations between the planned and delivered treatment. The aim is always to minimize these errors, but usually they cannot be totally eliminated.

The remaining errors are accounted for in the PTV formation, by adding a safety margin to the CTV.

Errors can be classified as random and systematic. Systematic errors have their origin in the treatment preparation and will influence all treatment fractions in an identical way [16; 20–22]. These errors mainly result because the target shape and position with respect to the isocentre are based on a single measurement [20]. Random errors, on the other hand, take place in the treatment delivery and do not have a systematic direction or magnitude [21; 22].

Random and systematic errors affect the dose distribution differently [21]. Random errors blur the dose distribution [1; 20]. In contrast, systematic errors cause a systematic shift of the dose distribution in respect to the target [16; 20; 21] (Figure 4). The effect of random errors, i.e. blurring of the dose distribution is easier to predict for each individual patient than the effect of systematic error [16]. Systematic errors have a much larger impact on the target dose than treatment delivery errors [21–23].

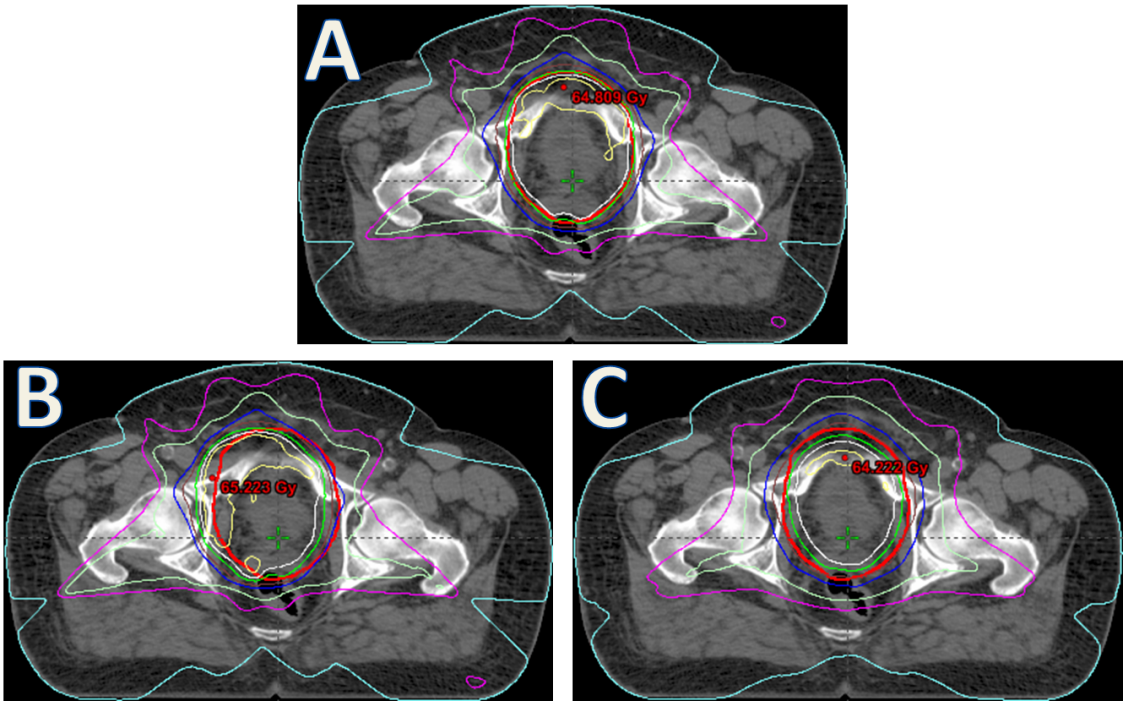

Figure 4: (A) The 95% isodose level of the dose distribution (green line) tightly surrounds the PTV when the dose is delivered without geometric errors. (B) Systematic deviation in the daily alignment of the field to the PTV causes a shift in the dose distribution with respect to the PTV. (C) Random errors in the alignment of the dose distribution and the PTV cause blurring of the dose distribution. The green 95% isodose level no longer surrounds the PTV. The PTV is the volume delineated with a red contour. The different dose levels, that is, the isodose lines are marked with different colours. For illustrative purposes, the errors in the isocentre position are 1 cm, which is an unrealistic error in a real RT treatment.

The variations in the treatment can also be classified as internal and external variations [17]. Internal variations are differences in the position, size and shape of the CTV [17]. Not all tissues are rigidly attached to the bony anatomy and thus, variations in the CTV positions can occur either directly or indirectly as the CTV is pushed by other moving organs and tissues. Internal variations patient and site-specific and can be affected by patient preparation protocols such as voiding instructions. External variations are deviations in the patient positioning and in the beam positioning. The external variations are affected by the patient positioning methods, the mechanical uncertainties of the equipment, dosimetric uncertainties (e.g. penetration of the beam), transfer errors from CT and simulator to the treatment unit, and human factors [17]. As well as variations between different treatment fractions (interfractional variation), there can be movement occurring during a treatment fraction (intrafractional variation). Both internal variations, such as organ motion, and external variations, such as patient movement relative to the beam position occur also during the treatment fractions.

2.1.4 Image-guided radiotherapy – minimizing errors

Safety margins are applied to account for geometric uncertainties in radiation therapy. In many cases these margins overlap organs at risk, which limits dose escalation [2]. Image-guided radiotherapy aims at improving the accuracy by imaging tumours and critical structures on the treatment machine immediately prior to irradiation [2].

There are multiple options for image guidance technologies available, including imaging devices both integrated and not integrated within the treatment room. A non-integrated option is a CT scanner outside the treatment room. Options that are integrated to the treatment room include kilovoltage (kV) X-ray imaging, active implanted markers [24; 25], ultrasound [26], megavoltage (MV) single slice CT (Tomotherapy) [27], conventional CT [28] and kV [29] and MV cone-beam CT [30]. Image guidance requires an imaging method to visualize the anatomy used as a surrogate for the target movement, a reference dataset and a method for correction of the error (e.g. translations of the treatment couch).

The information achieved from the imaging methods available on the treatment machine enables correction of the small deviations that are not visible just by comparing the location of the tattooed markings on the patient to the position of the laser lines. The imaging method affects what corrections can be made. If the target remains in a rigid position according to the bony anatomy, it is enough to visualize the bones for example with two-dimensional planar imaging. If the target is a soft tissue changing position with respect to the bones, 3-dimensional imaging method with the ability to distinguish the soft tissues is the only option. Adequate visualization is always a prerequisite for corrections.

The errors that can be corrected with image guidance depend on the imaging method used and the strategy used for correcting the errors. There are three different types of strategies for correction of errors: Offline corrections, online corrections and intrafraction corrections [2]. In offline correction the reaction to the image taken is

delayed to the subsequent fraction, whereas in online correction the reaction comes immediately after imaging, before the treatment. Intrafraction corrections are made with multiple images and corrections during each fraction.

The idea behind offline correction is that the margin selection is predominantly affected by systematic errors and less by random errors [2]. In offline correction one aims to correct the mean error of a patient without correcting the daily random variations. The advances in online imaging have made online corrections immediately after imaging feasible. The advantage of online correction is that it efficiently accounts for both systematic and random errors. A challenge is that the analysis and corrections should be performed quickly and the time pressure can affect the accuracy of the procedure [2].

Adaptive radiotherapy is image-guided RT taking a step further. In image-guided RT, the possible imaged deviations are corrected by moving the patient, but in addition, adaptive radiation therapy involves modifications to the treatment plan based on the information in the images. Yan et al. defined the adaptive radiation therapy as 'A radiation treatment process where the treatment plan can be modified using a systematic feedback of measurements' [8].

In offline ART a single adaptive treatment plan is generated using various repeated CT and/or CBCT scans [9]. However, adaptive radiotherapy can also be implemented on-line [8], modifying the plan daily according to imaging information. Online ART can in practice mean choosing the daily treatment plan from a library of pre-planned treatment plans based on CBCT imaging [9]. Adaptive radiotherapy is a solution for targets with organ motion being a significant source of error, such as the urinary bladder. Adaptive radiotherapy of the bladder is discussed later in this text. One remaining improvement would be online re-planning using volumetric imaging data [2]. In re-optimization of the treatment, the same problem as with also other online corrections is encountered, namely time pressure, which at present makes the re-planning mostly infeasible in clinical practice [2].

2.1.5 Margin recipies – accounting for errors

There are different approaches available for growing the PTV based on the GTV. In this chapter, the basic concepts of PTV formation are briefly addressed and the margin recipe of Van Herk et al [21], which was used to form the margin for lymph nodes in this study, is explained.

Most of the sources for systematic error can be assumed to be normally distributed and independent of each other and thus can be combined in quadrature to produce the combined systematic error $\mathbf{\Sigma}$ [15; 31]. Here the standard deviations of the systematic error component i will be denoted by $\mathbf{\Sigma}_i$.

Treatment delivery error components are also assumed to be normally distributed and independent. Treatment delivery errors generally take a different value at each treatment fraction and thereby have a Gaussian nature [15]. Thus, they also can be added in quadrature to form the total random error [31]. Also the delineation error is assumed to be Gaussian because of the lack of a more realistic model [15]. Treatment delivery error arises from random variation in organ position and movement (except

those induced by breathing, which will be discussed later) and patient set-up error [31]. The standard deviations of these random error components are denoted by $\boldsymbol{\sigma}_i$ and quadrature addition of these components gives the combined standard deviation $\boldsymbol{\sigma}$.

Van Herk and co-workers established a margin recipe to account for systematic (treatment preparation) errors and random (treatment delivery) errors separately. They mathematically modelled the blurring of the dose distribution as a consequence of the random errors as a convolution. In their work, they proposed a way to calculate the margin needed to compensate both for the random errors and for the systematic errors that generally cause a shift in the dose distribution. They calculated the probability that the cumulative dose to the CTV exceeds a given value for a population of patients and plotted the result as a dose–population histogram. Van Herk and co-workers also modeled the CTV with the presence of systematic errors as an extended CTV. Then, by reversing the procedure for computing dose–population histograms for this extended CTV, they established a way to derive treatment margins.[21]

The first step is to define an objective for the treatment. This means that a threshold dose parameter is defined for a specified probability level, i.e. a fraction of patients. This kind of an objective could be for example that the minimum dose to the CTV must be at least 95% of the prescribed dose for 90% of the patient population. [21]

The second step is to choose the volume C (for example an ellipsoid) representing the distribution of the preparation (systematic) errors so that 90% of the systematic errors fall into this ellipsoid. An ellipsoid with a vector radius of $\alpha\boldsymbol{\Sigma}$ is chosen. Here $\boldsymbol{\Sigma}$ is the combined standard deviation of the treatment preparation errors and it is a vector because the standard deviations may be different in different directions x, y and z. This volume C is a geometrical concept with which it is possible to construct the margin to be added to CTV to take the systematic variation into account. This volume, named extended CTV by Van Herk and colleagues [21] is called the systematic target volume (STV) in this text.

The next step is to ensure that even with random delivery errors the set dose threshold is fulfilled. Without treatment delivery errors, the chosen isodose surface D_{planned} (e.g. 95%) must be aligned with the STV. The extra margin to account for treatment delivery errors is the distance between the planned and actual 95% isodose surfaces D_{planned} and D_{blurred}, respectively. This distance can be calculated by using the 50% isodose surface, which does not change in position as a result of blurring, as a reference [21]. The distance can then be expressed as $\beta\boldsymbol{\sigma} - \beta\sigma_{\text{p}}$, where $\beta\boldsymbol{\sigma}$ is the distance between the 95% and 50% isodose surfaces of D_{blurred}, and $\beta\sigma_{\text{p}}$ is the distance between the 95% and 50% isodose surfaces of D_{planned}. σ_{p} is the standard deviation describing the width of the penumbra and $\boldsymbol{\sigma}$ is the total standard deviation of all treatment delivery variations including the penumbra. [21]

The total PTV margin

$$\mathbf{m}_{\text{PTV}} = \alpha\boldsymbol{\Sigma} + \beta\boldsymbol{\sigma} - \beta\sigma_{\text{p}}, \tag{2}$$

where $\mathbf{m}_{\text{PTV}}$, $\boldsymbol{\Sigma}$ and $\boldsymbol{\sigma}$ are vectors, which allows the usage of this equation to cal-

culate non-isotropic margins. In this formula, the specific value for α for 90% confidence in 3D is 2.5 [21]. This comes from the standard deviation of the 3D Gaussian distribution. The numerical value of β is different for each beam configuration in a treatment plan [32]. There are sources of error, which are recommended to be added to the total margin linearly and not by quadratic addition. These errors still need to be added to this formula. The PTV margin now becomes

$$\mathbf{m}_{\mathrm{PTV}} = 2.5\boldsymbol{\Sigma} + a + \mathbf{b} + \beta\left(\boldsymbol{\sigma} - \sigma_{\mathrm{p}}\right), \tag{3}$$

where a is the treatment planning system beam algorithm error and $\mathbf{b}$ is the breathing positional error. The probability distribution for the position of a target moving under the influence of breathing is not a Gaussian distribution [15]. The target spends most of the time around either of the two extreme positions, the inhalation and exhalation points and hence the probability distribution of the target has two peaks rising asymptotically at these extremes [32]. Any margin less than $\mathbf{b}$ will lead to target underdosage. The most practical approach to take the breathing-induced uncertainty of the target position into account is linear combination so that a margin of width $\mathbf{b}$ is added to both directions [15].

If the total error for each treatment fraction can be measured, one can calculate the total systematic error standard deviation $\boldsymbol{\Sigma}$ and the total random error standard deviation $\boldsymbol{\sigma}$. It is possible to estimate for example the effect of image guidance because the initial patient set-up to the skin markers is the same with and without image guidance. In this specific application, the amount of error is quantified by measuring the translations made in order to correct the errors in the initial set-up [16].

Table 1: Estimating the SD of random and systematic errors based on measurements in a population of patients. The numbers in this table could be the shifts of the patient (mm) in the left–right direction determined by comparing portal images taken before treatment to the DDRs reconstructed based on the planning CT. For each patient, the mean and SD of measurements of several fractions is determined. An estimate of the errors for a population of patients is calculated by different combinations of these values. Table modified from Ref. 16.

	Patient 1	Patient 2	Patient 3	Patient 4	
Day 1	2	4	1	3	
Day 2	1	–2	–1	–3	
Day 3	1	2	2	–2	
Day 4	1	0	2	1	
					Mean = $\mathbf{M}$ = 0.75
Mean	1.25	1	1	–0.25	SD = $\boldsymbol{\Sigma}$ = 0.68
SD	0.50	2.58	1.41	2.75	RMS = $\boldsymbol{\sigma}$ = 2.03

Van Herk et al. [16] describe the way to calculate the magnitude of the systematic and random errors (Table 1). By averaging all the mean shifts for the individual

patients, one obtains overall mean $\mathbf{M}$, which is the group systematic error. This error is expected to be small and the small deviations from zero are due to the imprecision of in the equipment (lasers) and procedure. By calculating the standard deviation of the individual means, one gets $\mathbf{\Sigma}$, an estimator of the systematic error standard deviation. The individual standard deviations give the standard deviation of the random error for each individual patient. The random error standard deviation $\boldsymbol{\sigma}$ is the group mean of the individual standard deviations, determined by calculating their root mean square. [16]

The photon penumbra width parameter σ_{p} can be measured by division of the distance between the 10% and 90% isodose level of a single beam at a typical treatment depth by 2.56 [15]. The penumbra dose is assumed to be described by the error function [15].

2.2 Accuracy of radiotherapy in treatment preparation – systematic errors

There are both geometric and dosimetric error sources in the treatment preparation as well as treatment delivery. In the next sections the whole radiation therapy treatment preparation process is briefly described, with special emphasis on the possible sources of error during each phase. Accuracy in the treatment preparation is essential, since the errors originating in treatment preparation are systematic and hence have a great effect.

2.2.1 Treatment simulation

Generally, the error sources in the treatment simulation emerge from three sources: the patient set-up, the geometric imaging error and the image quality. The patient set-up during the treatment is based on marks on the skin that are tattooed during the treatment planning CT session. Therefore, the motion of the skin with respect to the internal anatomy limits the set-up accuracy [15; 16; 20]. Skin mobility during treatment delivery causes an error, but this error varies randomly from day to day. Rather than in a position representative for the situation in treatment, the skin might be in an extreme position during the CT simulation, which causes systematic error during the treatment. The reproducibility of the patient positioning can be improved by immobilization methods, but because of the skin mobility, the set-up accuracy is never perfect [16].

The geometric imaging error in the CT includes the geometric uncertainties in the imaging room such as the alignment of the lasers and the indication of the couch position [15]. There is also uncertainty in the placing of the tattoos marking the location of the isocentre. These marks can be erroneous if the patient has moved between the time points of imaging and tattooing. This is especially detrimental if the body outline is rapidly changing at the place of the isocentre, e.g. the lateral location at the patient's cheek. Since the tattooing is done by hand, it is naturally not completely certain whether the markings exactly hit the locations of the positioning laser projections on the skin.

Computerized tomography is based on producing a 3D image set based on multiple two-dimensional projections aqcuired from different directions. The subject is scanned being divided to thin axial slices and each slice is divided into a matrix of 3-dimensional rectangular boxes called voxels [33]. The image is reconstructed by determining how much attenuation of the narrow x-ray beam occurs in each voxel of the reconstruction matrix and the attenuation values are represented as gray levels. At present, an iterative reconstruction algorithm is mostly used to solve the inverse problem of reconstructing the geometry of the slice based on the projections from different angles [34].

CT image quality is a potential source of errors. CT image quality is described in terms of contrast, spatial resolution, image noise and artifacts [35]. With CT it is possible to visualize structures with low contrast and discriminate with different tissues with similar densities [35]. If a poor quality CT scan leads to misinterpretation of the GTV, the error has an effect on the treatment plan and finally to the treatment and thereby can have a great effect on the outcome. In addition to the delineation, the image is used in the dose calculation. An artifact is any systematic discrepancy between the CT numbers in the reconstructed image and the real attenuation coefficients of the object [36]. In the case that this kind of discrepancies exists in the image, the image quality has the potential to affect the dose calculation.

Organ motion causes error both during treatment simulation and treatment. CT image represents just one arbitrary position that the moving organ had at the time of the imaging and systematically affects the dose distribution [12; 16; 20; 21]. Organ motion can also have an effect on the image quality.

2.2.2 Accuracy in radiation production

In this chapter the radiation production and the associated geometric errors are described. The dosimetric errors are reviewed in the chapter about treatment planning. The errors in the linear accelerator geometry are likely to remain relatively stable over the course of the treatment and thus result in a systematic error [15].

The linear accelerator is a device that accelerates electrons along a linear tract with the radio frequency (RF) power produced by a magnetron or a klystron. The electrons are boiled out of a hot cathode and accelerated to energy of up to 25 MeV. When producing photons, these electrons are made to hit a tungsten target where a portion of their energy transforms into bremsstrahlung, that is, photons. When producing electrons, the target is moved out of the way, letting the electrons pass (Figure 5). More detailed description of the electron acceleration and beam production is available in [13].

Both photon and electron beam shaping into a useful treatment beam happens in the radiation head of the linear accelerator. The beam characteristics are strongly influenced by the treatment head design [13]. There are a number of beam-shaping, localizing and monitoring devices in the radiation head. These include the bending magnet if used, the fixed primary collimator, the x-ray target, flattening filter, scattering foils for electron treatments, moveable secondary collimator jaws and the multileaf collimator. The primary collimator collimates the beam that then goes

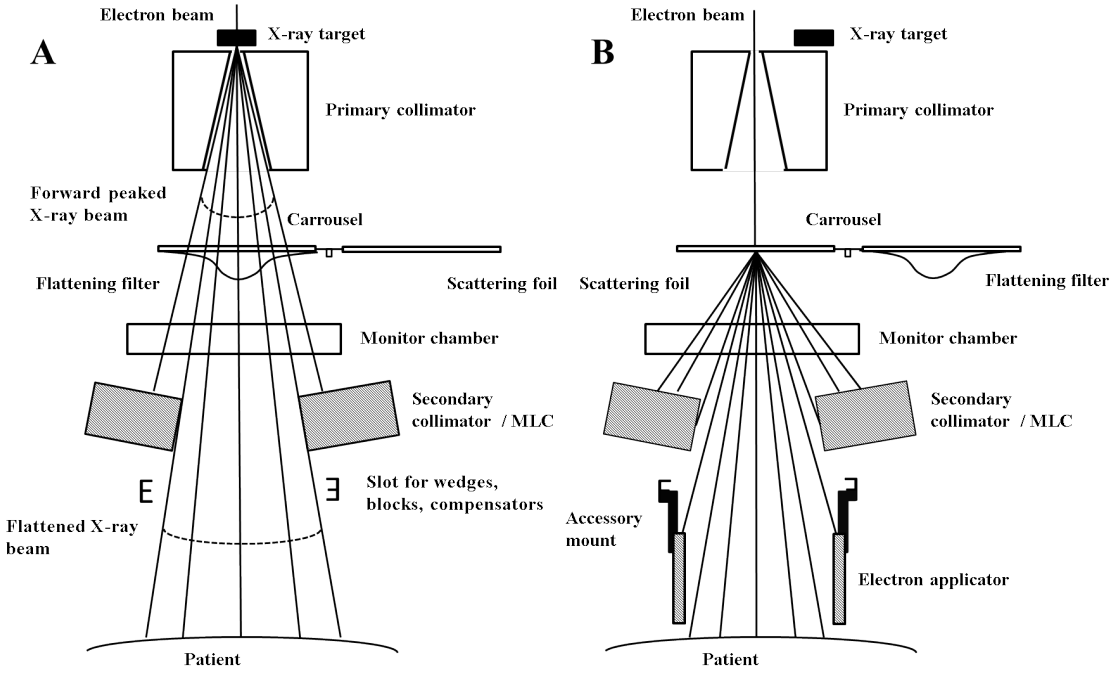

Figure 5: Schematic drawing of a linear accelerator treatment head. (A) Photon beam therapy. The X-ray target has been moved on the way of the beam and the carrousel is in a position where the beam goes through the flattening filter. The beam is formed with the secondary collimators and the multi-leaf collimator (MLC). (B) Electron beam therapy. The X-ray target has been moved out of the way of the beam and the carrousel is in a position where the beam goes through the scattering foil. The field is formed close to the patient with a block attached to the electron applicator. Figure modified from Ref. 13.

through the flattening filter or scattering foil (photon and electron treatments, respectively. The secondary collimator and the multileaf collimator perform the final beam shaping in photon treatments and in electron treatments, the beam shaping is done close to the patient with specially designed electron blocks. In the following, the different beam shaping procedures in the treatment head are reviewed with special emphasis on accuracy and error sources.

Magnets are used for focusing and tuning the electron beam as well as changing its direction in the case that the electron accelerator guide is not in line with the gantry. The accelerated electron beam is composed of electrons which all have different energies, are displaced radially and have their trajectories in different angles from the mean. The changes in mean energy, trajectory angle or displacements from the mean axis cause distortions in flatness of the electron beams.

If electrons are used, the beam is evened and spread to the required width with scattering foils. The photon beam needs to be flattened with a flattening filter in order to get an even beam to the patient. The braking radiation beam from the target has fluence, energy and angular distributions. The flattening filter effect depends on the distance and the shape of the filter is chosen so that an even dose is achieved at about 10 cm depth [13]. Angular or lateral displacements of the beam have an effect on the flattening result and it is thereby essential that the beam remains rigidly centred on the axis of the flattening filter.

There are two separate questions to be asked in estimating error in isocentre location. Firstly, one should find out if the radiation field isocentre of the treatment machine really is where it is thought to be. The place of the isocentre is affected by the mechanical properties of the treatment machine. The second question is whether the patient positioning laser indication shows this same precise isocentre.

The couch mechanical properties can cause geometric error, couch sagging [17]. It means that the couch position and angle somehow depend on the weight that is placed on the couch, i.e. the couch is not truly rigid but bends, producing distortions to the patient's body outline and to the position of the organs relative to the bones. Couch sag can be corrected for by imaging and with current treatment couches it is a problem mostly with heavy patients. There can be also gantry sagging, which must also be accounted for in the treatment planning.

The tolerance for each of the linear accelerator geometry error components mentioned above is defined by the national regulations and the clinic specific protocols. The mechanical properties of the linear accelerator are monitored regularly. The position indicators such as the lasers, light fields and the optical distance indicator are tested every day [37]. In Helsinki University Central Hospital, the field size is tested every month and the isocentre position is checked every 6 months. The gantry and collimator angle indication and the straightness and movements of the couch are checked by technicians every 4 months and by the physicists every 6 months [37].

The amount and quality of the produced radiation is monitored with an ionization chamber sampling the treatment beam. The units of the monitor chamber for the amount of radiation, the monitor units, are used in the treatment planning process to describe the actual dose to be given to the patient. The number of mon-

itor units needed to be produced in order to achieve a dose of one gray needs to be measured for each linear accelerator and each photon and electron energy. The properties of the produced beam are measured and used for the configuration of the machine to the treatment planning system and thus also need to be monitored regularly. In Helsinki University Central Hospital, the relative dose is measured 2 times a week. The field characteristics are measured more profoundly at least every 6 months and always when there is reason to suspect that they have changed [37]. The absolute dose produced with the accelerator may have a maximum ±2% deviation from the value that has been configured to the treatment planning system for the dose calculations [37]. The dosimetric errors are addressed in the chapter about treatment planning.

2.2.3 Target definition

Delineation of the GTV involves numerous geometric uncertainties and can be the greatest single source of geometric uncertainty in the treatment process [15]. Delineation errors are systematic for each individual patient, but have a stochastic nature over the whole population and thus cannot be estimated in advance for a single patient [20; 21]. The limited resolution of the imaging modalities causes uncertainty to the target definition. Different observers have been found to delineate the same volume differently (interobserver variability) and even the same observer never delineates the same volume exactly the same way when asked to repeat the delineation (intraobserver variability) [38; 39]. Even the imaging modality used has an effect [40]. It is hard to quantify the actual delineation error as there is no absolute truth available [15]. The differences between the institution guidelines according to the target volume formation have a significant effect on the result [19].

CTV to PTV margins needed to account for the uncertainties in patient positioning and movement, as well as alignment of the therapeutic beams, might depend on the irradiation technique selected [41; 42]. The more complex the field set-up, the steeper the dose gradients and thus, the more sensitive the plan is to set-up uncertainties [42].

2.2.4 Treatment planning and dose calculation

Treatment planning system error consists of three different components. The first is the possible error in the exact orientation of the image when the CT image set is transferred to the treatment planning system. The second component producing uncertainty is the automatic algorithm for forming the PTV by adding margins to the CTV. The third TPS error component is the error in drawing templates used for positioning and producing shield blocks for electron treatments. Another error of the treatment planning system, the photon beam algorithm error is present when the planned penumbra is too wide or too narrow compared to that of the measured dose distribution. This error causing either systematic underdosage or overdosage at the field border can be compensated for by the parameter a in Equation (3). [15]

Always when a new linear accelerator is acquired to the hospital, its individual MU–dose correspondence information is measured. This information is used to

configure a model, i.e. a quantitative machine [43]. In the treatment planning, the amount of monitor units needed to produce a specific dose distribution can then be calculated using this virtual treatment machine. Follow-up measurements need to be done periodically and if there are deviations from the original values, the model needs to be reconfigured [43]. The error due to machine configuration remains systematic for all patients.

Every model is a simplification and thus, the dose produced is not exactly the dose planned. According to the Finnish Radiation and Nuclear Safety Authority (Säteilyturvakeskus, STUK), there can be maximum 3% deviation in the reference point dose and 5% / 5 mm in target volume dose between the calculated and measured dose [44]. These are maximum deviations, but the aim is to maximize the accuracy.

2.3 Precision of radiotherapy in treatment delivery – random errors

The treatment delivery phase covers the whole treatment after the treatment preparation phase, essentially the patient set-up and radiotherapy on each treatment fraction. As mentioned previously, the random errors occurring in the treatment delivery impact the treatment differently each time and have a blurring effect on the dose distribution. In the next chapters the error sources inherent to the treatment delivery are discussed.

2.3.1 Positional imprecisions in treatment delivery

Treatment delivery is trying to mimic every aspect of the CT simulation situation as well as possible. The patient set-up should be reproduced as precisely as possible on each fraction of the treatment. The extent of gantry and table flexibility should be measured and compared between the CT and the treatment machine [15] and standardized if possible. Standardization is important also in the case of laser light systems, where variations in thickness of laser lights can cause significant uncertainty [15]. The immobilization devices used for the set-up should be checked regularly in order to maintain the geometric accuracy throughout the treatment [15].

In addition to deviations in these external factors, also changes in patient's clinical variables such as the bladder filling or weight can cause imprecision and should be evaluated [15]. Organ motion is an important source of uncertainty, in the case of the bladder even the main source of error [6; 20; 45–47]. The motion of the bladder will be discussed in more detail later in this text.

Organ motion can be divided into three categories: motion of the organs related to patient position changes, organ motion which occurs in-between fractions (interfraction), and motion that occurs during fractions (intrafraction) [12]. Position-related organ motion arises if the patient position during planning scan is different than during treatment [12].

Interfraction organ motion occurs when the position of the CTV changes from day to day. It is mainly associated with organs that are part of or close to the

digestive system, but can also be caused by changes in the condition of the patient, such as weight loss or gain [12]. Intrafraction motion is organ motion that occurs during the radiation fraction of the patient. In the case of the bladder, intrafraction motion causing geometric uncertainty arises from bladder and rectum filling and bowel gas movement. An additional source of uncertainty arises from intrafraction motion in the case that the radiation field includes a part of the intestinal system, where the realized dose can be influenced by the motion.

Organ motion can be tried to be restricted by using different protocols which aim to achieve a reproducible situation for the organ. If this is not enough to solve the problem, there are techniques such as gated RT, breath-hold techniques and tumour tracking than are used to sync the irradiation according to the motion [12]. When none of these techniques are available and also to compensate for the remaining positional uncertainty, the extent of the motion must be determined and margins can then be set to account for the organ motion.

2.3.2 CBCT image quality

Cone-beam computed tomography is an imaging method with which one can have 3-dimensional images of the patient at the time of the treatment. The equipment used for CBCT consists of an x-ray tube mounted on a retractable arm and an x-ray detector mounted opposite the tube and can be integrated with a medical linear accelerator. Cone-beam CT operates on the same principle as conventional fan-beam CT, except for that an entire volumetric image is acquired through a single rotation of the source and detector. This is possible, because a 2D-detector is used as opposed to the 1D-detectors used in conventional CT [48].

In the pelvic area, soft-tissue motion and deformation including gas pocket movement in the rectum occur regularly and result in severe imaging artifacts that may make the identification of soft-tissue boundaries extremely difficult [49]. These artifacts are even more severe than in conventional CT [50]. This is explained by the time needed for the imaging with each method. In conventional CT, each rotation of the scan can be completed within 1 second or less and organ and tumour motion is relatively small during this time. In a CBCT scan, however, the rotation speed of the gantry restrains the speed of the scanning and the acquisition of a full 360 degrees projection scan typically lasts for 1 min [50].

The treatment can be endangered by insufficient image quality of the treatment image guidance if the images are misinterpreted and for example a wrong translation is made causing treatment volume miss. It is possible to use different body restraints and breath-hold protocols to restrict the motion [50]. Smitsmans and co-workers introduced a dietary protocol to reduce the amount of moving gas and had a significant effect on the achieved CBCT image quality [51]. Motion of bowel gas during CBCT acquisition has been described to be particularly detrimental for image quality [49]. The CBCT image quality can be thought to indirectly indicate intrafraction (short term) and interfraction motion of tissues [51].

2.4 Radiotherapy of the urinary bladder

The bladder cancer is in Finland the most common cancer of the urinary tract and the fourth most common cancer type in males [52]. There are multiple different types of bladder cancer, the majority of which are restricted to the inner surface of the bladder and have a good prognosis [52]. These patients are mostly treated with bladder-sparing approaches such as transurethral resection. Roughly 25% of the bladder cancers has infiltrated to the muscular wall of the bladder when diagnosized and about 5–10% of these patients also have a metastasized cancer [52]. The patients with muscle-invasive bladder cancer are treated with radical surgery or radiotherapy, but the optimal choice of therapy is a topic of debate [45; 53]. Even with treatment, roughly half of the patients suffering from muscle invasive bladder cancer die in 5 years [52]. This text will concentrate on the treatment of muscle invasive bladder cancer.

The treatment of the muscle invasive bladder cancer varies based on how widely spread the disease is and the overall condition of the patient [52]. The primary method for treatment of muscle invasive bladder cancer has traditionally been radical cystectomy where the whole organ is surgically removed [45; 54]. Contraindications for cystectomy are usual among the high-aged patient population [45] and the possibility to remain bladder function has evoked interest to the bladder preserving treatment methods. Combined with other treatment modalities as the principal component of local treatment, radiotherapy has the potential for being an organ-preserving alternative [45; 55]. Muren et al. [45] and Milosevic et al. [56] provide a review of these combined-modality studies.

2.4.1 The challenges in the treatment

The bladder base is anchored at the level of the pelvic floor, but several surrounding structures affect its size and shape [57]. These structures include the anterior abdominal wall, small bowel, prostate, rectum and uterus. Also the degree of filling of the bladder itself affects the bladder shape and size [58] and it can even be the dominant source of bladder motion [47].

Several studies have found the bladder motion to be the most significant at the cranial and posterior part of the urinary bladder [20; 59; 60]. Meijer et al. believed the reason to be that in these areas the bladder can move freely without obstruction with the rectum and the sigmoid [20]. Meijer and co-workers observed the smallest variation in the ventral–caudal side of the bladder, where the bladder abuts on the symphysis [20].

McBain et al studied maximal bladder wall displacements in bladder cancer patients with cine-MRI and found them to be larger (median 27 mm, range 6–58 mm) and more variable in direction than those of the healthy controls (median 5.5 mm, range 0–7 mm) [47]. The tumour might change the normal physiological stretch pattern of the bladder [61]. McBain and colleagues suggested that there might be a tendency for bladder expansion occurring away from the tumour-bearing wall [47]. Muren et al. studied bladder motion during RT by means of weekly CT scans [6]. Patients were instructed to void before the treatment / repeat scanning

sessions. Bladder displacements as large as 29–36 mm were observed at the superior, left, anterior and posterior side of the bladder and the bladder displacements were in general largest at these four sides [6]. To give an example of the scale of bladder displacements possible during RT, Table 2 taken from Muren and colleagues' study is presented here.

Table 2: Summary of urinary bladder displacements observed in repeat CT scans. Table modified from Ref. 6.

	Inferior	Superior	Left	Right	Anterior	Posterior
Overall maximum (mm)	15	32	31	15	36	29
No. of scans with displacements $\leq$ 10 mm	6	29	14	5	24	16
No. of patients with at least one scan with displacements $\leq$ 10 mm	5	9	7	3	8	8
No. of scans with displacements $\leq$ 15 mm	0	12	4	0	12	2
No. of patients with at least one scan with displacements $\leq$ 15 mm	0	5	2	0	4	2
No. of scans scan with displacements $\leq$ 20 mm	0	7	4	0	6	1
No. of patients with at least one scan with displacements $\leq$ 20 mm	0	4	2	0	3	1

There are several technical challenges in accurate RT delivery to the bladder tumour [3; 4]. The bladder is a hollow, mobile organ whose position and volume vary significantly between different treatment sessions [3; 12; 45; 47; 57; 62; 63]. There is also a variable but continuous flow of urine into the bladder [45] which can cause intra-fraction motion. Tuomikoski et al. reported the observed maximal growth in the bladder dimensions during 15 minutes to be less than 10 mm in all orthogonal directions [61]. It is likely that the bladder shape in the planning CT scan differs from that during the course of the treatment resulting in a significant systematic error [62; 64].

An interesting question is whether the bladder movement, posing a challenge to bladder RT, could be controlled for or restricted. Several strategies to restrict the individual variations in bladder volume have been studied [4; 5; 46; 58; 65]. These strategies aim at making the situation of the bladder in the treatment as reproducible and controlled as possible, achieving a more successful treatment and possibly being able to use smaller margins. These strategies include for example different voiding or dietary protocols but also more invasive methods to restrict the bladder movement. The strategies for restricting the bladder volume variability are reviewed in this chapter.

Fluid intake restriction protocols have been suggested to control the intra-fraction volume change [46]. Muren et al. attempted to control the bladder volume by re-

stricting fluid intake prior to the treatment [65]. They reported that this fluid intake protocol failed to give any reduction in the margins required for the treatment [65].

Void protocols have also been suggested. Treating the bladder while empty minimizes the radiation field size. Further rationale for instructing the patient to void before treatment is to be able to reproduce the bladder volume as well as possible during the course of the treatment [46]. The empty bladder also increases patient comfort [46], which helps in maintaining the treatment position during the whole treatment fraction.

Instructing the patient to void might not be a magical solution. Although patients were asked to empty their bladder, significant variations in volume, up to 20–25%, remain [4; 5]. Bladder cancer patients have different degrees of bladder wall invasion that may impair the contraction and emptying of the bladder [4]. The tumour can significantly affect the ability to consistently empty the bladder. The bladder wall fixation due to the tumour may also affect the filling and emptying patterns of the bladder [4]. Bladder cancer typically occurs in the elderly, whose bladder function may be deteriorated [66–68].

One option would be to control the fluid volume in the bladder by using a Foley catheter [4]. This way it would be possible to insert an identical fluid volume to the bladder for RT planning and before each RT fraction. There are, however, multiple drawbacks such as bladder trauma, patient discomfort and possible bladder infections [4].

To stabilize the bladder volume and the shape of the bladder, Miralbell et al tested a urinary catheter balloon [58]. The procedure was unpleasant and produced painful bladder spasms in all of the eight patients [58]. Even with this procedure, bladder reproducibility accuracy was not perfect [58].

Especially in partial bladder irradiation, the image quality is a restricting issue [61]. Without adequate imaging information, one might risk missing the target [61]. Bladder visualization can be aided with different kinds of markers, such fiducial markers as well as different radio-opaque contrast media. With these markers it is possible to track the bladder movement [4]. The efficacy of the tracking depends on the ability of the markers to reliably and correctly represent the target volume position and whether they remain visible during the whole course of the treatment [69].

Soft-tissue visualization ability of the imaging method affects how well the changes in bladder shape and volume can be taken into account. Especially in partial bladder irradiation, tumour delineation in the CT image is problematic since the bladder tumour has often been resected before the RT treatment or the patient has received neoadjuvant chemotherapy and the visibility of the remaining scar tissue in CT is poor [54; 61; 70]. A CT scan might underestimate the mucosal borders of the tumour or overestimate them in the case that there is oedema following transurethral resection of the tumour [71]. As the markers are implanted in cystoscopy, they would allow marking the tumour borders and also aid the image registration process [61]. Without contrast agents, the tumour cannot be reliably detected in CBCT images [61]. On the other hand cystoscopy cannot show spread beyond the submucosa [4; 71].

Fiducial markers, such as titanium or gold seeds implanted in the mucosa of the bladder have been investigated [3; 24; 71]. Fiducial markers do not increase bladder toxicity due to standard cystoscopy [24] and are also voided without symptoms [3; 71]. Nevertheless, the procedure is invasive and associated with risks of bleeding, infection and bladder perforation [4]. Certain lesions may not be accessible with marker seeds [4]. It is also uncertain how many seeds are needed to accurately account for bladder wall movement [4]. As the implantation is based on cystoscopy, microscopic lesions cannot be visualized at all [4]. The accuracy of the procedure naturally relies on the physicians' skill [4]. In the case of the bladder, seed dropout is a possible drawback [71].

In addition to the fiducial markers, also radio-opaque contrast media have been suggested for radiotherapy of the bladder. Lipiodol® is a poppyseed oil that can act as a contrast agent [61]. Small drops of Lipiodol® are injected into the bladder wall through a flexible cystoscope during cystoscopy to mark the borders of tumour [61]. Several groups have reported using Lipiodol® for marking the target volume [25; 61; 69].

2.4.2 Conventional radiotherapy

The standard method for radiotherapy for muscle invading bladder cancer has traditionally been irradiation of the whole bladder and tumour with a 2–3-cm margin to a dose of 60–66 Gy [53; 62]. The set-up precision is verified with imaging, but since the soft tissues are poorly visualized with two-dimensional planar imaging, one cannot see the exact position or size of the bladder. Bladder movement cannot be controlled by external fixation devices used in the set-up and thus, no matter how well the bony anatomy agrees with the planning position, large margins have to be used in order to take the bladder movements into account. The clinical target volume is the whole bladder and visible tumour with large isotropic margins creating the planning target volume [46].

The total dose in the conventional radiotherapy treatment of the bladder is relatively low compared with doses used in other cancers such as prostate cancer, lung cancer and head and neck cancers [7]. As there is evidence of a dose–response relationship [7; 72], i.e. the higher the dose the better the outcome, dose escalation has been suggested to be a reasonable strategy to improve the radiotherapy of invasive bladder cancer [7]. Reduction of the margin could allow an escalation of the dose, but usage of an inadequate margin could lead to a large dose deviation inside the treatment target due to positional variation in the treatment process.

There are two key problems in the traditional approach [47]. The first is that the irradiated volume includes a large volume of normal tissue, especially the bladder itself and the small bowel [54]. The large irradiated normal tissue volume leads to high normal tissue toxicity and inhibits dose escalation [47; 54]. Radical radiotherapy of the bladder can cause serious side effects [20], both acute and long-term [59; 73]. These complications include bladder function decrease, cystitis, diarrhea, obstruction or constriction, fistula or perforation and ulceration, and can lead to undesired treatment interruptions [54; 59; 74]. Some complications may also require

surgery or even lead to the patient's death [59]. The second problem is that the approach may still be inadequate to account for bladder motion in up to 65% of the patients [62; 63].

More conformal irradiation techniques are based on the thought that the focusing the dose distribution to the target will be beneficial in two alternative ways. More focused radiation distribution is either less damaging to the normal tissue if maintaining the same prescription dose or improved local control may be obtained with equivalent normal tissue side effects if the prescription dose is increased [7; 71; 72]. Increasing the treatment dose and concomitant chemotherapy might be options to improve local control in the case of the bladder cancer [7; 71], provided that the normal tissue irradiation can be reduced. The increase in normal tissue sparing might also enable evolution of hyperfractionated treatment protocols that would be suitable for those patients who are not able to tolerate conventional treatment schedule lasting 6.5 weeks [9].

By conformal radiation therapy one implies to techniques in which the border of a certain reference isodose surface, e.g. 95% is matched to conform closely to the surface of the target volume [72]. Higher conformity of the dose requires imaging of the soft-tissue target, which is only possible with 3D imaging methods.

3-dimensional imaging at the time of the treatment allows visualization of the bladder. The information of the position and size of the bladder helps to eliminate the possibility for misses in the treatment, as one can account for the possible misalignment of the beams by making some correcting translations before the treatment. If the bladder is too big to fit into the treatment volume, the patient can be asked to void their bladder. Thus, ability to 3D-visualization adds to the probability of successful treatment and the reduction of set-up margins helps reduce the volume treated to a high dose [65; 75; 76]. Nevertheless, without being able to modify the treatment volume based on the imaging, large internal margins are still needed when treating the mobile bladder [6].

The 3D-imaging, however, offers much greater potential than merely repositioning the patient and avoidance of misses. If one has the ability to adapt the size of the treatment volume to the bladder size, one can reduce the irradiated volume thus avoiding the resulting unnecessary complications. Reduction of the irradiated volume might make dose escalation possible. This can be achieved with adaptive radiation therapy. In 2004, Muren et al. estimated the bladder to be one of the sites with the greatest potential benefit from equipment that is designed for localization of the tumour daily before the treatment [45]. Adaptive radiation therapy of the bladder has been one of the greatest improvements enabled by improved target localization. The assessment of Muren and colleagues could be judged to have been right. The next chapter reviews adaptive radiation therapy studies and the benefits achieved with adaptive treatment.

2.4.3 Adaptive radiotherapy

Adaptive radiotherapy (ART) treatment was first suggested by Yan [8]. The idea was to adapt the margin and the treatment dose individually for each individual patient

instead of using population-based margins and treatment doses. In the article of Yan, the adaptive prostate cancer treatment serves as an example of the application of the process [8]. Yan suggests defining the individual margins and treatment doses based on information gathered with electronic portal imaging and CT scans during the first a few fractions. This technique to create a single adaptive treatment plan for the rest of the treatment based on the imaging information acquired during the first fractions is called offline adaptive radiotherapy [9]. However, Yan also pinpoints that this process can be repeated if necessary during the entire treatment course, suggesting also the possibility of daily online adaptation. In online ART, the target volume is adapted before the treatment to represent the situation of the particular day, based on the imaging information of the treatment machine.

One way to implement online ART is that a library of pre-planned treatment plans is first created and the daily treatment plan is then selected from this library [9]. The ways to form this library and the ideas behind the methods differ. Since there are only a limited number of studies about bladder ART, the most essential studies of adaptive bladder radiotherapy, both offline and online, are reviewed in the following. It is easy to summarize the results of the studies: With ART it is possible to achieve improved CTV coverage [7; 40; 77] and / or reduction in the normal tissue (especially small bowel) irradiation [7; 9; 10; 61; 78–81]. Also the dose conformity can be higher with ART [40; 70].

The different ART protocols used are described in the text and the results as well as some elementary information of the studies are described in Table 3. As well as reviewing different adaptive radiation therapy protocols that have been suggested, the pros and cons in these methods are quickly reviewed and the different ideas behind the methods are compared. It can easily be seen that no ultimately superior method for adaptive radiation therapy has been invented yet, but all the suggested methods have their justifications as well as their downsides.

Offline adaptive radiotherapy is relatively simple to implement but it does not correct for random errors. Offline adaptive radiotherapy strategies have been used for both partial bladder irradiation and whole bladder irradiation [7; 40]. In offline ART, there is adaptation to the individual scale of bladder movements but not to the individual days' positional situation of the bladder.

Pos et al. evaluated the feasibility of offline adaptive radiotherapy with a partial bladder treatment [7]. They treated the bladder tumour plus a 2-cm margin and acquired five daily CT scans immediately before or after treatment. Based on the tumour volumes visible in these images, Pos and colleagues constructed a volume that encompassed all the GTVs visible in these scans, $\mathrm{PTV_{ART}}$ was constructed by expanding this $\mathrm{GTV_{ART}}$ with a 1-cm margin. Starting from the first week, the patients were treated to this $\mathrm{PTV_{ART}}$.

Foroudi and colleagues evaluated an offline adaptive protocol in practice and modeled an online adaptive protocol to be able to compare the CTV coverage and the dose conformity index between the conventional RT treatment and these optional adaptive methods [40]. In the offline process, five CBCT scans were acquired during the first week of treatment and the average of these volumes was expanded with a 1.5-cm margin to form the offline adaptive PTV. This volume was used for treatment

Table 3: A summary of the bladder adaptive radiotherapy studies and their key results. ART = adaptive radiotherapy, Ref. = Reference, S = Simulation, T = Treatment, WBI = whole bladder irradiation, PBI = partial bladder irradiation, SIB = simultaneously integrated boost.

Study	Ref.	N	S / T	WBI / PBI	Online / Offline	Key results compared to non-adaptive
Burridge et al. 2006	[78]	20	S	WBI	Online	Small (31 ± 23 cm^3) sparing of irradiated bowel volume
Pos et al. 2006	[7]	21	T	PBI	Offline	Better CTV coverage, 40% reduction of treatment volumes
Foroudi et al. 2009	[40]	5	T	WBI	Offline	Improved CTV coverage in 2/5 patients, higher conformity index
			S		Online	Yet better dose coverage than the offline method
Vestergaard et al. 2010	[10]	10	S	WBI	Online	Reduction of volume receiving high dose 33–34%
Foroudi et al. 2011	[79]	27	T	WBI	Online	29% reduction in V(normal tissue receiving ≤ 45 Gy)
Lalondrelle et al. 2011	[77]	15	S	WBI	Online	Fewer target misses
Murthy et al. 2011	[82]	10	T	WBI + SIB	Online	Plan-of-the-day technique feasible for ART
Tuomikoski et al. 2011	[9]	5	T	WBI	Online	On average 66 ± 36 cm^3 reduction in bowel volume receiving ≥ 45 Gy
Meijer et al. 2012	[70]	20	T	WBI + SIB	Online	Conformal dose distribution, Lipiodol® facilitated image guidance
Tuomikoski et al. 2013	[61]	5	T	PBI	Online	V(healthy bladder) receiving high doses smaller when treated with full bladder
Vestergaard et al. 2013	[80]	7	S	WBI	Online	V(tissue receiving $\geq 95\%$ of treatment dose) reduced to $\geq 66\%$ plan selection / 41% re-optimization
Vestergaard et al. 2014	[81]	20	T	WBI	Online	Reduction in PTV volumes, mean volume ratio of course-averaged PTV relative to non-adaptive PTV 0.70

from the third week onwards.

One could simplify that the more adaptive the method is, the more difficult and time-consuming it is to implement. Online adaptive radiotherapy is a step to the more adaptive direction from offline methods and online re-optimization is a further step onwards. However, although re-optimization has been successfully implemented in simulation [80], it is challenging to adapt into the clinical use where there are time constraints.

Burridge et al. were the first to model online adaptive radiotherapy for the bladder cancer [78]. They made conformal treatment plans using a four-field technique and an isotropic CTV–PTV margin of 15 mm. They created two additional target volumes by reducing the superior margin to 10 and 5 mm, which was estimated to represent the magnitude of the changes in bladder dimensions. The online adaptive method of Burridge and colleagues is easy to implement but since the reduction of margin in the superior direction is not based on data of the actual individual patient, there might be limitations to the method as the margins do not offer variability in all directions [78].

In the study of Foroudi et al., the online adaptive method was retrospectively simulated by creating three optional plans based on the first five CBCTs and the planning CT image [40]. The smallest was based on the smallest CTV, the largest on the union of all the CTVs of the images and the medium one on the average CTV volume. These optional volumes were expanded with a 5-mm margin. There were remaining five CBCT scans taken during the treatment for each patient and these were used in the simulation. In a later study, Foroudi and co-workers reported having used the online method for treating 27 patients [79].

Online adaptive radiotherapy requires daily imaging with the treatment machine, which produces some radiation dose to the patient. Kron et al. [83] studied the integral dose to the patient with the adaptive radiation therapy protocol of Foroudi et al. [40]. The group found out that the increase in dose conformity resulted in decreased overall radiation burden despite daily volumetric imaging [83]. Image guidance did not cause an increase to the integral dose.

In the library planning approach, there are many varieties that are based on capturing some of the bladder volume variation to the PTVs, but still employ different ideas. Lalondrelle et al. [77] and Tuomikoski et al. [9] employed an adaptive strategy where the library of adaptive PTVs is formed based on several repeat scans starting with a post-voiding planning CT scan, scanning every 15 minutes, with the attempt to capture the individual bladder filling pattern of the patient. Lalondrelle et al. examined bladder wall motion patterns during high-dose hypofractionated bladder radiotherapy and validated an adaptive planning strategy to prevent geographic miss [77]. The strategy was named adaptive-predictive organ localization (A-POLO). Tuomikoski et al. were able to reduce the dose to the intestinal cavity with their strategy employing 4 post-void CTs [9]. The fractionation schedule was conventional [9]. This method will be discussed in more detail later in this text, since this method is compared to the method introduced by Vestergaard et al. [10] in this study.

The strategies of Lalondrelle et al. [77] and Tuomikoski et al. [9] can be im-

plemented from the first fraction on, and thus, Lalondrelle and co-workers mention that the method be especially suited to hypofractionated radiotherapy in contrast to the methods utilizing the information from the first fractions [77]. In the approaches based on recording the bladder filling pattern, it is crucial to have a right combination of drinking and voiding protocols to be able to capture the maximal filling of the bladder without patient discomfort. In the studies of Lalondrelle and colleagues [77] as well as Tuomikoski and co-workers [9] there were cases where the volume change during the planning repeat CT scans was inadequate to represent all the filling states manifested during treatment.

In the study of Meijer et al [70] this challenge was addressed by first taking a scan with the full bladder and then with an empty bladder and then interpolating and extrapolating the needed alternatives to represent filling. However, it can be argued that it is useful to have a more detailed modeling of geometrical changes in the pelvic area than just two extreme conditions [61]. Also, making the patient go to the toilet between the two scans might induce changes to the geometrical situation in the pelvic area. To get the most descriptive and useful alternative plans when starting with a postvoiding scan, it is useful to the aim to a more effective hydration during the planning CT scans than during the treatment [61]. The time of image acquisition and irradiation during the course of the treatment should not exceed the time between the successive repeat planning scans [61].

In the protocol of Meijer et al., the library planning procedure was integrated with image guidance using Lipiodol® markers [70]. The whole bladder wall was irradiated with a simultaneous boost to the bladder tumour or tumour bed [70]. The GTV was marked with Lipiodol® and two successive planning scans were acquired, one with a full bladder and one with a voided bladder [70]. Six planning target volumes were created by interpolation and extrapolation based on the empty and full bladders [70].

An interesting question is whether to treat with an empty or full bladder. Usually, when the whole bladder is treated, it is beneficial to treat the patient with an empty bladder, to reduce the irradiated volume and to increase patient comfort. However, in partial bladder irradiation or when a simultaneously integrated boost (SIB) is given, it treating with a full bladder might help identify the tumour and to spare the rest of the bladder [82]. In their study, Tuomikoski et al. investigated the sparing of the healthy part of the bladder during partial bladder irradiation with Lipiodol® contrast agent markings around the tumour [61]. They obtained CBCT images every day before treatment, and almost weekly, also a post treatment scan was acquired. They studied the impact of having a full or an empty bladder during treatment to the sparing of the healthy parts of the bladder when treating only a part of the bladder. Treatment with full bladder was found to spare the healthy bladder. The authors used an ellipsoid model to predict the intrafractional changes in the bladder volume, which worked with an acceptable accuracy [61].

In all of the different approaches utilizing the bladder filling pattern, there is a concern whether the pelvic geometrical situation during the planning is representative of the patient anatomy during the treatment. Vestergaard et al. used CBCTs from the first week of treatment [10; 80]. They estimated that this approach is more

likely to capture the individual day-to-day pelvic organ motion patterns of the patient, when creating the library of adaptive plans [80]. It is more likely that there is more variety in rectum filling and bowel loop configurations when images acquired on a larger time scale are used. As mentioned previously, a similar idea was also behind the method of Foroudi et al. [40; 79].

Vestergaard et al. compared three different online adaptive radiotherapy methods, which all were based on forming a library of three plans and selecting the daily PTV of these alternative plans [10]. Method A utilized population-based margins while methods B and C used the bladder as seen in the CBCT scans of the first week. Method B did not require delineation of the bladder but method C did. The authors calculated the total dose distributions based on the planning CT and compared the ratios of the dose–volume histograms relative to the non-adaptive radiotherapy between the methods.

In a later study by Vestergaard and co-workers [80], two adaptive radiotherapy methods were compared. One of the methods was the same as method C in the previous study [10] and was based on forming three alternative planning target volumes based on the planning CT image and the CBCT-images of the first four fractions. The other method took a step further from the methods based on a library of plans and utilized daily re-optimization of the plan based on the CBCT-images in the treatment [80]. Deformable image registration was used to propagate the bladder contour from the planning CT to the CBCT-images. The method C is in routine use in Aarhus and there has been a recent clinical trial showing decreased planning target volume sizes [81]. The method is reviewed later in more detail, since it is compared to the Helsinki method [9] in this study.

Using information acquired during many fractions has also its downsides. If the method includes collecting imaging information during the first fractions, the first fractions have to be treated to the full PTV volume, which adds to the normal tissue dose even if it is lowered by the adaptive protocol. Vestergaard and colleagues suggested a way to overcome this hurdle [80]. If a boost treatment is included, it can be given before the actual treatment to be able to acquire the images without having to use the conventional treatment plan during the first fractions [80]. However, hypofractionated treatment is not possible with this kind of methods [77].

There are also approaches that use margins defined on a population basis [10] or just approximated non-individually [78; 82]. In these methods there is no attempt to track the individual bladder movements of the patient, and they are simple to implement, but require that the scale of movements is correctly estimated.

Murthy et al. studied MVCT-guided plan-of-the-day radiotherapy [82]. The planning CT and treatment were done with a full bladder, since the treatment included a simultaneously integrated boost to the bladder tumour. Patients not suitable for SIB were treated with an empty bladder [82]. The whole bladder was delineated on the planning kVCT scan and 6 adaptive PTVs were grown by adding isotropic margins from 5 mm to 30 mm in 5-mm steps. 6 IMRT plans were created for each patient. The MVCT images taken before treatment were automatically registered to the planning kVCT image by matching the bony anatomy and after that, the smallest possible PTV was selected by manually matching the bladder to

fit inside the PTV volume with a 2–3-mm margin [82].

As well as adaptation of the planning target volume size, there can be adaptation to the position of the bladder or to the position of the tumour. Wright et al. compared three different strategies for correction of the isocentre [76]. The first was no translation of the isocentre, the second was an optimal translation of the isocentre to maximize the overlapping CTV volumes between the repeat CTV and the planning CTV. The third was a shift to the tumour location, studied for 6 possible locations of the tumour, which is the most relevant when considering the tumour boost [76]. For each of the three strategies, Wright et al used an algorithm to formation of both anisotropic and isotropic margins by finding the PTV enclosing all possible repeat CTVs, and the daily adaptation PTV enclosing only the CTV of the day [76]. They compared the achieved volume overlaps between the bladder of the planning CT scan and the repeat scan.

Wright et al. found the daily translations to the tumour position and volume adaptation to the CTV of the day to increase the average percentage volume overlap by 20% to 79–82% for the various tumour positions, compared to the optimization of all repeat CTVs [76]. The achieved volume overlap was similar with no translation of the isocentre and slightly higher with optimal translation according to the bladder. They concluded that the translation of the isocentre according to the tumour position did not lead to increased normal tissue irradiation compared with no translation Optimal translation of the isocentre according to the tumour position was superior in terms of normal tissue sparing [76].

2.5 Helsinki and Aarhus methods

2.5.1 Introduction

In the method used in Helsinki University Central Hospital developed by Tuomikoski et al., four treatment planning CT images with different bladder filling states are acquired and based on the CTV volumes delineated on the images, a set of treatment plans are made [9]. The plan of the day is chosen based on the visible extent of bladder wall in CBCT images, i.e. the CTV. The position of the PTV in the treatment is adjusted to the daily bladder position with soft-tissue registration.

In the method used in Aarhus University Hospital [10; 80], the treatment plan for the first week is made based on one treatment planning CT image with large margins. CBCT-images of the patient are taken every day during the first week and three alternative planning target volumes are constructed based on Boolean operations to the the bladder contours delineated in the treatment planning CT image and the four CBCT images. These CBCT images are registered to the treatment planning CT image based on bony anatomy in patient positioning. During the course of the treatment, the plan of the day is chosen of separate plan selection volumes (PSVs) [10; 80].

There are three major differences between the methods: the way to form the PSVs, the way to register the treatment CBCT images to the planning CT image and the different treatment margins. Table 4 and Figure 6 visualize a comparison

of the methods.

Table 4: Comparison of the Helsinki and Aarhus methods.

	Before the treatment			Treatment					
Helsinki	Treatment planning CT	CTV definition	Treatment planning	CBCT imaging	Choice for the plan of the day	Radio-therapy			
	Patient drinks 8 dl of water and empties the bladder. CT imaging is performed immediate-ly and every 15 minutes (4–5 consecu-tive CT scans)	The radiation oncologist delineates the CTV to the CT scans	A set of 4–5 alternative plans are made based on the CTVs	Before each fraction a CBCT scan is taken. Soft tissue registra-tion between the CBCT and CT	The plan of the day is chosen of the optional CTVs, fitting the bladder to the smallest possible CTV				
	Before the treatment			The first week of the treatment			Rest of the treatment		
Aarhus	Treatment planning CT	CTV definition	Treatment planning for the first week	CBCT imaging and treatment	CTV definition	Treatment planning	CBCT imaging	Choice for the plan of the day	Radio-therapy
	Patient empties the bladder and CT imaging is done	The radiation oncologist delineates the CTV to the CT scan. The lymph nodes are usually included	A plan with margins large enough to account for bladder volume variation is made	Before each fraction a CBCT scan is taken. The plan with large margins is used	The radiation oncologist delineates the CTV to the CBCT images. Based on the CTV volumes in CT and CBCT images 3 alternative PTVs are formed	3 alterna-tive plans are made based on the alterna-tive PTVs	Before each fraction a CBCT scan is taken. Bony anatomy registra-tion between the CBCT and CT	The plan of the day is chosen of the optional PSVs	

2.5.2 Helsinki method

In the Helsinki method, the idea is to determine the changes of volume and shape of the bladder due to filling. The patients drink 8 dl and empty their bladder. Four repeated CT scans are acquired in supine position using a knee and feet fixation system. The scans are taken with a 15-min interval between the successive scans, the first scan being acquired shortly after voiding. The images are imported in the treatment planning system. The images are registered to the first image with the empty bladder with an automized rigid registration algorithm of the TPS based on the bony anatomy. [9]

The bladders plus areas of extravesical extension representing the CTVs in the

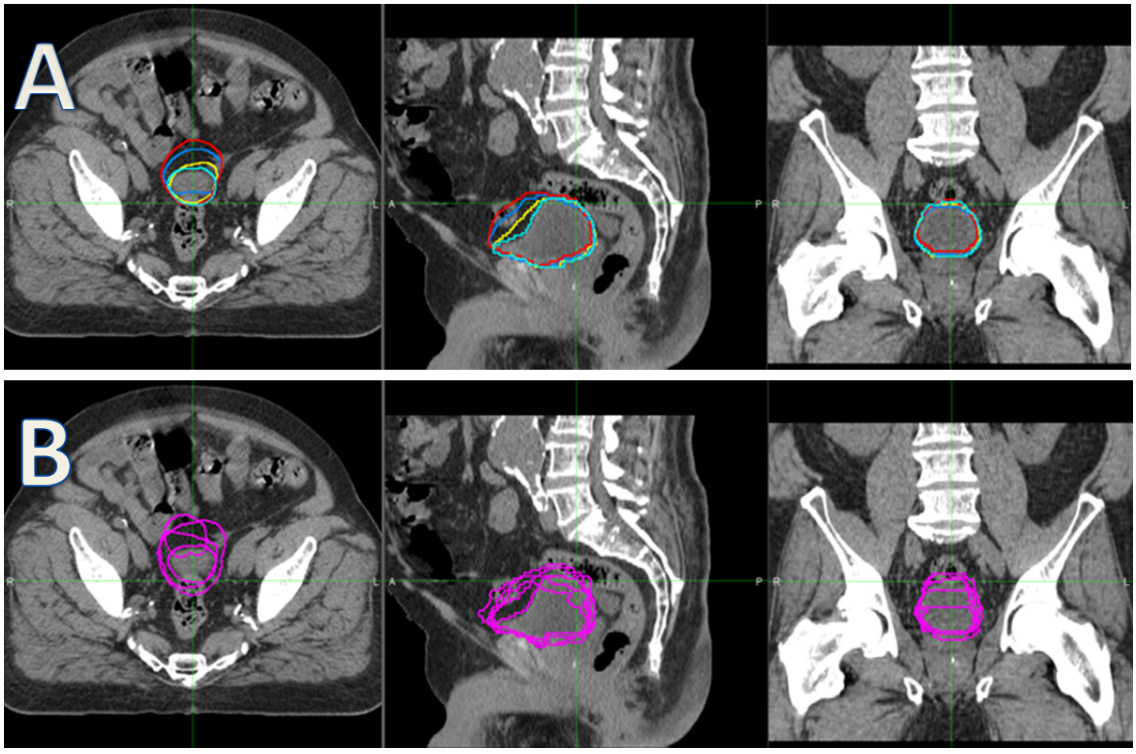

Figure 6: The ideas behind the Helsinki (A) and Aarhus (B) methods. In the Helsinki method (A), the objective is to catch the individual bladder filling pattern of the patient. Repeat CT images are aqcuired every 15 minutes, starting from the empty bladder (cyan) and stopping after 45 minutes (red). The bladder contours in these images are used as a starting point when producing the planning target volume. In the Aarhus method (B), the bladder contour of the planning CT image is combined with four CBCT scans aqcuired on consecutive treatment days of the first week of treatment to produce the starting point for the PTV formation. The aim of the Aarhus method is to catch changes in the bladder form and position over time.

treatment planning images are manually contoured by a radiation oncologist and the contours are then used to form the alternative planning target volumes. This way the patients' individual bladder filling pattern is defined. Also the surrounding normal structures are delineated by the radiation oncologist. These structures include the rectum, the intestinal cavity and the femoral heads. The patients usually receive fractionated RT that is divided in two parts. The elective part, which is given first, includes the whole bladder (and in some cases the lymph nodes) as elective treatment volume and is usually treated to 45–50.4 Gy with 1.8-Gy fractions. The boost part includes only the tumour with margins and this volume is treated to a total dose of 10–20 Gy in 2-Gy fractions, depending on the patient tolerance. [9]

The planning target volume is formed by anisotropically extending the CTVs with anterior and cranial margins of 10 mm and lateral, posterior and caudal margins of 15 mm [9]. The treatment plans are made with volumetric arc therapy or intensity-modulated radiation therapy techniques. 4 treatment plans for the whole bladder and 4 plans for the boost are made.

The patient is instructed to void their bladder prior to each treatment session. The treatment is delivered based on the daily CBCT acquisition and the online registration of the CBCT images to the planning CT image is made with an automatic soft-tissue registration algorithm. According to the current procedure in Helsinki, the radiographers choose the plan with the smallest PTV for the specific treatment fraction so that the bladder visible in the CBCT image fits inside the planning CT bladder. In the Helsinki method, no separate plan selection volume is formed but the planning CT bladder, i.e. the CTV, is directly used as the PSV. The whole CTV–PTV margin thereby accounts for the intrafractional changes.

2.5.3 Aarhus method

In the Aarhus method, the idea is to account for the day-to-day changes in the bladder shape and position. One treatment planning CT scan is taken after the patient has emptied their bladder and the images are imported and registered in the treatment planning system. The clinical target volumes for the bladder, including the bladder wall and its contents, and for the lymph nodes are delineated. In the Aarhus method, the lymph nodes are often included in the treatment. The total dose of the treatment is 60 Gy in 2-Gy fractions. [10]

The PTV for the first week of the treatment is formed as follows: First, an internal target volume (ITV) covering the internal variations in the bladder position is formed by adding an anisotropic margin to the bladder CTV. The margin width is 20 mm anterior and superior, 15 mm posterior and 10 mm in the remaining directions. To account for the external setup variations a margin of 5 mm in the axial plane and 8 mm in the cranial–caudal direction is applied. The treatment is delivered after set-up based on CBCT acquisition and online image registration based on bony anatomy. This applies to the whole course of the treatment. [10]

After the treatment of the first week has been given, 3 alternative PTVs for the adaptive treatment are formed based on the CBCT images taken during the first four fractions and the planning CT scan. The CTVs are delineated on each image

and the images are registered using the bony-anatomy match [10]. The small PSV is the volume covered by at least two of these five bladder contours plus a 3-mm margin to compensate the registration of the images based on bony anatomy. The medium PSV is the union of these five bladder volumes plus the same 3-mm margin. To form the small and medium PTVs, a 5-mm intrafraction margin is added to these composite CTVs (Figure 7). The large PTV is the same as the PTV of the first week's treatment [10]. The treatment plans are made with IMRT planning [80].

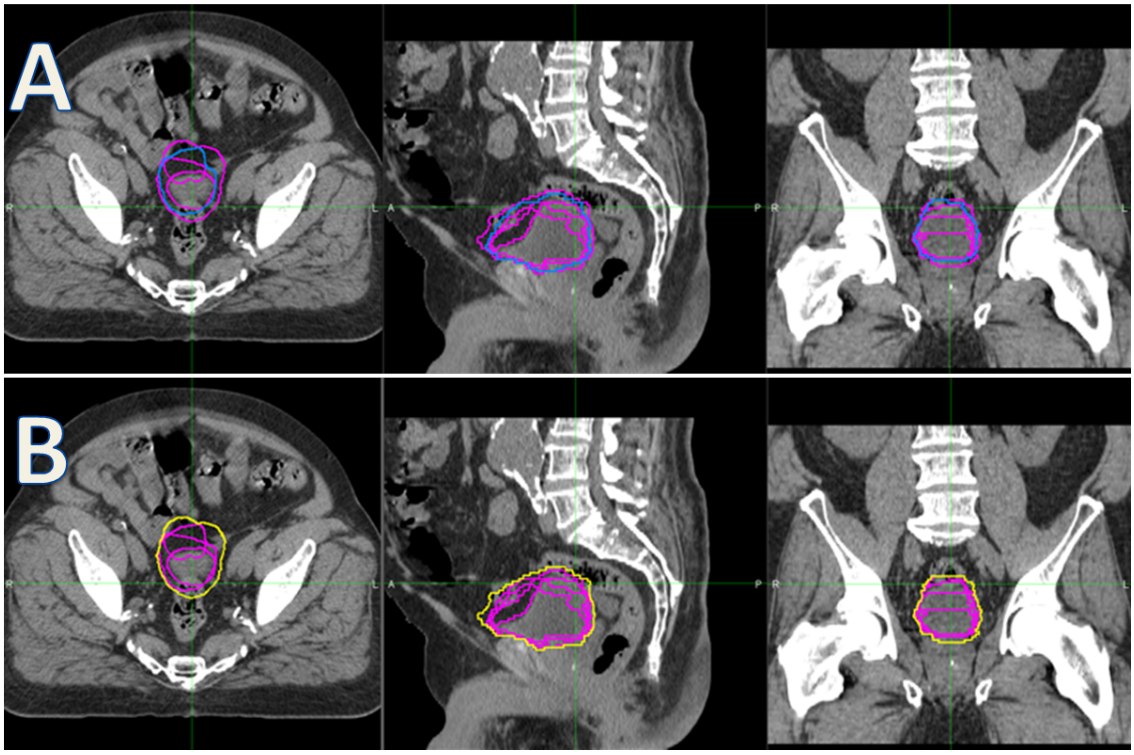

Figure 7: The small (A) and medium (B) composite CTV in the Aarhus method. The small composite CTV is the volume covered by at least two of the 4 CBCT and 1 planning CT bladders. The medium composite CTV is the union of these five bladders. The PSVs are formed by adding a 3-mm margin.

3 Methods

3.1 Patients

In total 10 patients with muscle invasive bladder cancer were retrospectively selected for the study. 8 males (patients 1–8) and 2 females (patients 9–10) were selected in order to represent the typical population of bladder cancer patients. The patients had been treated in Helsinki University Central Hospital between 2010 and 2014. 4 of the patients, 1 female and 3 male, had been treated with Varian Clinac iX with the OBI kV on board imaging system. 6 patients, 1 female and 5 male, had been treated with Electa Axesse machine. This linear accelerator is also equipped with a kV on board imaging system, called XVI. Patients 1, 3, 5 and 10 had been treated with the Varian linear accelerator and the rest with the Elekta linac. 6 of the patients had received a whole bladder treatment and 4 a treatment for the whole bladder with the pelvic lymph node areas included (patients 5, 6, 7 and 10).

The CBCT images taken during the treatment were used as the material for this study. The patient needed to have received at least 30 fractions of treatment in order to have an adequate number of CBCT-images to be included into the analysis. The patients had been treated to varying doses and the amount of images taken during the treatment varied between the patients. However, the Aarhus University hospital usually treats the patients to a total dose of 60 Gy in 30 2-Gy fractions [10] and thus, the total amount of 30 images was chosen to be included to the analysis. An additional prerequisite was that four planning CT series had to have been successfully acquired in order to be able to form the PTVs according to the Helsinki method.

3.2 Simulating the treatment

3.2.1 Image registrations

There were three kinds of registrations in the study: bony-anatomy based registrations, centroid-based registrations and registrations based on soft-tissue anatomy. All of the images were first registered based on bony anatomy. The bladder contours delineated in the CBCT-images were transformed into the treatment planning CT according to this registration. These bony-anatomy matches were also utilized as such to evaluate the hits and misses in the Aarhus method and the modified Helsinki method where the bony-anatomy match was used.

The radiotherapy planning CT image and the CBCT images were registered using bony-anatomy matching. Here an automatic tool in MIM® medical image management software (MIM Software Inc., Cleveland, OH, USA) was first used to match the images together approximately. After this, the software's box-based assisted alignment tool was used to refine the registration. The MIM® software uses a registration algorithm which does the matching based on both soft tissues and bony anatomy. However, the focus was on the bones while evaluating the quality of the registration. The bones surrounding the bladder were included to the box. The femoral heads were included but the rest of the femur was excluded, since the

patient's legs could be in a slightly different position. The symphysis was included, but the anterior abdominal wall was excluded to avoid the breathing movement to influence the matching. Respectively, the spinal cord was included but the soft tissues lying more posteriorily were excluded from the box. Superiorily the box reached at least the superior border of the CBCT image. An example of the region of interest for the image registrations is shown in Figure 8.

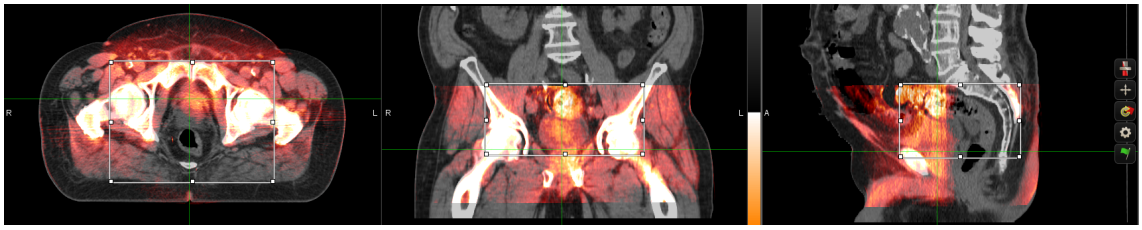

Figure 8: The box-based alignment region of interest.

In Helsinki University Central Hospital, rotational variations are currently not corrected for with table rotations in the case of bladder patients. To be able to follow the procedure of the treatment as precisely as possible, the matching of the images was done without rotation. In Aarhus University Hospital the current procedure includes correction for small rotational deviations, but as this is a recent change in the procedure, this was not taken into account, in order to simplify the analysis.

In the later phases of the analysis there were also registrations based on the mass gravity centres of the daily bladders and the alternative PSVs. The centroids of the bladders and the alternative PSVs were found with the automatic tool of the MIM® software and manually aligned with the MIM® software transformation tool. The tool finds the mass gravity center of the contour, treating all voxels as same density.

In the Helsinki method, a soft-tissue registration is made between the treatment planning CT and the treatment CBCT images. When comparing the original non-modified methods, this soft-tissue registration could not be performed in the exact same way as in the treatment. On the treatment machine there is automatic software for soft-tissue matching and the radiographers are allowed to refine the result if it is not satisfactory. In the MIM® software, there is no such tool. The soft-tissue registration in the Helsinki method was simulated by using the centroid registration as an objective starting point and refining this registration manually to get the bladder of the day to fit into the smallest possible PSV, trying to keep the required translations as small as possible. It is emphasized that all the analyses were performed retrospectively and they did not have any effect on the patients' actual treatments.

3.2.2 Delineation of the bladders

For the 10 patients, the bladders and intestinal cavities in the CBCT images were delineated in cooperation with a radiation oncologist. Even though the pelvic lymph node areas had been included to the treatment area or some patients in the actual treatment, for the purpose of this simulation only the bladder was included to the

target area. The CBCT images of 30 fractions of the treatment were included to the analysis. In the case that there were more than 30 images available, the 30 first images were taken into analysis. If the patient had been imaged twice during the fraction, pre and post treatment, the first of the images was chosen.

The bladder was delineated utilizing axial, coronal and sagittal directions of the image. In the case of partial volume artifacts, the larger volume was contoured if in doubt. The guideline 'err on the generous side' [49] was hence followed.

3.2.3 Target volumes

The target volumes were formed according to three different ways: 1) using Helsinki method as such, using the Helsinki method margins, 2) forming the PSV according to Helsinki method, but using Aarhus margins, and 3) using the Aarhus method.

In the Helsinki method, the CTVs on the four treatment planning CT images taken immediately after emptying the bladder (CT0) and every 15 minutes (CT15, CT30, CT45) were expanded with anisotropic margins to form the alternative PTVs. The bladder was used as the CTV as such, assuming for the purpose of this study that the subclinical growth would be restricted to the bladder walls. According to the current procedures in the treatment in Helsinki, the bladders delineated on the treatment planning images, i.e. the CTVs, were used as plan selection volumes.

In the Aarhus method there were three alternative planning target volumes: small, medium and large. Each of these planning target volumes were constructed differently. Whereas in the Helsinki method the PTV was formed by adding margins to the bladder which was straightforwardly used as the CTV, in the Aarhus method additional PSVs were formed in order to form the PTV. The treatment planning CT scan (CT0) and the CBCT-images of the first four treatment fractions were used to form the small, medium and large PSVs as described earlier in this text.

In order to be able to compare the Helsinki and Aarhus methods to form the PSV, without that the comparison would be influenced by the margins or the image registration method, the Helsinki adaptive RT method was modified. The Helsinki method to form the CTV was combined with Aarhus method margins to form this modified method. The way and the margins to form the alternative PSVs and PTVs according to the modified and non-modified Helsinki and Aarhus methods is summarized in Table 5. To make the margin formation quicker and more easily reproducible, an automated workflow for the MIM® software was designed. The result was checked manually for all of the margins.

3.2.4 Selection of the daily target volumes

After creating the alternative PTVs and PSVs for each method, the simulation of the treatment continued with the selection of the daily treatment volumes. The same basic principles applied for all methods: the smallest possible treatment volume was chosen so that the bladder of the day fit into the corresponding PSV. In this chapter, the treatment volume selection procedure is reviewed for all of the evaluated methods.

Table 5: PTV formation in each method. Directions: ant. = anterior, post. = posterior, sup. = superior, inf. = inferior, lat. = lateral

Method	PTV	Bladder contours to start with	Operation before margin addition	PSV margin	Intrafraction margin
Helsinki actual	PTV A–D	4 Planning CTs, 15 min intervals	None	0 mm	anisotropic ant. & sup. 10 mm lat., post. & inf. 15 mm
Helsinki modified	PTV A–D	4 Planning CTs, 15 min intervals	None	isotropic 3 mm	isotropic 5 mm
Aarhus actual & modified	PTV S	Planning CT & 4 CBCTs	At least two bladders (Figure 7)	isotropic 3 mm	isotropic 5 mm
	PTV M	Planning CT & 4 CBCTs	Union (Figure 7)	isotropic 3 mm	isotropic 5 mm
	PTV L	Planning CT	None	anisotropic ant. & sup. 20 mm post. 15 mm remaining 10 mm	anisotropic sup. & inf. 8 mm remaining 5 mm

It seems natural to start with the Aarhus method, since in that method the registrations between the treatment planning CT and CBCT images are the same bone-based registrations used when transforming the bladders from the CBCT images to the treatment planning CT. The selection of the PTV was done by looking at the contours of both the bladder of the day and the alternative PSVs and simply choosing the smallest PSV into which the bladder contour would fit. The contours were allowed to coincide but the bladder could not come out of the PSV contour so that there would be a gap between the delineated contours. The same principle as in the Aarhus method was followed when choosing the smallest Helsinki method PSV created using Aarhus margins that would cover the bladder. The PSVs were examined one by one, starting from the smallest and comparing them to the bladder of the day as described earlier.

The procedure of treatment volume selection is a bit more complicated for the methods including some other way to register the images than the bone match. The principle of these image registrations was described earlier in the related chapter. The bladders were in the CBCT images and the possible PSVs in the treatment planning CT so that changing the registration between these images changed the position of the contours in respect to each other. There were concerns of how to perform these registrations objectively and so a compromise was made. Matching the mass gravity centres of the contours was thought to simulate the soft-tissue match well enough. Both Aarhus and Helsinki methods now used this centroid match and the margins of Aarhus method.

Matching based on the contour centroids was performed as follows. Starting with the smallest PSV, the centroids of the PSVs were matched with the bladder centroid one by one and the one covering the whole bladder was chosen. If the bladder was not covered by even the largest PSV, it was recorded if at least the largest PTV covered it. If not, the severity of the miss was noted.

The soft-tissue registration belonging to the Helsinki method was performed using the centroid match as a starting point. Each PSV, starting with the smallest one, was evaluated until the smallest possible PSV was found. However, after matching the centroids, it was also tested whether the bladder could fit into the PSV by making some translations. If, for example the smallest PSV was clearly too small for the bladder, the next smallest one was matched based on the centroids. If the bladder did not fit the PSV with the centroid match, it was evaluated if it could be made to fit by making a small translation. The aim was to find the smallest possible PSV that would cover the bladder but also to do this with as little translations as possible. If even the largest PSV did not cover the bladder, it was checked whether the largest PTV would cover the bladder without any translations. If not, it was clarified whether it was possible to get the bladder into the PTV by making some translations.

3.2.5 Comparison of the plan selection frequencies with those in the treatment

The plan selection frequencies were compared with the plan selection frequencies observed in the actual treatment. The plans with which the patients had been treated were listed for each fraction. In this simulation the bladder was used as the target as such, but in the treatment the regions of extravesical tumour expansion were also included. For some of the patients (5, 6, 7 and 10) the lymph nodal areas were also included to the treatment volumes and bony-anatomy registration was used. These patients were left out to have a more representative selection of patients treated with the Helsinki method. Nevertheless, the PTVs in the treatment might not have been the same as in the simulation for all of the patients, as the treatment protocol can be adjusted to the individual needs of the patient by the treating oncologist.

For some of the patients, there were less than four different options for a treatment plan. In these cases the bladder expansion between some sequential CT scans had probably not been strong and the treating oncologist had decided that there is too little difference between the two bladders for both options to be useful. To be able to make some rough comparison of the selected volumes, the plan made based on the post-void planning CT was named as A, the plan made based on the 15 minutes CT image was named B and so forth.

There had been different fractionation schedules in the treatment and usually a booster had been included, and hence the treatment with the PTVs formed according to the described Helsinki method had not lasted for 30 fractions. The relative ratios of the frequencies of the treatment plans were calculated.

3.3 Feasibility of soft-tissue image registration when irradiating pelvic lymph nodes

When treating the bladder and the lymph node areas, if the patient's position is adjusted based on the CBCT images so that the bladder is in an optimal position with regards to the PTV, an error is induced to the lymph node region. The lymph nodes are in a relatively stable position with respect to the bony anatomy, so regarding the lymph nodes, it would be ideal to adjust the patient's position based on bony-anatomy registration, which is the case in the treatment if the lymph nodal areas are included to the target volume. The eligibility of the soft-tissue registration in the case of treatment of both the whole bladder and the lymph nodes was further examined by a simulation. It was calculated, how large a CTV–PTV margin needs to be added to the lymph nodes in order to correct for the error caused by registration of the images based on soft tissues and not the bony anatomy. The formula (3), which was introduced by van Herk et al. [21], was used.

First, the translations from bony anatomy to soft-tissue anatomy in each direction x, y and z on each treatment fraction were calculated for individual patients. The coordinate system was that used by the MIM® software. Here the x direction was the lateral direction with the positive direction pointing to the left. Coordinate

y was the anterior posterior axis and the positive direction was the posterior direction. The z axis was in the cranial caudal direction, the positive direction being the caudal direction. The coordinate system is visualized in Figure 9.

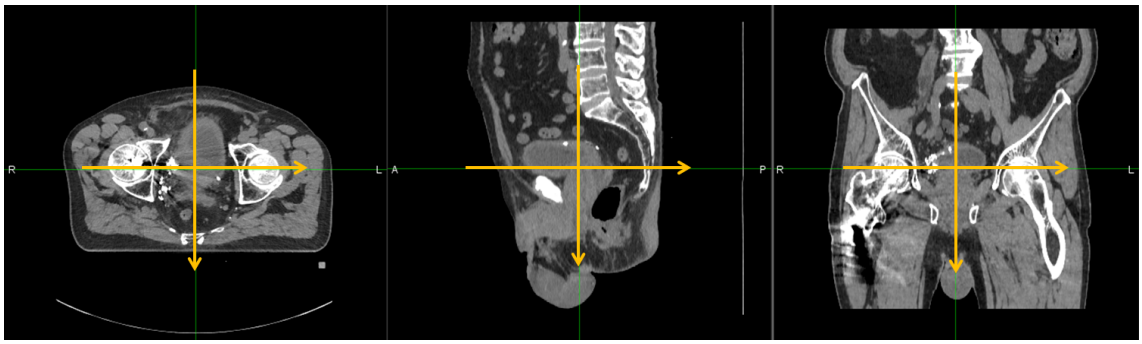

Figure 9: The coordinate system in the MIM® Software. The positive directions are indicated by the arrows. When performing an image registration, the planning CT image was chosen as the primary image. This means that in all the registrations, the CBCT image is moved according to the planning CT image.

The coordinates indicating the translation between the treatment planning CT image and CBCT image acquired before treatment were listed for each fraction of each individual patient, separately for the soft-tissue registration and the bony-anatomy registration. The coordinates of soft-tissue registration were subtracted from the coordinates of bony-anatomy registration. The individual means and standard deviations for each patient were calculated by taking the average and standard deviation across all fractions for each patient. The group systematic error M was the mean of the patients' individual means and $\boldsymbol{\Sigma}$ was the standard deviation of the individual means, which represents the standard deviation of the systematic error. The standard deviation of the random error, $\boldsymbol{\sigma}$, was calculated as a root mean square (4)

$$R\left(x\right) \equiv \sqrt{\langle x^2 \rangle} \tag{4}$$

of the individual standard deviations, where the $\langle ... \rangle$ stands for the arithmetic mean.

The penumbra width parameter σ_{p} was calculated by dividing the measured penumbra width by 2.56 [15]. Based on the 6 MV photon inline profile measurements for HUCH linear accelerator 6 the distance between the 10% and 90% dose levels of a single beam at a typical treatment depth (10 cm) was calculated. The field size used in the measurements was 10 cm x 10 cm. The distance between these dose levels was 2.07 cm. As the respective distance for linear accelerator 3 was similar (1.99 cm), we decided to use the linear accelerator 6 penumbra width value for all the patients for simplicity. Thus, the value of parameter σ_{p} was 8,1 mm. The treatment planning system photon beam algorithm error, a, was approximated to be at most half of a typical calculation grid size of 3 mm. Hence, the calculation grid size was the limiting factor.

The breathing error **b** was assumed here to be zero. Respiratory-induced prostate motion has been found to be less than 1 mm in the vast majority of fractions in

all directions in the supine position [84–86]. The bladder motion induced by the breathing has not been studied to our knowledge but it can be assumed to be similar to the prostate motion due to respiration. As the movement is assumed to be modest compared to the bladder movement in total, the breathing positional error **b** was set to be zero.

The parameter β which depends on the field set-up was taken from [32]. The total number of the irradiating beams in a typical IMRT-plan for bladder RT is 7, but we used the value for a 6 field plan. The formula introduced by McKenzie et al. for calculating the value of the parameter β underestimates the value of the parameter at high beam numbers [32]. McKenzie and colleagues report that up to 6 beams, the table is satisfactory. However, as the parameter decreases as the number of the beams increases, it was considered safe to use the β value for a 6-field plan also for the 7-field plan as it would at worst overestimate the margin needed. As there are no parallel or opposing beams on the IMRT plans, the parameter β value in the x and y directions was 0.52 and in the z direction it was 1.64.

3.4 Statistical analysis

Statistical methods were used in the analysis of the results. These methods included linear regression modeling, the F-test for statistical significance of the regression coefficients, the paired t-test and the Pearson correlation coefficients. These methods are briefly described.

In linear regression analysis, the goal is to model the relationship between the dependent variable y and one or more explanatory variables x with a linear equation. The equation

$$y_i = f\left(x_i; \beta\right) + \epsilon_i \tag{5}$$

describes how the variation of variable x explains the variation of variable y_i. β is the parameter vector containing the regression coefficients. The term ϵ_i is the error term that catches all other factors influencing the dependent variable y, other than x. Other than forming a model to explain some phenomenon with possible explanatory variables, linear modelling can be used to quantify how strongly y is influenced by the x that is suspected to be related to y. The value of parameter β is chosen so that the values of the error terms ϵ_i are minimized. In this analysis, this curve fitting problem was solved with the least squares method, which minimizes the quadratic sum of the error terms

$$\sum_{i=1}^{n} \epsilon_i^2 = \sum_{i=1}^{n} \left(y_i - f\left(x_i; \beta\right)\right)^2 \tag{6}$$

The regression coefficients can be tested with the F-test. The F-test is performed using formula

$$F = \left(n - 2\right) \frac{R^2}{1 - R^2} \tag{7}$$

The R^2 value of the model describes how many per cent of the variation of the dependent variable can be explained by the explanatory variable(s). The $n-2$ is the number of degrees of freedom. If the value of F is large, this suggests the null hypothesis that the regression coefficients are all zero to be false.

The paired t-test can be used when it is reasonable to arrange the observations as pairs [87]. In the t-test the differences between the numbers in the pair are calculated and the mean of these differences is assumed to be zero. The t-test quantity is

$$t = \frac{\bar{D}}{s_D/\sqrt{n}}, \tag{8}$$

where

$$\bar{D} = \frac{1}{n}\sum_{i=1}^{n} D_i \tag{9}$$

and

$$s_D^2 = \frac{1}{n-1}\sum_{i=1}^{n}\left(D_i - \bar{D}\right)^2 \tag{10}$$

The paired t-test assumes that the values are normally distributed, but if the number of observations is large enough ($n > 40$) it can be safely used even for clearly skewed distributions [87].

The Pearson correlation coefficients can be calculated according to the formula

$$r_{xy} = \frac{\sum_{i=1}^{n}\left(x_i - \bar{x}\right)\left(y_i - \bar{y}\right)}{\sqrt{\sum_{i=1}^{n}\left(x_i - \bar{x}\right)^2}\sqrt{\sum_{i=1}^{n}\left(y_i - \bar{y}\right)^2}}, \tag{11}$$

where $\bar{x}$ is the arithmetical mean of the values of x and $\bar{y}$ is the arithmetical mean of the values of y.

4 Results

4.1 Bladder volumes during the course of the treatment

Based on the delineated bladders on the CBCT images, some statistics of the observed bladder volumes were calculated (Table 6). In the patient population, the bladder volumes during treatment ranged from 42 ml to 343 ml. Daily bladder volumes were observed throughout the treatment (Figure 10).

Table 6: Bladder volumes of each patient (ml). The mean bladder volume across the treatment fractions, the standard deviation (SD) of the bladder volume and the minimum as well as maximum bladder volumes are presented.

	V(bladder)			
Patient	Mean [ml]	SD [ml]	Min [ml]	Max [ml]
1	145	31	106	223
2	106	22	76	176
3	108	22	69	163
4	112	39	80	251
5	157	35	123	266
6	90	28	42	156
7	131	24	102	198
8	188	43	145	343
9	112	49	51	271
10	121	53	59	227

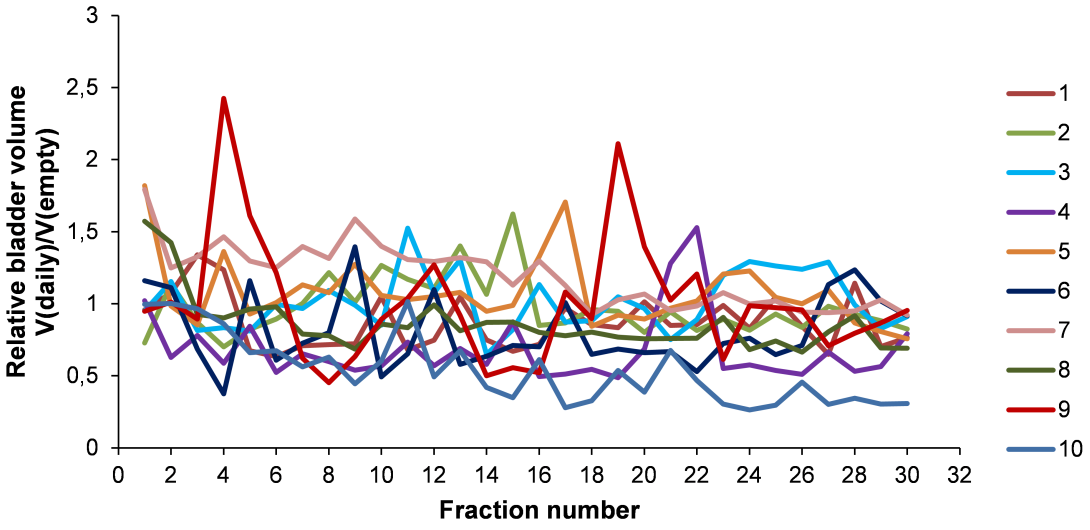

Figure 10: The daily bladder volumes relative to the volume of the empty bladder on the planning CT scan.

There seemed to be a trend that the bladder volumes decrease during the treatment (Figure 10). A linear regression line was fitted with the least squares method. A model was constructed to explain the bladder volume variations during the course of the treatment with the increasing fraction number. Based on the regression lines fitted to the bladder volume data of individual patients, 8 of the 10 patients studied had a decreasing tendency in the bladder volume during treatment. Only patients 3 and 6 had a positive regression coefficient. A linear regression curve was fitted to describe how the fraction number (time) affected the bladder volume.

The F-test found at least one of the regression coefficients to differ statistically significantly from zero. The fraction number had a significant negative coefficient of –1.28 ($p < 0.001$), meaning that the bladder volumes significantly decreased as a function of the treatment fraction. However, a linear relationship with the fraction number is not enough to explain all the variations in the bladder volume ($R^2 = 0.06$, adjusted $R^2 = 0.06$). The change in the fraction number explained only 6% of the bladder volume value variations.

On 67% (20/30) of the fractions the bladder had a smaller volume than in the planning CT scan. One can ask if the bladder volume in the planning scan is representative of the bladder volumes during the course of the treatment. However, the bladder volume also varied during treatment (Figure 11). On patients 1, 2, 3, 5 and 7 the maximum bladder volume in the treatment exceeded the volume of the 45 minute CT scan bladder.

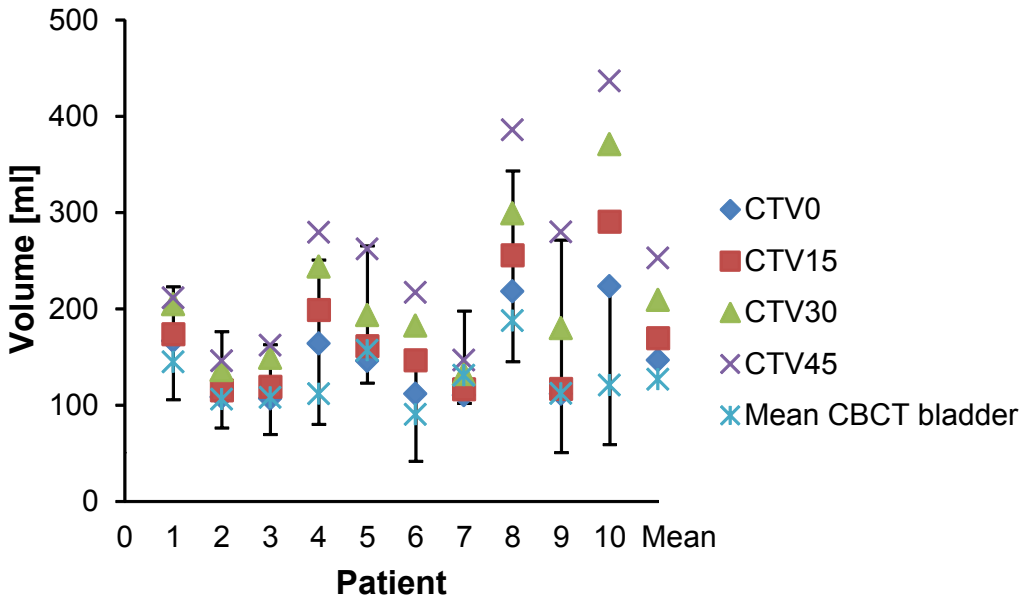

Figure 11: Individual bladder volume change due to filling measured from the planning CT scans taken during an hour. The error bars around the mean CTCB bladder represent the range of the bladder volumes during treatment.

4.2 Comparison of Aarhus and Helsinki methods

4.2.1 Plan selection frequencies and hitting the target

There are three procedural differences between the methods: The method to form the CTV, the CTV–PTV margins and the method for registration between the planning CT and CBCT images. The purpose was to compare the Helsinki and Aarhus methods for forming the CTV. We wanted to see the effect of only the CTV forming method without the effects of the margins and the registration method. Also the non-modified methods were compared. The success of the radiotherapy treatment depends on whether the target is hit or missed. The compared methods were evaluated in this respect. The frequencies of the selected PTVs were listed and the success of the treatment fractions was reported.

In the next figures, the frequencies of the different PTV selections in the different methods are presented. The black and white scale represents the safe zone, where the bladder of the day has fit into the plan selection volume, in the case of the Helsinki method, one of the treatment planning CTVs. The red colour indicates the worst case, where the bladder of the day has not fit into even the largest PTV. In the cases marked with yellow colour, the largest PSV was not adequate but at least the bladder fit into the PTV in the beginning of the treatment. In these cases one cannot be certain whether the intrafractional changes in the bladder size are still accounted for. In red and yellow cases patient would be asked to void their bladder again. These situations would hence not pose a threat to the success of the treatment but would be inconvenient and slow down the treatment.

To equalize all the other components than the way to form the CTVs between the different methods, we first decided to try and change the registration method and the CTV–PTV margins of the Helsinki method to those of the Aarhus method. That is, the margins were according to the Aarhus method and the registration of the images was done based on the bony anatomy.

When using the bone match, the Aarhus margins were clearly not adequately large when the Helsinki method for forming the CTV was used (Figure 12). The PTV is frequently too small in the simulation when applying this modified method. The Aarhus method, being non-modified, worked properly and will be addressed later in this chapter.

The next way of comparison of PSV formation was to utilize the Aarhus method margins and Helsinki method registration for both methods (Figure 13). In Helsinki, the method to register the treatment CBCT images to the planning CT image is soft-tissue matching, which was simulated with the centroid registration for the objectivity of this comparison.

The Aarhus method with the centroid match seemed to be applicable. For Helsinki method, compared to the bony-anatomy registration, the centroid registration decreased the rate of inadequate PTVs. However, in some cases, the planning target volumes would not have covered the CTV in the modified Helsinki method with the Aarhus method margin and centroid match.

The next step was to compare the plan selection frequencies of the methods as such, non-modified (Figure 14). Based on this simulation, the majority of the chosen

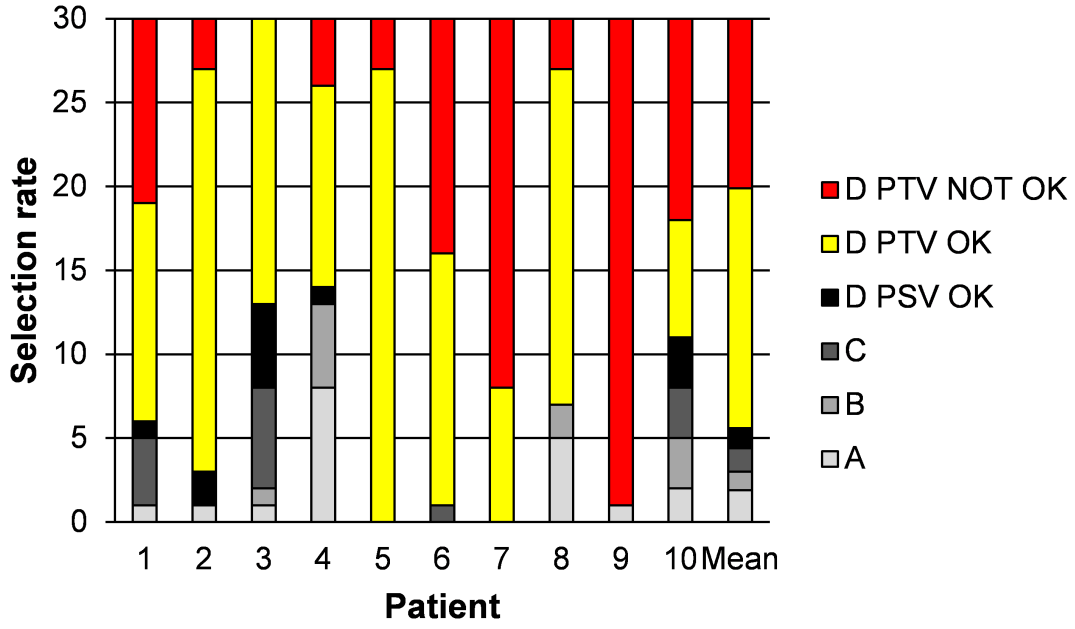

Figure 12: Plan selection frequencies with the modified Helsinki method for each patient. The planning target volumes were formed with the Helsinki method, but using the Aarhus method margins. The planning CT and treatment CBCT images were registered based on bony anatomy.

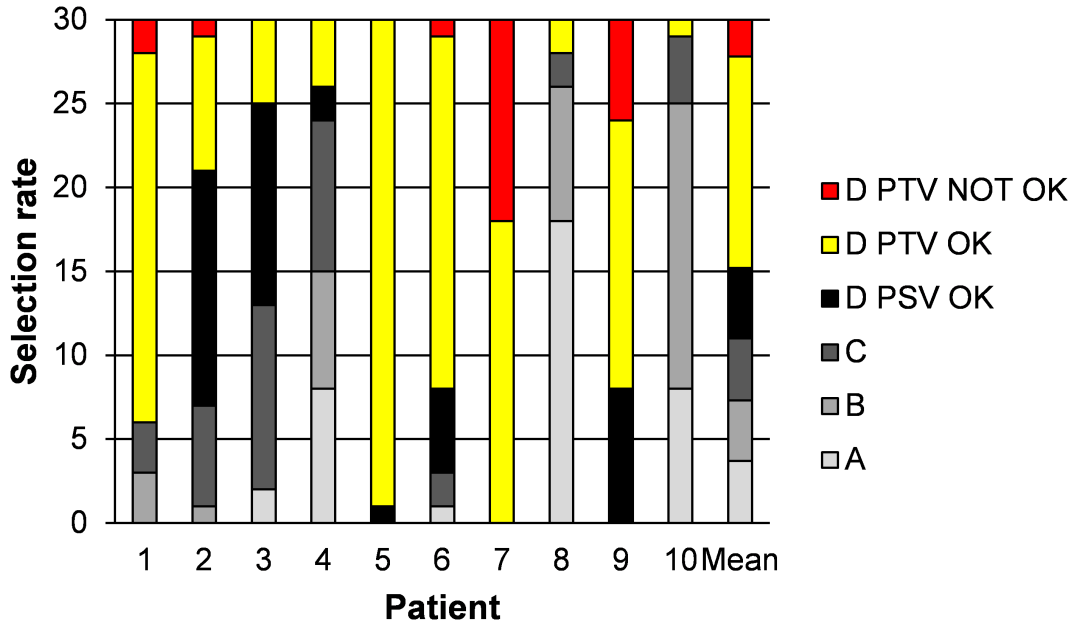

(a) Helsinki method with centroid registration and Aarhus margins

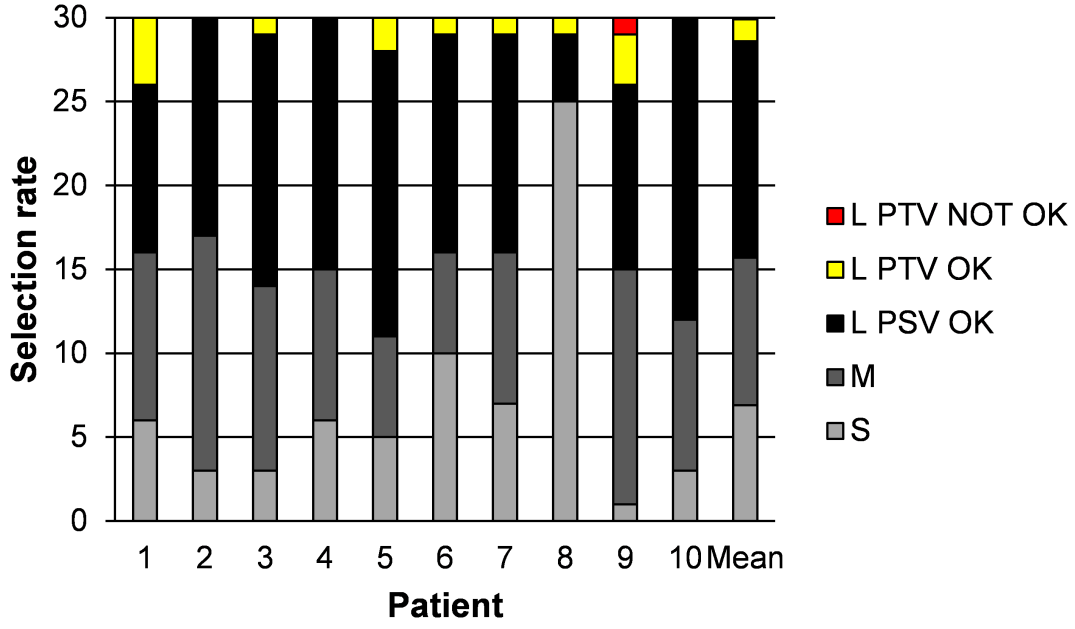

(b) Aarhus method with centroid registration

Figure 13: (a) Plan selection frequencies with the modified Helsinki method for each patient. The planning target volumes were formed with the Helsinki method but using Aarhus method margins. (b) Plan selection frequencies with the modified Aarhus method for each patient. The planning target volumes were formed with the Aarhus PTV formation method using the Aarhus method margins. In both (a) and (b), the planning CT and treatment CBCT images were registered based on a point match of the centroids of the bladder and the PTV. This was thought to adequately simulate the soft-tissue matching.

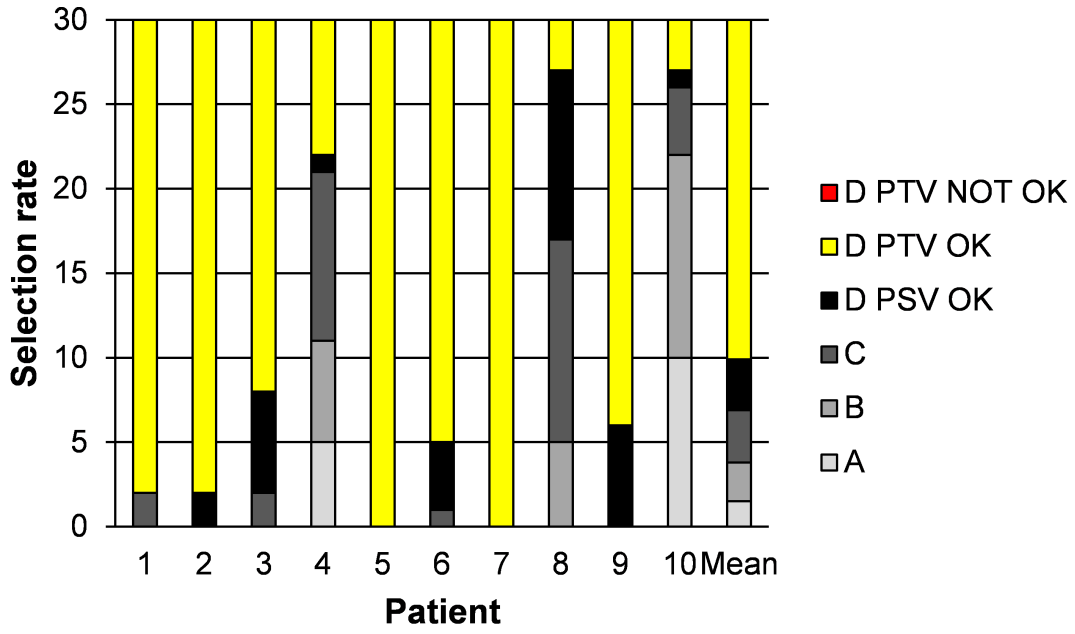

(a) Helsinki method

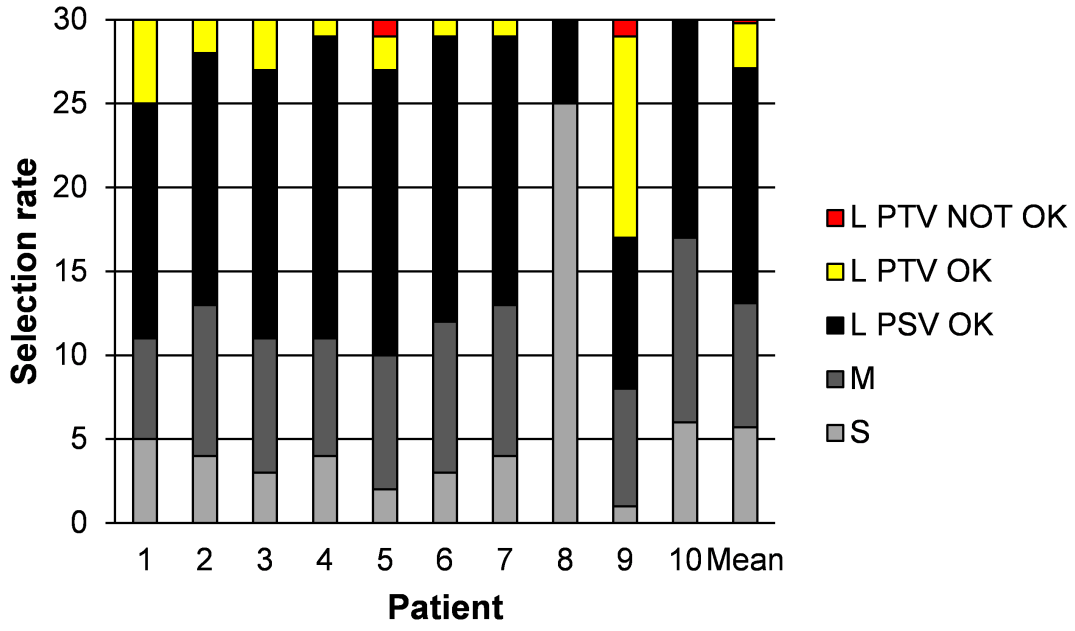

(b) Aarhus method

Figure 14: (a) Plan selection frequencies with the Helsinki method for each patient. The planning target volumes were formed with the Helsinki method using the Helsinki method margins and the planning CT and treatment CBCT images were registered based on soft-tissue anatomy. (b) Plan selection frequencies with the Aarhus method for each patient. The planning target volumes were formed with the Aarhus method using the respective margins and the planning CT and treatment CBCT images were registered based on bony anatomy.

treatment plans in the actual Helsinki method would have been the ones with the largest planning target volume (Figure 14a). For some patients, the largest planning target volume PTVD was even the only one ever chosen. The method doesn't hence seem to be truly adaptive. However, one must pinpoint that since the PTVs are not frequently too small as they were in the modified Helsinki methods, the method seems to work. Also, in the Helsinki method, part of the adaptation comes through the soft-tissue registration and the ability to make transformations to the position of the patient according to the position and shape of the bladder.

In the Aarhus method the chosen alternative PTVs were quite evenly distributed and also the smallest plans were chosen often (Figure 14b). In the case of some patients, there are also some fractions where even the largest PTV volume was inadequate.

4.2.2 PTV and PSV volumes

To analyze the differences between the methods and to understand how the target volumes available guided the plan selection, the PTVs and PSVs were compared between the methods. The PTV volumes (Figure 15) and the PSV volumes (Figure 16) of the modified Helsinki and Aarhus methods were first compared.

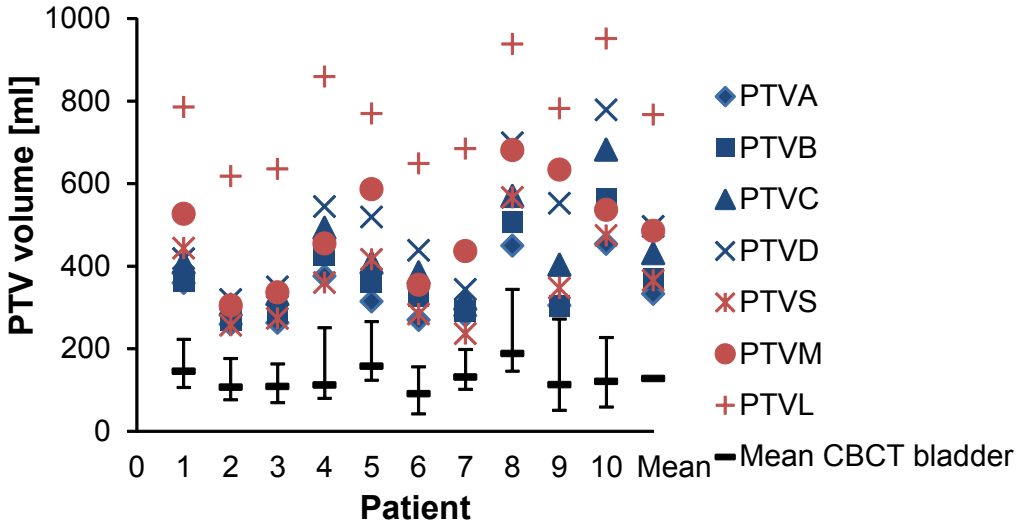

Figure 15: PTV volumes of individual patients in the modified Aarhus and Helsinki methods with centroid and bony-anatomy registration. The error bars indicate the range of the CBCT bladder volumes observed during the treatment.

In the case of the modified methods using centroid or bony-anatomy registration, Aarhus margins were used also for the Helsinki method PTV formation. This resulted in smaller PTVs for the Helsinki method, as the CTV–PTV margin was

added to a single bladder contour instead of the composite volumes used in the Aarhus method. There is also more variation in the Aarhus planning target volumes, providing a wider range of possible choices (Figure 15).

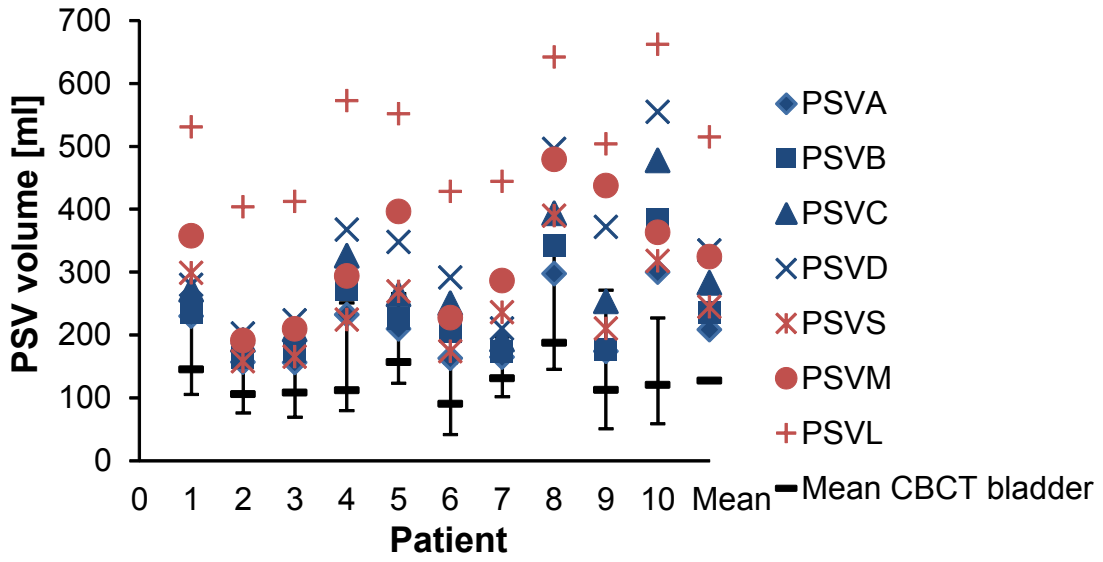

Figure 16: PSV volumes of individual patients in the modified Aarhus and Helsinki methods with centroid and bony-anatomy registration. The error bars indicate the range of the CBCT bladder volumes observed during the treatment.

In the modified methods, the PSV volumes are formed by adding a 3-mm margin to the planning CT bladders in the case of the modified Helsinki method and to the composite volumes in the case of the Aarhus method. As for the PTV volumes, the Aarhus method PSV volumes have a wider range and are larger than the modified Helsinki method PSV volumes (Figure 16).

When comparing PTVs of the clinically used Aarhus and Helsinki methods (Figure 17), one can observe that the Aarhus PTVs again have a wider range in volume. The smallest PTV is smaller and the largest PTV is larger than in the Helsinki method. However, just by comparing the volume of the bladders during treatment and the PTV volumes in each method, one can say that the PTVs in both methods should be able to accommodate the bladder volumes observed during the treatment.

Plan selection volumes are the volumes where the daily bladder needs to fit in order for the PTV to be selected, that is, the PSVs of the clinically used methods (Figure 18). In the case of the Helsinki method, the daily bladder has to fit inside one of the planning CT bladders. The available PSV volumes are smaller in the Helsinki method. As the intra-fraction margin in the Aarhus method is 5 mm, it is 10–15 mm in the Helsinki method.

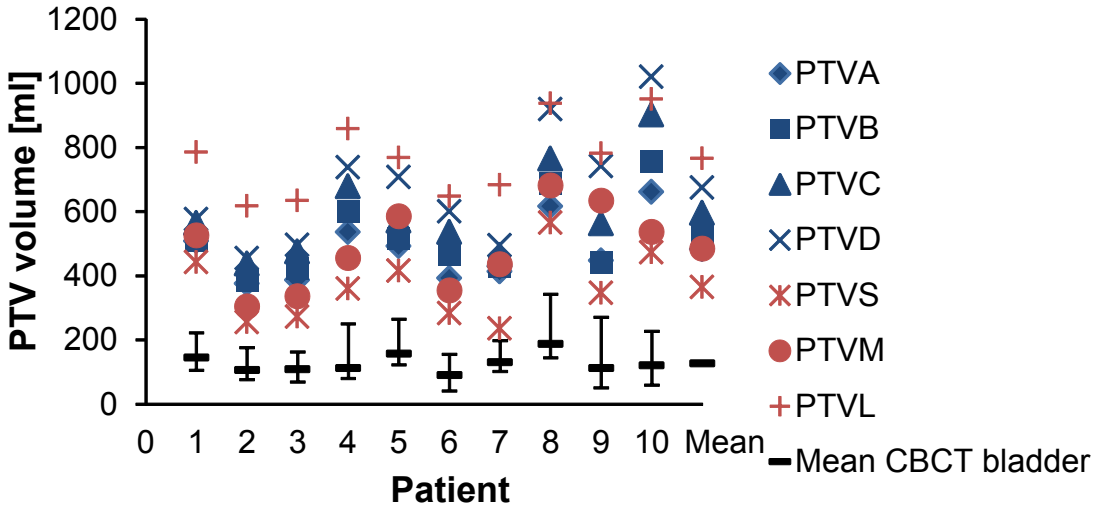

Figure 17: PTV volumes of individual patients in the actual Helsinki and Aarhus methods. The error bars indicate the range of the CBCT bladder volumes observed during the treatment.

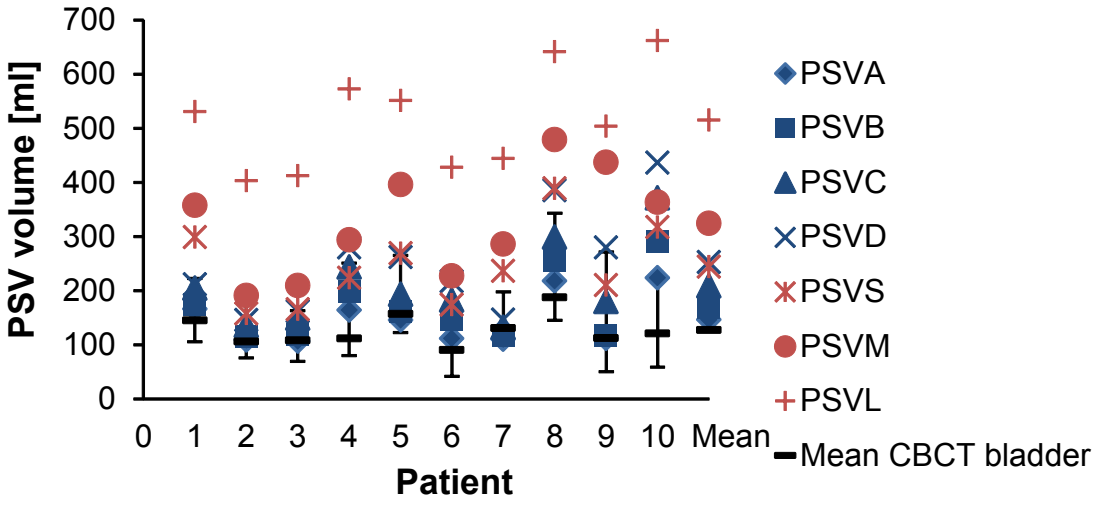

Figure 18: PSV volumes of individual patients in the actual Helsinki and Aarhus methods. The error bars indicate the range of the CBCT bladder volumes observed during the treatment.

4.2.3 Further comparison of methods

The objective of the study was to compare the way to form the CTV in each method. To do this, all the other differences between the methods were made equal between the methods. Two ways to do this were tried, first to register the images in both methods according to the bony anatomy and use the Aarhus margins for both methods and secondly to register the images in both methods with the centroid registration and use the Aarhus margins for both methods. Also, to compare the methods as they are clinically used, we simulated the treatment according to both methods as they are actually done. The plan selection frequencies were compared in the previous chapter but the methods were also compared in more detail. In this chapter, these analyses are presented.

According to the diagrams about plan selection frequencies (Figures 12–14) there were some cases that the largest PTV was inadequate to accommodate the CTV of the day. In these situations the patient would have been requested to void their bladder again, which would have slown down the treatment. Of the 300 fractions, the number of occations when there was bladder volume outside the PTV was 100 for the Helsinki method with bony-anatomy registration and Aarhus margins. The maximum volume of bladder outside the PTV was 14 ml. These figures indicate that the modified Helsinki method would not have functioned in the treatment. Hence, there was no point in comparing this modified method to the non-modified and functioning Aarhus method and further discussion was omitted.

The second way to compare the PSV formation ways between the methods was to use the centroid registration as a surrogate for the soft-tissue registration. Both methods now used this centroid registration and the margins of the Aarhus method were used for the Helsinki method as well. The different alternative planning target volumes were quite evenly chosen in both methods (Figure 13). This indicated that the methods work and the volume of the chosen PTV seems to be adapted to the volume of the bladder. In the modified Aarhus method, the distribution of the chosen plans was even more even than in the modified Helsinki method.

PTV outside bladder volumes can be used as a surrogate for the volume of normal tissues, particularly intestinal cavity volume, irradiated to the treatment dose. These volumes are listed in Table 7 for each method in the comparison.

Table 7: PTV outside bladder volumes for each of the compared methods. The mean and median value, as well as the standard deviation and the range of the PTV volume outside bladder are reported.

PTV volume outside bladder	Mean [ml]	Median [ml]	SD [ml]	Min [ml]	Max [ml]
Aarhus – bony-anatomy registration	494	515	168	113	865
Helsinki – soft-tissue registration	504	517	120	279	805
Aarhus – centroid registration	468	491	182	112	892
Helsinki – centroid registration with Aarhus margins	314	300	90	143	556

The chosen PTV volumes were found to be significantly smaller in the modified Aarhus method than those in the non-modified Aarhus method, as was indicated by the paired comparison t-test (t =2.97, $p < 0.01$). There was only one fraction where the largest PTV volume was too small, whereas there were two such fractions in the actual clinically used Aarhus method. The severity of the miss was 1 ml for the modified method and 5 ml for the non-modified method. There was no difference in the volume of bladder outside PTV. However, the PTV volume outside the daily bladder was smaller for the modified Aarhus method with centroid registration (t = 2.97, $p < 0.01$).

The Helsinki method was modified both in respect of the registration method and the margins. There were 22 occasions where the largest PTV was not adequate, the largest bladder volume outside the PTV being 3 ml, whereas there were none in the simulated clinically used method. Not surprisingly, the chosen PTV volumes were statistically significantly different between the modified and non-modified Helsinki method. The PTVs of the non-modified Helsinki method were larger than those of the modified method ($t = 48.59$, $p < 0.001$). The bladder volume outside PTV was significantly smaller in the non-modified method ($t = –2.71$, $p < 0.01$). However, as was expected since the PTV volumes were larger in the non-modified method, the PTV–bladder volumes were significantly smaller for the modified Helsinki method ($t = 47.49$, $p < 0.001$).

The average volumes of the patients' chosen PTVs during the treatment were compared between the modified Aarhus and Helsinki methods with the centroid registration (Figure 19). It seems that the PTVs chosen according to the modified Aarhus method are on average larger for all 10 patients. To test whether the visible difference is statistically significant, the paired t-test was applied. The t-test indicated that the Aarhus modified PTV volumes were larger than the Helsinki modified PTV volumes ($t = –16.29$, $p < 0.001$). As could be anticipated from the number of missed fractions, the bladder outside PTV volumes were larger for the modified Helsinki method ($t = –2.67$, $p < 0.01$). As the PTVs of the modified Aarhus method were found to be significantly larger, so were also the PTV–bladder volumes (t = 16.30 and $p < 0.001$).

The average volume of the PTVs chosen for treatment on each fraction was compared between the clinically used non-modified Aarhus and Helsinki methods. According to the paired t-test there was no statistically significant difference between the PTV volumes of these actual methods (Figure 20). The bladder outside PTVs volumes did not differ between the methods either, nor did the PTV outside bladder volumes.

To analyse the plan selection statistically, correlations between the bladder volume and the chosen PTVs were calculated. If there were no correlation, there would be reason to suspect that the method is not truly adaptive.

The fraction number had a statistically significant ($p < 0.001$) negative (correlation coefficient = –0.25) correlation with the bladder volume. The fraction number also had a significant ($p < 0.001$) correlation with the Aarhus method PTV volume, both with the modified and non-modified method. The correlation coefficients were –0.26 in the case of the non-modified method and –0.31 for the modified method,

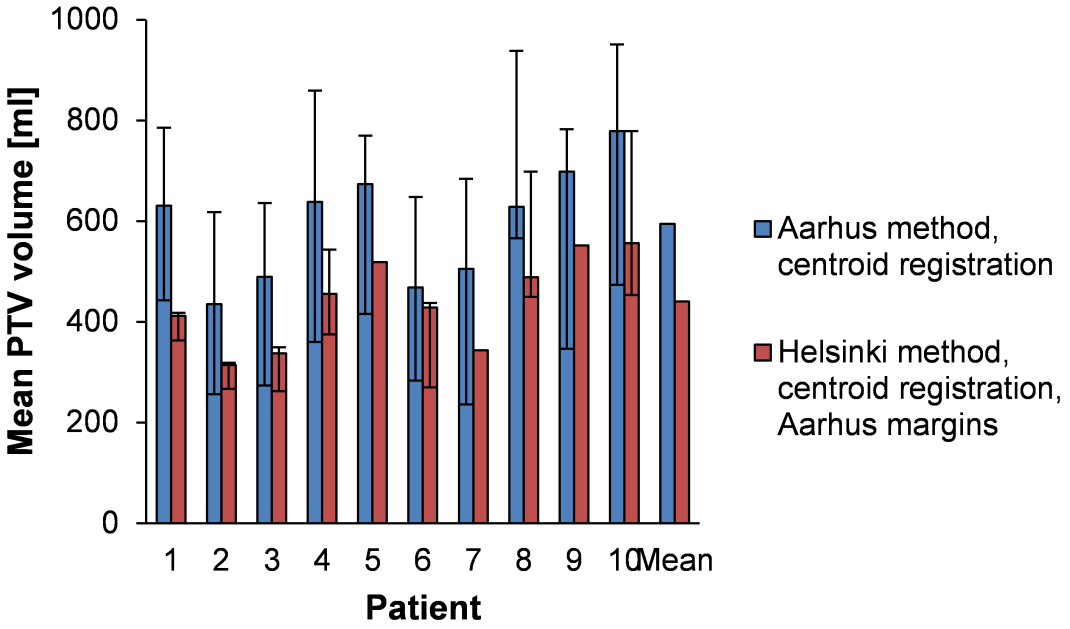

Figure 19: The volumes of the patients' PTVs chosen during the treatment averaged across the fractions. Comparison of the modified methods with centroid registration.

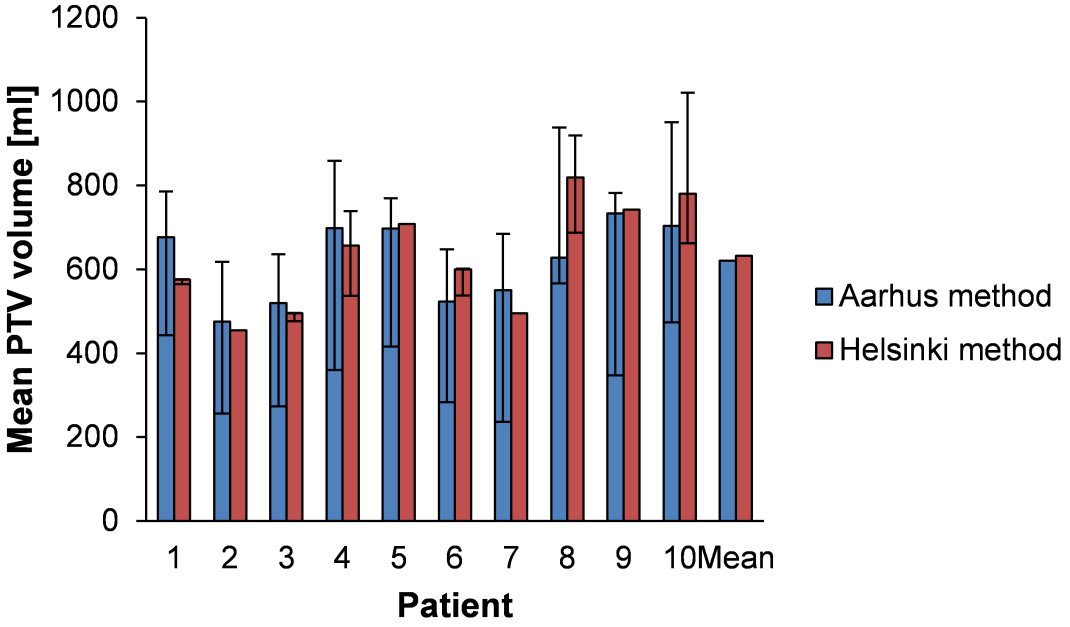

Figure 20: The volumes of the patients' PTVs chosen during the treatment averaged across the fractions. Comparison of the actual methods.

and thus the PTV volume decreases when the fraction number increases. The same tendency was observed with the Helsinki PTV volumes (correlation coefficients –0.11 for the non-modified method and –0.07 for the modified method with the centroid registration), but the correlation did not reach statistical significance. However, part of the adaption comes from the positioning of the PTV according to the bladder in the Helsinki method.

The correlation of the bladder volume to all PTV volumes was positive (0.45 and 0.47 for the non-modified and non-modified Aarhus methods and 0.44 and 0.33 for the modified and non-modified Helsinki methods) and the correlations reached statistical significance for all the methods ($p < 0.001$). This was logical, since the choices for the PTVs were made based on the daily bladders. There was also a significant positive correlation between the mean PTV volumes chosen according to each method, when the correlations were examined pairwise between all the methods ($p < 0.001$).

4.2.4 Plan selection frequencies in simulation and in treatment

To see if the simulation realistically represents the methods, the treatment plans used in the actual treatment were recorded. In the case of Helsinki method, only those patients were included (1, 2, 3, 4, 8, 9), who had not had a treatment of the lymph nodal regions. These patients had had a similar treatment as in the simulation, a treatment to the bladder with the Helsinki method with the soft-tissue registration (Figure 21a).

Compared to the treatment (Figure 21a), the selected plans in the simulation were larger and the distribution of the plan selections was less even (Figure 21b). The same tendency was observed when comparing the simulated (Figure 22b) and actual (Figure 22a) Aarhus method plan selections. The plan selections in treatment in AUH were obtained from the study of Vestergaard et al. [81] in order to see the typical plan selection frequencies in the treatment according to the Aarhus method. It needs to be emphasized that the patients in the treatment in AUH and the patients in this simulation were different and therefore, the frequencies are not as straightforwardly comparable than in the Helsinki method. The smaller plans were more often selected for treatment in the real treatment than in the simulation.

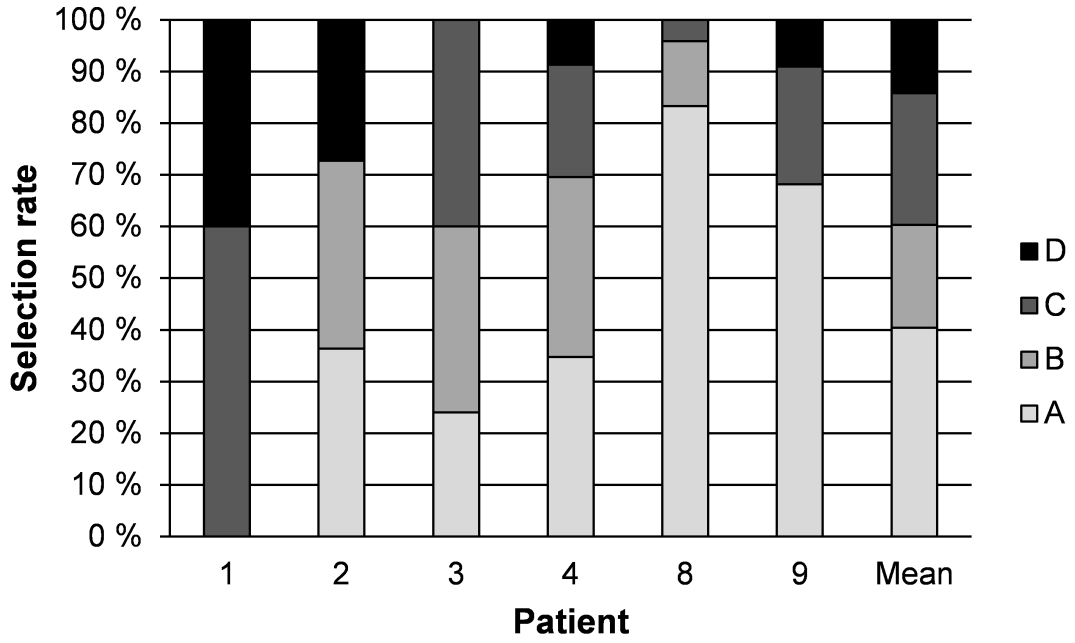

(a) HUCH treatment

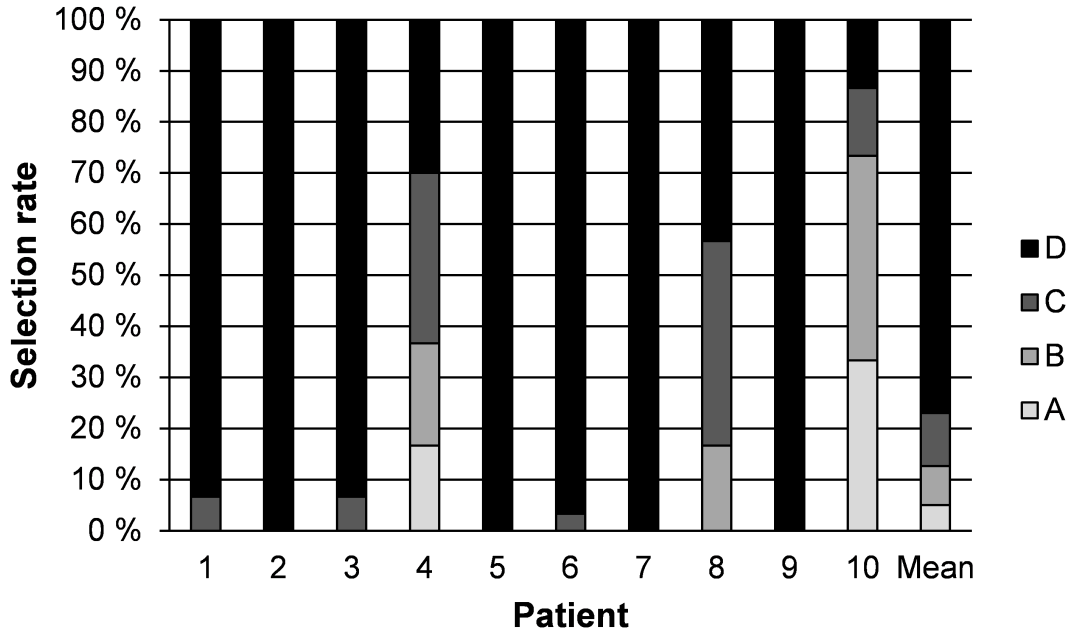

(b) HUCH simulation

Figure 21: (a) Plan selection rates in the actual treatment in HUCH for the patients who did not receive treatment of the lymph nodes. (b) Plan selection rates in the simulation according to Helsinki method.

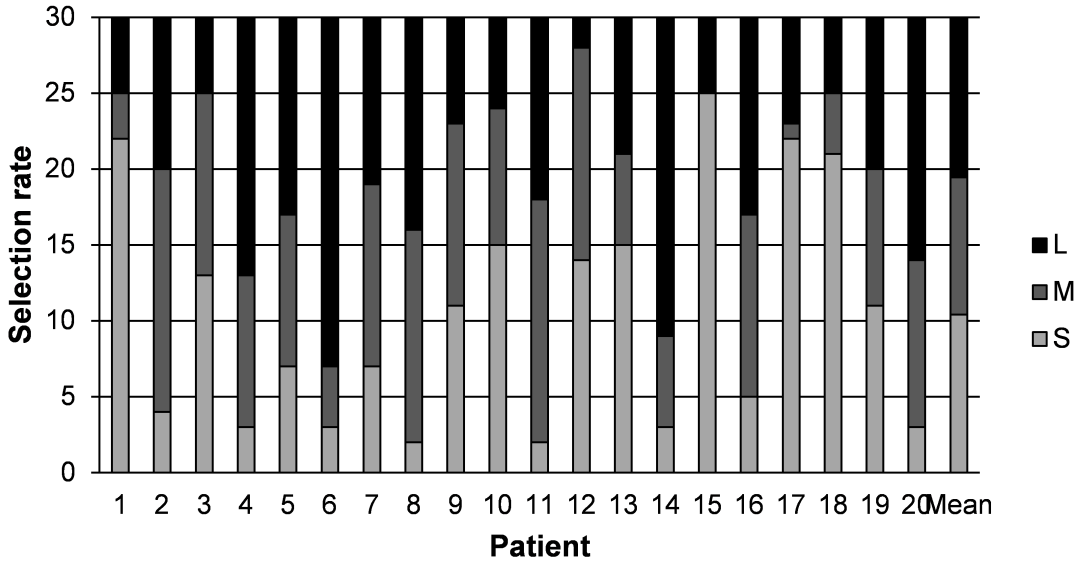

(a) Aarhus treatment

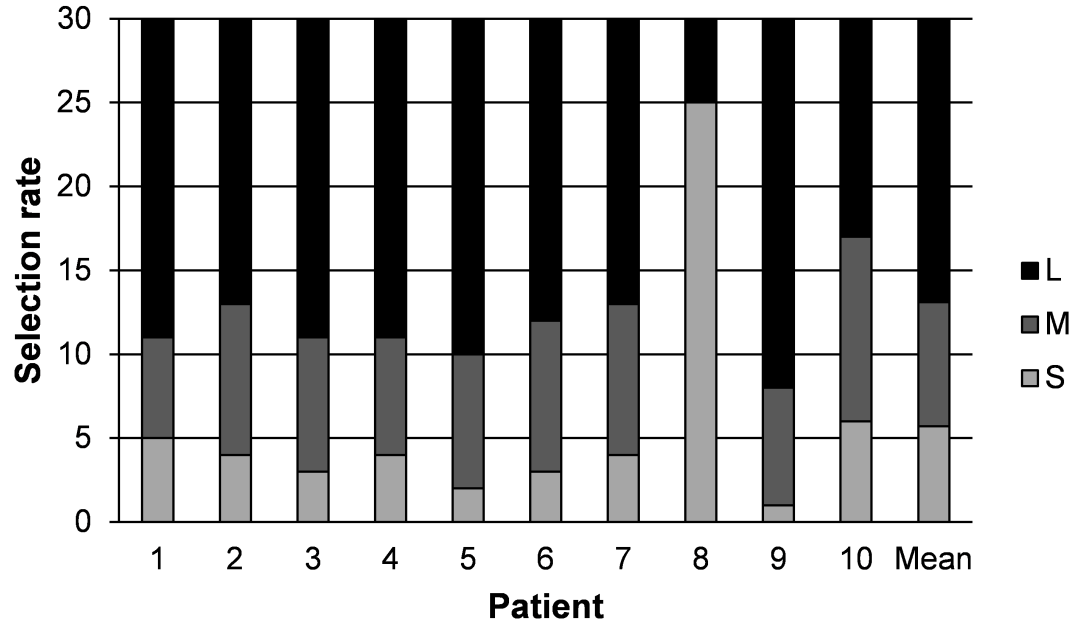

(b) Aarhus simulation

Figure 22: (a) Plan selection rates in the actual treatment in AUH. Modified from Ref. 81. (b) Plan selection rates in the simulation according to the Aarhus method. The patients in the comparison are different since the treatment according to the Aarhus method has been given in AUH. 13 of the AUH patients have also had their lymph nodes treated [81], but they can be included in the comparison since the Aarhus method employs bony-anatomy registration.

4.3 Translations between bony-anatomy and soft-tissue registration

The systematic shifts between bony-anatomy and soft-tissue registrations (mm) in different directions were listed for each patient (Figure 23). Some statistics of the displacements were calculated (Table 8).

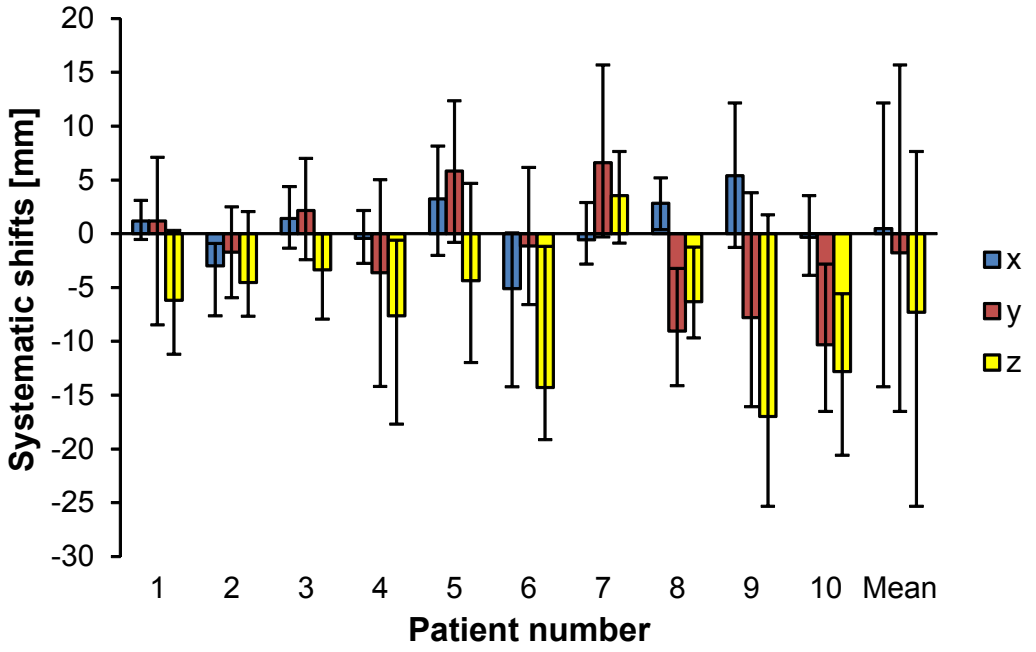

Figure 23: Mean shifts between the registration based on bony anatomy and that based on soft-tissue anatomy. The solid bars represent the mean shift in each direction. The error bars represent the range of shifts. Directions: x = left–right; y = anterior–posterior; z = superior–inferior.

Table 8: The displacements between the registrations based on bony anatomy and those based on soft-tissue anatomy.

	Mean displacement [mm]	Median displacement [mm]	Mean SD of patients [mm]	Maximum displacement (absolute value)[mm]
x: left–right	0.5	0.6	1.7	14.3
y: anterior–posterior	–1.8	–1.5	3.5	16.5
z: superior–inferior	–7.3	–6.5	3.4	25.3

4.4 The CTV–PTV margin for lymph node treatment with soft-tissue registration

The translations from soft-tissue anatomy to bony-anatomy registration coordinates were used to calculate the individual means and standard deviations of the error due to the soft-tissue registration in the hypothetical situation that the lymph nodes were treated with soft-tissue registration. From these quantities, the overall mean error $\mathbf{M}$, the standard deviation of the systematic error $\boldsymbol{\Sigma}$ and the standard deviation of the random error $\boldsymbol{\sigma}$ were calculated (Table 9).

Table 9: Individual means and standard deviations of the translations from bony anatomy to soft-tissue registration during treatment. Based on these figures, also the systematic mean error, the standard deviation of the systematic error, and the standard deviation of the random error were calculated. Directions: x: left–right, y: anterior–posterior, z: superior–inferior.

	Individual mean				Individual SD		
Direction	x	y	z		x	y	z
Patient	[mm]	[mm]	[mm]		[mm]	[mm]	[mm]
1	–1.2	–1.2	6.2		1.0	4.4	3.0
2	3.0	1.7	4.6		1.3	2.3	2.7
3	–1.4	–2.2	3.4		1.4	2.3	1.9
4	0.4	3.6	7.6		1.3	4.0	4.4
5	–3.2	–5.8	4.4		1.9	3.2	3.8
6	5.1	1.1	14.3		3.3	2.8	4.1
7	0.6	–6.6	–3.5		1.3	4.1	2.3
8	–2.9	9.0	6.3		1.0	2.6	1.9
9	–5.4	7.8	17.0		3.0	5.5	5.8
10	0.3	10.3	12.8		1.9	3.8	3.7
M	–0.5	1.8	7.3	$\boldsymbol{\sigma}$	1.9	3.7	3.6
$\boldsymbol{\Sigma}$	3.1	5.9	6.0				

The margin based on the formula (3) was calculated for all directions x, y and z. The margin in x direction was

$$\begin{aligned} m_{PTV,\mathrm{x}} &= 2.5\Sigma_{\mathrm{x}} + a + \beta\,(\sigma_{\mathrm{x}} - \sigma_{\mathrm{p}}) \\ &= 2.5 \cdot 3.1 \text{ mm} + 1.5 \text{ mm} + 0.52(1.9 \text{ mm} - 8.1 \text{ mm}) = 6.0 \text{ mm}. \end{aligned}$$

The margin widths in the y and z directions were calculated respectively by using the y and z direction values for the vector quantities. The margin widths in x, y and z directions were 6.0 mm, 14.1 mm and 9.1 mm, respectively. The success of the treatment fractions, were these margins used, was evaluated by checking whether the margin is larger than the absolute value of the translation (Figure 24). If the margin was inadequate, the treatment fraction was judged to be failed, even if a small miss usually does not have an impact on the resulting total dose, unless it is

repeated many times at the exactly same location. On average, 65% of the treatment fractions would have been successful, would the van Herk margin have been used.

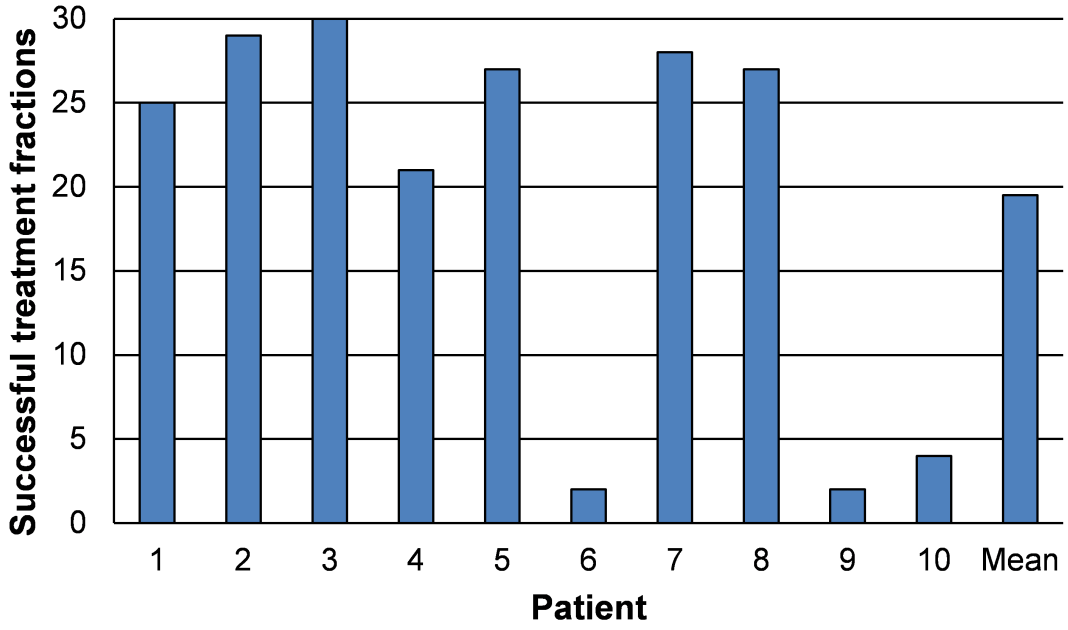

Figure 24: The number of successful treatment fractions with the margin of van Herk [21], listed for each individual patient.

5 Discussion

5.1 Bladder volumes observed during the treatment

The range of the bladder volumes observed during treatment was 42–343 ml. McBain et al. studied bladder volume variation with cine-MRI imaging. In their cohort of 10 patients they observed similar empty bladder volumes of the range from 55–395 ml. The imaging method is different and thus, the results should be interpreted carefully. It could be awaited that the bladder volumes observed during treatment would be larger than those observed when studying the empty bladder, since the treatment cannot always be given immediately after the patient has voided their bladder. In our study, this was not the case as the mean empty bladder volume in the planning CT scans was 147 ml and the mean CBCT bladder volume was 127 ml. A similar observation was made by Muren and colleagues [6]. Muren et al studied in total 129 repeat CT scans taken during the treatment of 20 patients and observed an overall mean bladder volume of 143 ml [6]. The average planning scan bladder volume was 206 ml [6].

In 67% of the CBCT scans, the bladder volume was smaller than in the CT scan with empty bladder. Similarly, in the study of Muren et al. the bladder volumes were smaller than in the planning situation in 85% of the repeat scans [6].

In this study, also a trend of decreasing bladder volumes during the treatment was observed. This trend was reported before by Pos and colleagues [63]. Mangar and co-workers [88] found the bladder filling rate and bladder size to have been unaffected by RT in their study but reported that the bladder filling rate could have been found to be decreasing due to RT, had more patients been included. Lebesque et al. found the bladder volume to decrease with time over the course of the treatment [89]. McBain et al. found significantly decreasing bladder volume during treatment in 5 of 20 patients and conducted that radiotherapy can directly influence the physical properties of the bladder in some cases [46]. A similar trend of bladder decrease during prostate cancer radiotherapy has been reported by many authors [90–94].

Yee and colleagues found a similar trend of bladder decrease [4]. They reported the CBCT-derived bladder and PTV volumes to be 10–17% smaller relative to those derived from the planning CT. Yee and co-workers estimated this to be a result of a combination of several factors. Firstly, the patient can develop a more consistent daily bladder-emptying routine prior to RT during the course of the treatment. Secondly, antitumour effects from RT may cause the bladder tumour to diminish, facilitating improved bladder emptying [4]. Thirdly, acute RT cystitis may increase the urinary frequency, which results in smaller bladder volumes during RT [4].

In some patients, exceptionally large bladder volumes were observed on some fractions even though the bladder volume variation was otherwise of a smaller range. These might be occasions when the patient has received chemotherapy. The hydration required prior to chemotherapy can increase the diuresis level and the bladder filling rate [95]. One potential limitation of this study is that the bladder contours were not delineated by a radiographer or an oncologist. However, the precision

should be adequate for the purpose of the comparison between two methods, which was the main goal of the study.

5.2 Modified methods

Combining the Helsinki method PSV formation method with the Aarhus method margins and the bony-anatomy registration led to high number of fractions where the largest PTV was inadequate. The number of fractions when the patient would have had to void their bladder again was 100 out of 300, which would have slowed down the treatment process immoderately. The combination of the PSV formation and the Aarhus margins resulted in clearly too small PTVs to be used if bony-anatomy registration is used.

Modifying the Helsinki method to employ Aarhus margins and the bony-anatomy registration was not successful, as the method did not function properly after the modifications. However, this analysis showed that if one wishes to use either of the methods, they should not be modified. Also, the result shows that when creating a method for adaptive radiotherapy of the bladder, one must consider precisely how to apply previously developed methods to the current situation. Even a modification that seems small can cause a large negative effect.

The other way to simulate the treatment with modified methods was to use the centroid registration for both methods. In the Helsinki method, there are four different plan selection volumes which are the bladder contours delineated in four CT images acquired every 15 minutes starting from the post-void situation. The Aarhus method PSVs are formed by using Boolean operations to achieve a composite volume of the bladders in the first four treatment CBCT images and the planning CT image, expanded with a 3-mm margin. In this simulation with the centroid registration, this same 3-mm margin was applied to the Helsinki method CTVs to form the PSVs.

The PSV formation method of HUCH was based on tracking the bladder filling pattern. That of Aarhus was based on tracking the day-to-day positional variance of the bladder. The other differences between the methods were equalized and the Helsinki method used the margins of the Aarhus method and centroid registration. The Aarhus method, on the other hand, employed centroid registration. When making these equalizations, the following results were observed. The planning target volumes chosen during the treatment in the simulation according to the Aarhus method were on average larger than those of the Helsinki method. On the other hand, there were some fractions with inadequate PTV volume with the Helsinki method. The plan selections were more evenly distributed according to the Aarhus method.

There were 22 fractions with the modified Helsinki method where the largest PTV volume was inadequate to cover the bladder of the day. Either the margins were insufficient or the centroid registration did not model the soft-tissue registration sufficiently. These factors probably both had an effect. Asking the patient to void again for 22 times out of 300 is still in the tolerable range and the method was hence found to work adequately to be compared with the modified Aarhus method.

The additional 3-mm margin made the plan selections of the Helsinki method more evenly distributed than in the simulation of the actual Helsinki method. It can be asked whether addition of this kind of a margin would be beneficial for the method. Apparently there were many fractions in the simulation of the actual clinically used Helsinki method, where the PSV volume was inadequate and the limiting factor would necessarily not have been the PTV volume. If the plan selection volumes are frequently too small even if the PTVs were not and thus cause the unnecessary selection of larger PTV volumes, this is of course an unwanted situation. However, the plan selections in the treatment have apparently been more evenly distributed than in the simulation and also the smaller PTVs have been selected.

5.3 The actual methods

The basic ideas behind Helsinki and Aarhus methods are different. The Helsinki method aims to record the individual pattern of bladder filling while Aarhus method is based on recording the day-to-day positional variation of the bladder. The strengths and possible weaknesses of the methods should be compared from these points of view.

The positional variation is accounted for in the Helsinki method by using the soft-tissue registration. The strength of this approach is that the planning target volumes can be smaller when they can be moved to an optimal position with respect to the bladder. Wright et al. found that an optimal translation with respect to the bladder did not increase healthy tissue irradiation in comparison to no translation [76]. Also, the optimal translation was superior in terms of normal tissue sparing, when optimizing the PTV margins based on the daily bladder. The soft-tissue registration is hence a logical option if one wishes to have the smallest possible PTV volume.

With the PTVs accounting for bladder volume variation due to filling, the method is not sensitive to those occasions when the bladder emptying has not been successful. Bladder cancer patients might have difficulties in emptying the bladder properly and asking the patient to go to the toilet again slows down the treatment, which can be an important issue in a busy radiotherapy department.

The downside of the soft-tissue registration is that it is infeasible when treating the lymph node areas. The lymph nodes remain in a stable position with respect to the bony anatomy and thus, the current practice is to register the treatment CBCT images to the treatment planning CT with the bony-anatomy registration when treating these areas. In this study, the margin widths required for treatment of the lymph nodal areas with soft-tissue registration were calculated and will be discussed later.

The benefits of the bony-anatomy registration are that it is easy to perform and that the lymph nodal areas can be treated at the same time without having to think about any additional margins to the lymph nodes. However, there might be a need for larger PTV options when registering the images based on bony anatomy and not based on the bladder.

The limitation of the PSV formation based on the bladder filling pattern is

that the optional PTVs are formed based on the situation of a single hour. If the situation is unrepresentative of the situation in the treatment (e.g. the rectum filling is exceptionally large), it might be difficult to find good options for the daily PTVs during the treatment. In this case, larger PTVs get chosen more often and even they might not be enough to suit the bladder. A renewed CT scan and treatment planning might be acquired.

Using the bladder positional variation during the first four fractions and the planning scan as a starting point for the target volume formation is more robust to the unrepresentative situations during one day. At worst, these situations merely cause unnecessary expansion of the treatment volume and not the need for re-planning. Five scans of the patient has been suggested to be optimal number of scans to form the PTV [96], with which a reasonable part of the bladder positional variation is captured to the composite volumes. This is essential, since the registration based on bony anatomy does not in itself account for the variation of the bladder position.

One suboptimal issue in the Aarhus method is that it requires a week of irradiation with larger margins. However, they have suggested giving the boost treatment during the first week eliminating the need for the larger margins during the first few fractions [81].

The actual Helsinki and Aarhus methods used in the treatment were compared as such, non-modified. The comparison showed no statistically significant difference between the methods. However, in the simulation according to the Aarhus method, the selection frequencies of the alternative planning target volumes were more evenly distributed, as for the Helsinki method, the large planning target volumes were the most frequently selected. Based on this study, both methods are equal in terms of normal tissue sparing, which is an encouraging result. Additional confidence in the result would be achieved by including more patients to the comparison. The respective studies have had similar numbers of patients (Table 3). The group of 10 patients included in this study was thought to be adequate but a larger group would have been challenging, as the bladder delineation is time-consuming. The PTV volume is a good measure of the healthy tissue irradiation, but to be able to get more detailed information on the doses to specific normal tissues, it would be interesting to calculate the daily dose distributions.

One limitation in the objectivity of the comparison was the lack of an automatic soft-tissue registration algorithm, that is available on the treatment machine in HUCH. The plan selections according to the Helsinki method based on soft-tissue anatomy were done by using the centroid registration as a starting point and trying to make as little translation as possible. However, basically the optimal position of the bladder could be searched arbitrarily. At the treatment machine, the radiographers can make adjustments to the result of the automatic registration. Careful consideration was obeyed when making adjustments, keeping the reasonable scale of translations in mind. The Aarhus method simulation based on bony-anatomy matching did not have this same limitation.

The plan selection frequencies in treatment and in the simulation were compared to see how well the simulation represented the clinical situation for both Aarhus and Helsinki methods. An interesting observation was that the largest PTV alternatives

are the ones the most frequently chosen, as the frequencies of the treatment plans chosen in the real treatment are not like this. Before drawing any conclusions of the methods and in which situations each of them should be applied, one has to consider how well the simulation represents the methods in treatment.

The PTVs used in the treatment are always situation-based and depend on the decisions made by the physician. This is known to be the situation at least in HUCH and this kind of variation exists also in AUH [81]. Therefore, the size of the volumes used in the simulation and those used in the treatment might differ.

In the comparison of the plan selection frequencies between simulation and treatment according to the Helsinki method, the amount of data of the plan selection rates in the treatment was modest. This was due to the fact that some patients included in the study (patients 5, 6, 7 and 10) had received a treatment of the lymph nodal areas in addition to the whole bladder irradiation. With these patients, the planning target volumes naturally differ drastically between the simulation and treatment and since also the registration method in these cases differed from the reported method, these patients were decided to be left out of the analysis. The remaining data for six patients may not be enough to give a comprehensive view on the plan selection frequencies in HUCH in general. However, the comparison was considered to give some idea of how well the study simulated the real situation.

For Aarhus method, there was more data to compare the simulated plan selections with. In a recent study of Vestergaard et al., the plan selection frequencies during the treatment of 20 patients were reported [81]. The patients in the treatment were thus not the same as in the simulation. Individual differences occur but in addition to those, there might be differences between the AUH and HUCH protocols. As many as 13 patients of this group had received lymph node treatment in addition to whole bladder irradiation [81], but the patients could be included in this comparison, because Aarhus method employs bony-anatomy registration. Naturally, treating the pelvic lymph nodes added extra space to the bladder PTV especially in the cranial direction where the lymph nodal PTV and bladder PTV overlap.

In AUH, patients are given frequent feedback of the bladder emptying success of the day and also, if the bladder emptying seems not to have been successful, the patient is sent to the toilet. The Helsinki method PTVs, on the other hand, are formed based on the bladder filling pattern of the patient and even though the patients are instructed to come to the treatment with an empty bladder, the patient is not necessarily asked to void again in case of an unexpected delay between the voiding and the treatment. Since the simulation is done with imaging information of the HUCH patients, the Aarhus method requirements of a totally empty bladder might not be fulfilled, increasing the chosen PTV volumes. One additional difference to be considered is that in AUH, rotational corrections around the anterior–posterior axis are possible whereas this simulation included only translational corrections. It should be mentioned, though, that the possibility to correct the couch rotational deviations is a relatively new addition to the AUH protocol. Hence, some of the patients in the Vestergaard and colleagues' study [81] might have been treated without correcting the couch rotation around the anterior–posterior axis.

During the treatment, different people make decisions of the plans of the day.

The criteria for plan selection might not have been exactly the same despite the instructions. At least in HUCH there has been some evolution in the protocol for plan selection. It was reported in the paper of Tuomikoski et al. [9] that the plan selection was done by seeing that the bladder of the day fit into the PTV with a margin of 3 mm, at that time thought to sufficiently account for the intrafractional bladder filling. Hence, it is not straightforward to compare these plan selection frequencies.

The level of uniformity of the protocols might be different in AUH and HUCH, since it is reported that the people working with the adaptive treatments all have to take a course in AUH [81]. However, for both methods, inter-observer variation might affect the plan selections in the treatment. In the simulation this inter-observer variability is eliminated, since all the decisions about the plans are made by a single observer. The variability is further decreased by having the CBCT bladder contours visible during plan selection. Observing if the bladder contours fit inside the plan selection volume makes the procedure reproducible and reduces errors. However, this might not represent the real life plan selection, where one pixel of the bladder can be outside the plan selection volume and is left unnoticed. An error of this scale is insignificant to the treatment result. Also, the imprecision of the hand while delineating the bladder might lead to situations where the bladder contour crosses the plan selection volume contour and leads to selection of a larger PTV volume even if the border of the bladder would in reality have fitted into the PSV. This is true for Aarhus method as well as for the Helsinki method.

One reason for the selection of on average larger PTVs in the Helsinki method simulation might also be that in the group of 10 patients included to the study, there were two patients with a peculiar-shaped elongated bladder. If the bladder is in a different position in the planning CT image than in the treatment, the effect is larger with an unusually long bladder, compared to the regularly shaped one. The special shape of the bladder is better accounted for in the Aarhus method, where the composite volumes of the bladders during the first fractions are more likely to compensate for the effects of bladder form changes. An unrepresentative planning scan situation may have stronger effects on the success of the Helsinki method, and also in this simulation there was at least one patient with rectum filling during the planning CT scans.

5.4 The CTV–PTV margin for lymph node treatment with soft-tissue registration

The formula (3) which was introduced by van Herk [21] accounts for only the deviations of the random and systematic errors and assumes the mean systematic error $\mathbf{M}$ to be small [16]. The authors note that this error often deviated significantly from zero because of inaccuracy of the equipment (lasers) and procedure [16]. These deviations are small.

The situation in this simulation of the treatment including the lymph nodes is a bit different from the prerequisites of van Herk and co-workers [16]. In this case, we intentionally correct the error in the bladder positioning and therefore produce an

error to the lymph nodes. Thus, for the lymph nodes, the mean error **M** deviates from zero in all directions. The magnitude of the mean translation on a population basis is unknown and cannot be determined with the sample of 10 patients included into this study. It would thus require additional analyses to clarify whether the formula of van Herk (3) [21] is truly applicable to this situation.

For the purposes of this simulation, the van Herk formula (3) is adequate, since the systematic error correction would not have to increase the margin. A reasonable strategy to take the systematic error into account, margin would be added in the direction of the error and reduced from the opposite side. Of course, the direction of the error would be hard to estimate in advance, but for the simulation of the lymph node treatment with the soft-tissue registration, the van Herk margin is a good guess for the margin width extending the PTV.

Van Herk et al. calculated their margin recipe on the basis of a dose–population histogram and it should ensure that for 90% of the patient population, the minimum dose to the CTV must be 95% of the nominal dose or higher [21]. If this requirement is filled or not, is difficult to estimate based on this approach of merely comparing two digits. If, for example, the bladder would on one treatment fraction be 1 mm out of the PTV, this would not have a devastating effect in reality. However, when just checking if the margin is larger than the translation, this fraction would be judged as missed. Therefore, it is likely that the calculated margin would in fact lead to the situation defined by van Herk. On average 65% of the treatment fractions were judged to succeed in this analysis and it is likely that considering the severity of the misses, the goal set by van Herk [21] could be achieved.

The margin was not sufficient for patients 6, 9 and 10. There were only 2 successful treatment fractions for patients 6 and 9 and 4 successful treatment fractions for patient 10. These patients had a large positive mean shift (14.3 mm, 17.0 mm and 12.8 mm) in the z-direction. This indicates that CBCT image was moved cranially when changing the registration from the bony-anatomy registration to soft-tissue registration. The other patients had much smaller translations in the z-direction (Figure 23).

The margin widths calculated with the van Herk formula (3) were realistic (the margin in x, y and z-directions 6.0 mm, 14.1 mm and 9.1 mm, respectively). There are two options: to add a larger margin to the lymph nodal areas and match based on the bladder or to add a larger margin to the bladder and register the images based on the bony anatomy. The treated volume can be reduced if the latter option is chosen. Hence, those patients whose condition requires treatment of the lymph nodes should have the treatment CBCT-images and the treatment planning CT image registered based on the bony anatomy, which is the current practice also in HUCH, where soft-tissue registration is usually employed. One option would be to use the Aarhus method in the cases when the bony-anatomy registration has to be applied, since the method already employs matching based on the bones.

6 Conclusions

Urinary bladder adaptive radiotherapy has been shown to both avoid target misses by increasing precision and enable smaller target volumes in the treatment. This leads to fewer side effects and can enable dose escalation, which has been suggested to improve the outcome of the bladder cancer radiotherapy. However, up to this point, no consensus of the optimal strategy of adaptive bladder radiotherapy has been reached.

In this study two bladder ART methods were compared by means of a simulated treatment. The Helsinki method was based on tracking the individual bladder filling pattern of the patient. The bladder contours with different filling status were used to form the alternative CTVs. The idea of the Aarhus method was to record the bladder positional variations during the first fractions of treatment and to use these in order to form the CTVs. For 10 patients, the bladder contours in CBCT images of 30 treatment fractions were contoured. Using these contours as an objective measure of whether the bladder of the day fit inside the plan selection volume contour, the daily PTVs were chosen according to both methods.

The original aim was to study the impact of the PSV formation method to the results. The way to form the PSV was one of the three differences between the methods. The other differences were the PSV–PTV margins and the method to register the treatment planning CT to the treatment CBCT images when adjusting the patient's position. The aim was to equalize the other differences between the methods to be able to solely compare the impact of the PSV formation method.

The first way to equalize the differences between the methods was to employ bony-anatomy registration and Aarhus method margins for both methods. This combination with the Helsinki PSV formation method resulted in clearly too small PTVs and the comparison with the Aarhus method would not have been reasonable.

Since the comparison using Aarhus method margins and registration methods was unsuccessful, the second option to compare the methods was to still use Aarhus method margins, but to register the images based on soft tissues as in the Helsinki method. It was thought that if soft-tissue registration would be used for both methods in the comparison, the objectivity of the matching would be hard to ensure. There was no automatic algorithm available for this simulation, although the registration of the images is done automatically on the treatment machine. A compromise was made to use the centroid registration, where the mass gravity centres of the bladder and PSV contours would coincide, for both methods. The Aarhus method margins were again used for both methods.

Using centroid registration had only a minor effect on the Aarhus method. The Helsinki PSV formation method, however, combined with the centroid registration and the Aarhus margins resulted in significantly smaller PTV volumes compared to the modified Aarhus method with the centroid registration. The PTVs were evenly selected in the simulation of both methods, but even more so according to the Aarhus method, where also the smaller PTVs were chosen more often.

In addition to the comparison of the modified methods, the methods were compared as such, as used in the treatment. There was no statistically significant

difference between the methods in terms of normal tissue sparing. The plans were again distributed more evenly according to the Aarhus method. It was noticed that the plan selections included the smaller alternative plans more often according to the modified Helsinki method where the PSV is formed by expanding the CTV with a 3-mm margin than according to the actual method where the PSV is the CTV. Thus, it might be a reasonable improvement to the Helsinki method to increase the plan selection volume margin. However, the plan selections in the actual treatment were compared to the simulation and it was observed that the smaller plans had been more frequently selected in the treatment than in the simulation. The daily bladder contours used in the simulation for the sake of objectivity might have had an effect on the plan selection frequencies, which on the other hand might have had an effect on the mean PTV volumes. It would be useful to repeat the analysis without having the contours visible to see how the plan selection would be without contours, even with concerns of objectivity.

Both methods have their strengths as well as their downsides. The soft-tissue registration of the Helsinki method is a logical choice if one wishes to get the full potential out of image guidance. Also, since the Helsinki method is based on tracking the bladder filling pattern, empty bladder is not necessarily required to the treatment, which can be beneficial when treating patients with urinary deficiency. In Aarhus those patients who have difficulties in consistently voiding their bladder would benefit of a treatment according to the Helsinki method.

The simulation of treatment with soft-tissue match encouraged to continue using the bony-anatomy match when treating the lymph nodal regions in addition to whole bladder irradiation. This is the practice in HUCH. However, it is not clear whether the mean volume of the selected planning target volumes is the same according to the Helsinki method using soft-tissue registration and the bony-anatomy match and thus, one cannot know if a similar reduction of treatment volumes can be gained with the bone registration combined with the Helsinki method. With the Aarhus methods these patients would get the treatment according to a well established protocol that is designed to work with bony-anatomy registration. I recommend using the Aarhus method for these patients.

The Aarhus method is not as sensitive as the Helsinki method to an unrepresentative situation in the planning scan. For HUCH I would suggest replanning the treatment according to the Aarhus method in the cases when there is reason to believe that the planning scan failed to represent the treatment situation. The first week's treatment could be given with the Helsinki method and if the largest PTV had been frequently selected merely because the patient's anatomy had changed from the treatment planning CT, the Aarhus PTVs could be designed based on the first CBCT scans. However, it needs to be emphasised that this hasn't frequently occurred in treatment.

The main finding of this study was that there was no difference in the mean PTV volume for the study population of 10 patients. Since both Helsinki and Aarhus methods have been found to result in diminished small bowel irradiation compared to the conventional bladder cancer radiotherapy treatment, no method can be judged superior to the other regardless of the situation.

References

[1] Leong J. Implementation of random positioning error in computerised radiation treatment planning systems as a result of fractionation. Physics in medicine and biology. 1987;32(3):327–334.

[2] van Herk M. Different styles of image-guided radiotherapy. Seminars in radiation oncology. 2007;17(4):258–267.

[3] Mangar S, Thompson A, Miles E, Huddart R, Horwich A, Khoo V. A feasibility study of using gold seeds as fiducial markers for bladder localization during radical radiotherapy. The British Journal of Radiology. 2007a;80:279–283.

[4] Yee D, Parliament M, Rathee S, Ghosh S, Ko L, Murray B. Cone beam CT imaging analysis of interfractional variations in bladder volume and position during radiotherapy for bladder cancer. International Journal of Radiation Oncology Biology Physics. 2010;76(4):1045–1053.

[5] Mangar S, Miller N, Khoo V, Hansen V, McNair H, Horwich A, et al. Evaluating inter-fractional changes in volume and position during bladder radiotherapy and the effect of volume limitation as a method of reducing the internal margin of the planning target volume. Clinical Oncology. 2008;20(9):698–704.

[6] Muren LP, Smaaland R, Dahl O. Organ motion, set-up variation and treatment margins in radical radiotherapy of urinary bladder cancer. Radiotherapy and Oncology. 2003;69(3):291–304.

[7] Pos FJ, Hart G, Schneider C, Sminia P. Radical radiotherapy for invasive bladder cancer: What dose and fractionation schedule to choose? International Journal of Radiation Oncology Biology Physics. 2006;64(4):1168–1173.

[8] Yan D, Vicini F, Wong J, Martinez A. Adaptive radiation therapy. Physics in medicine and biology. 1997;42(1):123–132.

[9] Tuomikoski L, Collan J, Keyriläinen J, Visapää H, Saarilahti K, Tenhunen M. Adaptive radiotherapy in muscle invasive urinary bladder cancer–an effective method to reduce the irradiated bowel volume. Radiotherapy and Oncology. 2011;99(1):61–66.

[10] Vestergaard A, Søndergaard J, Petersen JB, Høyer M, Muren LP. A comparison of three different adaptive strategies in image-guided radiotherapy of bladder cancer. Acta Oncologica. 2010;49(7):1069–1076.

[11] Lahtinen T, Holsti LR, Grénman R. Kliininen säteilybiologia. Duodecim; 1997.

[12] Langen K, Jones D. Organ motion and its management. International Journal of Radiation Oncology Biology Physics. 2001;50(1):265–278.

[13] Karzmark C, Nunan CS, Tanabe E. Medical electron accelerators. McGraw-Hill, Incorporated, Health Professions Division; 1993.

[14] Khan FM. The physics of radiation therapy 4th ed. Lippincott Williams & Wilkins; 2010.

[15] Wilkinson JM. Geometric uncertainties in radiotherapy. British Institute of Radiology; 2003.

[16] Van Herk M. Errors and margins in radiotherapy. Seminars in radiation oncology. 2004;14(1):52–64.

[17] ICRU Report 83. Prescribing, Recording, and Reporting Photon-Beam Intensity-Modulated Radiation Therapy (IMRT). International Commission on Radiation Units and Measurement: Bethesda, MD, USA; 2010.

[18] ICRU Report 50. Prescribing, Recording, and Reporting Photon-Beam Therapy. International Commission on Radiation Units and Measurement: Bethesda, MD, USA; 1993.

[19] Ketting CH, Austin-Seymour M, Kalet I, Unger J, Hummel S, Jacky J. Consistency of three-dimensional planning target volumes across physicians and institutions. International Journal of Radiation Oncology Biology Physics. 1997;37(2):445–453.

[20] Meijer GJ, Rasch C, Remeijer P, Lebesque JV. Three-dimensional analysis of delineation errors, setup errors, and organ motion during radiotherapy of bladder cancer. International Journal of Radiation Oncology Biology Physics. 2003;55(5):1277–1287.

[21] van Herk M, Remeijer P, Rasch C, Lebesque JV. The probability of correct target dosage: dose-population histograms for deriving treatment margins in radiotherapy. International Journal of Radiation Oncology Biology Physics. 2000;47(4):1121–1135.

[22] van Herk M, Remeijer P, Lebesque JV. Inclusion of geometric uncertainties in treatment plan evaluation. International Journal of Radiation Oncology Biology Physics. 2002;52(5):1407–1422.

[23] Engelsman M, Damen EM, De Jaeger K, van Ingen KM, Mijnheer BJ. The effect of breathing and set-up errors on the cumulative dose to a lung tumor. Radiotherapy and Oncology. 2001;60(1):95–105.

[24] Shimizu S, Shirato H, Kitamura K, Shinohara N, Harabayashi T, Tsukamoto T, et al. Use of an implanted marker and real-time tracking of the marker for the positioning of prostate and bladder cancers. International Journal of Radiation Oncology Biology Physics. 2000;48(5):1591–1597.

[25] Chai X, van Herk M, van de Kamer JB, Remeijer P, Bex A, Betgen A, et al. Behavior of lipiodol markers during image guided radiotherapy of bladder cancer. International Journal of Radiation Oncology Biology Physics. 2010;77(1):309–314.

[26] Mohan DS, Kupelian PA, Willoughby TR. Short-course intensity-modulated radiotherapy for localized prostate cancer with daily transabdominal ultrasound localization of the prostate gland. International Journal of Radiation Oncology Biology Physics. 2000;46(3):575–580.

[27] Mackie TR. History of tomotherapy. Physics in medicine and biology. 2006;51(13):R427–R453.

[28] Court L, Rosen I, Mohan R, Dong L. Evaluation of mechanical precision and alignment uncertainties for an integrated CT/LINAC system. Medical physics. 2003;30(6):1198–1210.

[29] Jaffray DA, Siewerdsen JH, Wong JW, Martinez AA. Flat-panel cone-beam computed tomography for image-guided radiation therapy. International Journal of Radiation Oncology Biology Physics. 2002;53(5):1337–1349.

[30] Pouliot J, Bani-Hashemi A, Chen J, Svatos M, Ghelmansarai F, Mitschke M, et al. Low-dose megavoltage cone-beam CT for radiation therapy. International Journal of Radiation Oncology Biology Physics. 2005;61(2):552–560.

[31] On target: ensuring geometric accuracy in radiotherapy. The Royal College of Radiologists, Society and College of Radiographers, Institute of Physics and Engineering in Medicine; 2008.

[32] McKenzie AL, van Herk M, Mijnheer B. The width of margins in radiotherapy treatment plans. Physics in medicine and biology. 2000;45(11):3331–3342.

[33] Goldman LW. Principles of CT and CT technology. Journal of nuclear medicine technology. 2007;35(3):115–128.

[34] Ginat DT, Gupta R. Advances in Computed Tomography Imaging Technology. Annual Review of Biomedical Engineering. 2014;16(1):431–453.

[35] Goldman LW. Principles of CT: radiation dose and image quality. Journal of nuclear medicine technology. 2007;35(4):213–225.

[36] Barrett JF, Keat N. Artifacts in CT: Recognition and Avoidance. Radiographics. 2004;24(6):1679–1691.

[37] Hämäläinen T. Laadunvalvonta: Kiihdyttimet. Helsingin ja Uudenmaan sairaanhoitopiiri. HYKS Syöpätautien klinikka; 2009.

[38] Fiorino C, Reni M, Bolognesi A, Cattaneo GM, Calandrino R. Intra-and inter-observer variability in contouring prostate and seminal vesicles: implications for conformal treatment planning. Radiotherapy and Oncology. 1998;47(3):285–292.

[39] Nishioka K, Shimizu S, Kinoshita R, Inoue T, Onodera S, Yasuda K, et al. Evaluation of inter-observer variability of bladder boundary delineation on cone-beam CT. Radiation Oncology. 2013;8(1):185–191.

[40] Foroudi F, Wong J, Haworth A, Baille A, McAlpine J, Rolfo A, et al. Offline adaptive radiotherapy for bladder cancer using cone beam computed tomography. Journal of medical imaging and radiation oncology. 2009;53(2):226–233.

[41] Samuelsson A, Mercke C, Johansson KA. Systematic set-up errors for IMRT in the head and neck region: effect on dose distribution. Radiotherapy and Oncology. 2003;66(3):303–311.

[42] Worthy D, Wu Q. Dosimetric assessment of rigid setup error by CBCT for HN-IMRT. Journal of Applied Clinical Medical Physics. 2010;11(3):38–63.

[43] Varian Medical Systems. Eclipse Algorithms Reference Guide, Version 86. Palo Alto, USA; 2008.

[44] Sädehoidon laitteiden käytönaikaiset hyväksyttävyysvaatimukset. Säteilyturvakeskus, Helsinki; 2011.

[45] Muren LP, Smaaland R, Dahl O. Conformal radiotherapy of urinary bladder cancer. Radiotherapy and Oncology. 2004;73(3):387–398.

[46] McBain CA, Green M, Stratford J, Davies J, McCarthy C, Taylor B, et al. Ultrasound imaging to assess inter-and intra-fraction motion during bladder radiotherapy and its potential as a verification tool. Clinical Oncology. 2009;21(5):385–393.

[47] McBain CA, Khoo VS, Buckley DL, Sykes JS, Green MM, Cowan RA, et al. Assessment of bladder motion for clinical radiotherapy practice using cine–magnetic resonance imaging. International Journal of Radiation Oncology Biology Physics. 2009;75(3):664–671.

[48] Jaffray D, Siewerdsen J. Cone-beam computed tomography with a flat-panel imager: initial performance characterization. Medical physics. 2000;27(6):1311–1323.

[49] Weiss E, Wu J, Sleeman W, Bryant J, Mitra P, Myers M, et al. Clinical evaluation of soft tissue organ boundary visualization on cone-beam computed tomographic imaging. International Journal of Radiation Oncology Biology Physics. 2010;78(3):929–936.

[50] Li T, Schreibmann E, Yang Y, Xing L. Motion correction for improved target localization with on-board cone-beam computed tomography. Physics in medicine and biology. 2006;51(2):253–267.

[51] Smitsmans MH, Pos FJ, de Bois J, Heemsbergen WD, Sonke JJ, Lebesque JV, et al. The influence of a dietary protocol on cone beam CT–guided radiotherapy for prostate cancer patients. International Journal of Radiation Oncology Biology Physics. 2008;71(4):1279–1286.

[52] Joensuu H, Roberts PJ, Kellokumpu-Lehtinen PL, Jyrkkiö S, Kouri M, Teppo L, et al. Syöpätaudit. 5., uudistettu painos. Helsinki: Kustannus Oy Duodecim; 2013.

[53] Sengeløv L, von der Maase H. Radiotherapy in bladder cancer. Radiotherapy and Oncology. 1999;52(1):1–14.

[54] Pos F, Remeijer P; Elsevier. Adaptive management of bladder cancer radiotherapy. Seminars in radiation oncology. 2010;20(2):116–120.

[55] Fokdal L, Høyer M, von der Maase H. Radical radiotherapy for urinary bladder cancer: treatment outcomes. Expert Review of Anticancer Therapy. 2006;6(2):269–279.

[56] Milosevic M, Gospodarowicz M, Zietman A, Abbas F, Haustermans K, Moonen L, et al. Radiotherapy for bladder cancer. Urology. 2007;69(1):80–92.

[57] Harris S, Buchanan R. An audit and evaluation of bladder movements during radical radiotherapy. Clinical Oncology. 1998;10(4):262–264.

[58] Miralbell R, Nouet P, Rouzaud M, Bardina A, Hejira N, Schneider D. Radiotherapy of bladder cancer: relevance of bladder volume changes in planning boost treatment. International Journal of Radiation Oncology Biology Physics. 1998;41(4):741–746.

[59] Fokdal L, Honoré H, Høyer M, Meldgaard P, Fode K, von der Maase H. Impact of changes in bladder and rectal filling volume on organ motion and dose distribution of the bladder in radiotherapy for urinary bladder cancer. International Journal of Radiation Oncology Biology Physics. 2004;59(2):436–444.

[60] Lotz HT, Pos FJ, Hulshof MC, van Herk M, Lebesque JV, Duppen JC, et al. Tumor motion and deformation during external radiotherapy of bladder cancer. International Journal of Radiation Oncology Biology Physics. 2006;64(5):1551–1558.

[61] Tuomikoski L, Korhonen J, Collan J, Keyriläinen J, Visapää H, Sairanen J, et al. Implementation of adaptive radiation therapy for urinary bladder carcinoma: Imaging, planning and image guidance. Acta Oncologica. 2013;52(7):1451–1457.

[62] Turner SL, Swindell R, Bowl N, Marrs J, Brookes B, Read G, et al. Bladder movement during radiation therapy for bladder cancer: implications for treatment planning. International Journal of Radiation Oncology Biology Physics. 1997;39(2):355–360.

[63] Pos FJ, Koedooder K, Hulshof MC, van Tienhoven G, González González D. Influence of bladder and rectal volume on spatial variability of a bladder tumor during radical radiotherapy. International Journal of Radiation Oncology Biology Physics. 2003;55(3):835–841.

[64] Sur R, Clinkard J, Jones W, Taylor R, Close H, Chaturvedi A, et al. Changes in target volume during radiotherapy treatment of invasive bladder carcinoma. Clinical Oncology. 1993;5(1):30–33.

[65] Muren LP, Redpath AT, Lord H, McLaren D. Image-guided radiotherapy of bladder cancer: bladder volume variation and its relation to margins. Radiotherapy and Oncology. 2007;84(3):307–313.

[66] Madersbacher S, Pycha A, Schatzl G, Mian C, Klingler CH, Marberger M. The aging lower urinary tract: a comparative urodynamic study of men and women. Urology. 1998;51(2):206–212.

[67] Nordling J. The aging bladder – a significant but underestimated role in the development of lower urinary tract symptoms. Experimental gerontology. 2002;37(8):991–999.

[68] DuBeau CE. The aging lower urinary tract. The Journal of urology. 2006;175(3):S11–S15.

[69] Pos F, Bex A, Dees-Ribbers HM, Betgen A, van Herk M, Remeijer P. Lipiodol injection for target volume delineation and image guidance during radiotherapy for bladder cancer. Radiotherapy and Oncology. 2009;93(2):364–367.

[70] Meijer GJ, van der Toorn PP, Bal M, Schuring D, Weterings J, de Wildt M. High precision bladder cancer irradiation by integrating a library planning procedure of 6 prospectively generated SIB IMRT plans with image guidance using lipiodol markers. Radiotherapy and Oncology. 2012;105(2):174–179.

[71] Hulshof MC, van Andel G, Bel A, Gangel P, van de Kamer JB. Intravesical markers for delineation of target volume during external focal irradiation of bladder carcinomas. Radiotherapy and Oncology. 2007;84(1):49–51.

[72] Dahl O, Kardamakis D, Lind B, Rosenwald JC. Current status of conformal radiotherapy. Acta Oncologica. 1996;35(S8):41–57.

[73] Fokdal L, Høyer M, von der Maase H. Treatment outcome and prognostic variables for local control and survival in patients receiving radical radiotherapy for urinary bladder cancer. Acta Oncologica. 2004;43(8):749–757.

[74] Kavanagh BD, Pan CC, Dawson LA, Das SK, Li XA, Ten Haken RK, et al. Radiation dose–volume effects in the stomach and small bowel. International Journal of Radiation Oncology Biology Physics. 2010;76(3):S101–S107.

[75] Redpath AT, Muren LP. CT-guided intensity-modulated radiotherapy for bladder cancer: isocentre shifts, margins and their impact on target dose. Radiotherapy and Oncology. 2006;81(3):276–283.

[76] Wright P, Redpath AT, Høyer M, Grau C, Muren LP. The normal tissue sparing potential of adaptive strategies in radiotherapy of bladder cancer. Acta Oncologica. 2008;47(7):1382–1389.

[77] Lalondrelle S, Huddart R, Warren-Oseni K, Hansen VN, McNair H, Thomas K, et al. Adaptive-predictive organ localization using cone-beam computed tomography for improved accuracy in external beam radiotherapy for bladder cancer. International Journal of Radiation Oncology Biology Physics. 2011;79(3):705–712.

[78] Burridge N, Amer A, Marchant T, Sykes J, Stratford J, Henry A, et al. Online adaptive radiotherapy of the bladder: small bowel irradiated-volume reduction. International Journal of Radiation Oncology Biology Physics. 2006;66(3):892–897.

[79] Foroudi F, Wong J, Kron T, Rolfo A, Haworth A, Roxby P, et al. Online adaptive radiotherapy for muscle-invasive bladder cancer: results of a pilot study. International Journal of Radiation Oncology Biology Physics. 2011;81(3):765–771.

[80] Vestergaard A, Muren LP, Søndergaard J, Elstrøm UV, Høyer M, Petersen JB. Adaptive plan selection vs. re-optimisation in radiotherapy for bladder cancer: A dose accumulation comparison. Radiotherapy and Oncology. 2013;109(3):457–462.

[81] Vestergaard A, Muren LP, Lindberg H, Jakobsen KL, Petersen JB, Elstrøm UV, et al. Normal tissue sparing in a phase II trial on daily adaptive plan selection in radiotherapy for urinary bladder cancer. Acta Oncologica. 2014;53(8):997–1004.

[82] Murthy V, Master Z, Adurkar P, Mallick I, Mahantshetty U, Bakshi G, et al. 'Plan of the day' adaptive radiotherapy for bladder cancer using helical tomotherapy. Radiotherapy and Oncology. 2011;99(1):55–60.

[83] Kron T, Wong J, Rolfo A, Pham D, Cramb J, Foroudi F. Adaptive radiotherapy for bladder cancer reduces integral dose despite daily volumetric imaging. Radiotherapy and Oncology. 2010;97(3):485–487.

[84] Dawson LA, Litzenberg DW, Brock KK, Sanda M, Sullivan M, Sandler HM, et al. A comparison of ventilatory prostate movement in four treatment positions. International Journal of Radiation Oncology Biology Physics. 2000;48(2):319–323.

[85] Malone S, Crook JM, Kendal WS, et al. Respiratory-induced prostate motion: quantification and characterization. International Journal of Radiation Oncology Biology Physics. 2000;48(1):105–109.

[86] Lin Y, Liu T, Yang X, Wang Y, Khan MK. Respiratory-Induced Prostate Motion Using Wavelet Decomposition of the Real-Time Electromagnetic Tracking Signal. International Journal of Radiation Oncology Biology Physics. 2013;87(2):370–374.

[87] Mellin I. Todennäköisyyslaskenta ja tilastotiede: Kaavat. Tilastolliset menetelmät: Kaavat [Opetusmoniste]; 2008.

[88] Mangar SA, Scurr E, Huddart RA, Sohaib SA, Horwich A, Dearnaley DP, et al. Assessing intra-fractional bladder motion using cine-MRI as initial methodology for Predictive Organ Localization (POLO) in radiotherapy for bladder cancer. Radiotherapy and Oncology. 2007b;85(2):207–214.

[89] Lebesque JV, Bruce AM, Guus Kroes A, Touw A, Shouman T, van Herk M. Variation in volumes, dose-volume histograms, and estimated normal tissue complication probabilities of rectum and bladder during conformal radiotherapy of T3 prostate cancer. International Journal of Radiation Oncology Biology Physics. 1995;33(5):1109–1119.

[90] Antolak JA, Rosen II, Childress CH, Zagars GK, Pollack A. Prostate target volume variations during a course of radiotherapy. International Journal of Radiation Oncology Biology Physics. 1998;42(3):661–672.

[91] Stroom JC, Koper P, Korevaaar GA, van Os M, Janssen M, de Boer HC, et al. Internal organ motion in prostate cancer patients treated in prone and supine treatment position. Radiotherapy and Oncology. 1999;51(3):237–248.

[92] Frank SJ, Dong L, Kudchadker RJ, De Crevoisier R, Lee AK, Cheung R, et al. Quantification of prostate and seminal vesicle interfraction variation during IMRT. International Journal of Radiation Oncology Biology Physics. 2008;71(3):813–820.

[93] Orio PFI, Merrick GS, Allen ZA, Butler WM, Wallner KE, Kurko BS, et al. cExternal beam radiation results in minimal changes in post void residual urine volumes during the treatment of clinically localized prostate cancer. Radiation Oncology. 2009;4:26–34.

[94] Zellars RC, Roberson PL, Strawderman M, Zhang D, Sandler HM, Ten Haken RK, et al. Prostate position late in the course of external beam therapy: patterns and predictors. International Journal of Radiation Oncology Biology Physics. 2000;47(3):655–660.

[95] Foroudi F, Pham D, Rolfo A, Bressel M, Tang CI, Tan A, et al. The outcome of a multi-centre feasibility study of online adaptive radiotherapy for muscle-invasive bladder cancer TROG 10.01 BOLART. Radiotherapy and Oncology. 2014;111(2):316–320.

[96] Wright P, Redpath AT, Høyer M, Muren LP. A method to individualize adaptive planning target volumes for deformable targets. Physics in medicine and biology. 2009;54(23):7121–7133.